

BIOACTIVE GEL-GLASSES:  
PROCESSING AND REACTION MECHANISMS

By

MARIVALDA DE MAGALHÃES PEREIRA

A DISSERTATION PRESENTED TO THE GRADUATE SCHOOL  
OF THE UNIVERSITY OF FLORIDA IN PARTIAL FULFILLMENT  
OF THE REQUIREMENTS FOR THE DEGREE OF  
DOCTOR OF PHILOSOPHY

UNIVERSITY OF FLORIDA

1994

To my dad, Carlos,  
whose memory is a constant source of  
strength and motivation to pursue my best.

## ACKNOWLEDGMENTS

I wish to express my sincere appreciation to the chairman of my committee, Dr. Larry Hench, for introducing me to the field of biomaterials and for his guidance and assistance through the course of this study. Very special thanks go to Dr. Arthur (Buddy) Clark for his continued encouragement and advice. I would also like to thank Professors James Adair, David Clark, E. Dow Whitney and Dinesh Shah for their guidance and participation as committee members.

I am very grateful to those individuals whose time and expertise contributed to this work. Guy LaTorre provided numerous hours of technical assistance, always with patience and useful suggestions. Dr. Jon West always had a word of advice and helpful comments. I thank Dr. Bamiduro Oguntebi and Dr. Harold Stanley of the University of Florida College of Dentistry for their expert work in the pulp capping study and Mary Stone for the preparation of the histological samples. Thanks go also to Richard Crockett and Wayne Acree for expert SEM and EMP work and to Fernando Araújo for providing some of the silica gel samples. I especially thank Allyson Barrett for her technical assistance in several

steps of this work and for her friendship and support, which helped me through some difficult times.

I wish also to thank my family and all my friends for their love and moral support during my stay in the United States. My very special thanks go to my best friend Flay for being present, for listening, for sharing the many feelings that are part of the experience of a graduate student.

Finally, I wish to thank my husband, Gio, for his love, support and companionship, and for his very own way of making things seem a lot easier and lighter.

Financial support from the Brazilian Government--*Conselho Nacional de Desenvolvimento Científico e Tecnológico*--is gratefully acknowledged. Acknowledgment is also made of the support of the U.S. Air Force Office of Scientific Research Grant Nº F49620-92-J-0351 and National Institute of Dental Research Grant Nº P50DE09307-01.



## TABLE OF CONTENTS

	<u>Page</u>
ACKNOWLEDGMENTS.....	iii
LIST OF TABLES.....	ix
LIST OF FIGURES.....	x
ABSTRACT.....	xiv
 CHAPTERS	
1 INTRODUCTION.....	1
1.1 Bioactive Materials.....	1
1.2 Sol-Gel Processing of Bioactive Glasses.....	5
1.3 Calcium Phosphate Formation on Bioactive Glasses.....	11
1.4 Calcium Phosphate Formation on Pure Silica Substrates.....	16
1.5 Objectives.....	19
2 HOMOGENEITY OF BIOACTIVE SOL-GEL DERIVED GLASSES IN THE SYSTEM $\text{CaO-P}_2\text{O}_5\text{-SiO}_2$ .....	21
2.1 Introduction.....	21
2.2 Homogeneity of Multicomponent Gels.....	22
2.2.1 Gel Preparation Stage.....	23
2.2.2 Postgelation Stage.....	29
2.3 Experimental Procedures.....	30
2.3.1 Materials.....	30
2.3.2 Gel Preparation.....	31
2.3.3 Postgelation Treatment.....	34
2.3.4 Homogeneity Measurement.....	36
2.4 Results and Discussion.....	37

2.4.1	Gel Derived Glasses Prepared with Calcium Nitrate.....	37
2.4.2	Gel Derived Glasses Prepared with Calcium Alkoxide.....	40
2.5	Conclusions.....	47
3	CALCIUM PHOSPHATE FORMATION ON SOL-GEL DERIVED BIOACTIVE GLASSES IN VITRO.....	50
3.1	Introduction.....	50
3.2	Experimental Procedures.....	51
3.2.1	Materials Preparation.....	51
3.2.2	Characterization Measurements.....	51
3.2.3	<u>In Vitro</u> Testing.....	53
3.3	Results.....	55
3.3.1	Characteristic Features of the Gel-Glasses.....	55
3.3.2	<u>In Vitro</u> Calcium Phosphate Formation...	60
3.4	Discussion.....	68
3.5	Conclusions.....	78
4	EFFECT OF TEXTURE ON THE RATE OF HYDROXYAPATITE FORMATION ON SILICA GEL SURFACE.....	79
4.1	Introduction.....	79
4.2	Experimental Procedures.....	81
4.2.1	Preparation of Sol-Gel Derived Glasses.	81
4.2.2	Soaking in Solutions.....	83
4.2.3	Analysis of Surface Structure.....	87
4.2.4	Ion Concentration Analysis.....	88
4.3	Results.....	88
4.3.1	Effect of Composition of Sol-Gel Derived Glasses on Hydroxyapatite Formation.....	88
4.3.2	Effect of Solution Parameters on Hydroxyapatite Formation.....	94
4.3.3	Effect of Texture on the Hydroxyapatite Formation.....	94
4.3.4	Morphology of Hydroxyapatite Formed on Silica Gels with Different Textures....	103
4.4	Discussion.....	111
4.5	Conclusions.....	118

5	MECHANISM OF HYDROXYAPATITE FORMATION ON SILICA SUBSTRATES: A REVIEW.....	119
5.1	Introduction.....	119
5.2	Effect of Solution Parameters on Apatite Formation.....	121
5.3	The Silica-Rich Gel Layer Requirement.....	123
5.4	Soluble Silicates Species on Apatite Nucleation.....	125
5.5	Porous vs. Dense Substrates.....	127
5.6	Effect of Surface Charge.....	129
5.7	Effect of the Texture of Silica.....	130
5.8	Hydroxyl Groups as Nucleation Sites for Hydroxyapatite.....	132
5.9	Hydroxyl Concentration as a Rate Determining Factor in Hydroxyapatite Formation.....	137
5.10	Conclusions.....	139
6	<u>IN VIVO</u> EVALUATION OF BIOACTIVE SOL-GEL DERIVED GLASSES.....	141
6.1	Introduction.....	141
6.2	Experimental Procedures.....	143
6.2.1	Experimental and Control Materials.....	144
6.2.2	Pulp-Capping Procedure.....	146
6.2.3	Microscopic Examination.....	150
6.2.4	Scanning Electron Microscopy Examination.....	150
6.3	Results.....	150
6.3.1	Microscopic Observations.....	150
6.3.2	SEM Observations.....	152
6.4	Discussion.....	154
6.5	Conclusions.....	158
7	CONCLUSIONS AND SUGGESTIONS FOR FUTURE WORK.....	160
	REFERENCES.....	166
	BIOGRAPHICAL SKETCH.....	178

## LIST OF TABLES

<u>Table</u>	<u>Page</u>
2.1 Nominal Compositions of Gel-Glasses (in mole %). ....	32
2.2 Ion Concentration (mM) of SBF and Human Blood Plasma.....	48
3.1 BET Data for Bioactive Gel-Glasses. Gelation Time=3 days.....	61
3.2 BET Data for Bioactive Gel-Glasses. Gelation Time=5 days.....	61
4.1 Nominal Compositions of Gel-Glasses (in mole %). ....	82
4.2 BET Data of Gel-Glasses Treated at 600°C.....	82
4.3 BET Data of Gel-Silica Glasses and Porous Vycor Treated at 600°C.....	84
4.4 BET Data of 1S1.2 Gel-Silica Glasses Treated at 400, 600 and 800°C.....	84
4.5 Ion Concentration (mM) of SBF and Human Blood Plasma.....	86
5.1 Nominal Ca Concentration in the SBF Solutions.....	122
5.2 Measured Ca and P in SBF Solutions Before and After Maintaining at 37°C for the Period Indicated.....	122
5.3 Texture of Gel-Silica Glass 1S3.1 Treated at the Indicated Temperature and Correspondent Hydroxyl Coverage.....	138
5.4 Induction Time (Days) for Nucleation of Hydroxyapatite on Gel-Silica Glass 1S3.1.....	138
6.1 Composition of Experimental Materials in Mole %....	145
6.2 Experimental Design for Pulp Capping Treatment.....	148



## LIST OF FIGURES

<u>Figure</u>	<u>Page</u>
1.1 Processing steps in making bioactive gel-glasses by the sol-gel method.....	7
1.2 FTIR reflection spectra of 58S sol-gel derived glass.....	10
2.1 Drying schedules of gels.....	35
2.2 Heterogeneity level (HL) of calcium nitrate derived gels, reference procedure (R) and slow drying rate.....	38
2.3 Heterogeneity level (HL) of calcium nitrate derived gels, varying condensation pH.....	39
2.4 DTA curves for calcium nitrate and calcium alkoxide derived gels .....	41
2.5 Calcium nitrate and calcium alkoxide derived gel-glasses.....	43
2.6 Heterogeneity level (HL) of calcium alkoxide derived gels .....	44
2.7 FTIR spectra of four randomly selected samples of S60 calcium alkoxide derived gel-glasses.....	45
2.8 FTIR spectra of three samples of S60 calcium alkoxide derived gel-glasses and of 45S5 melt derived glass after reaction in SBF for 20hours....	46
3.1 Drying schedule for calcium alkoxide derived gels..	52
3.2 Partial densification schedule for calcium alkoxide derived gels.....	52
3.3 DTA and TGA curves for gel S60.....	56
3.4 X-ray diffraction spectra for calcium alkoxide derived gel-glasses.....	58

3.5	FTIR spectra of gel-glasses treated at 700°C.....	59
3.6	FTIR spectra of gel-glasses after reaction in Tris buffer for: a) 5 hours; b) 24 hours; c) 360 hours..	62
3.7	FTIR spectra of gel-glasses after reaction in SBF for: a) 5 hours; b)12 hours; c) 20 hours.....	65
3.8	Concentration of Ca, P, and Si in Tris buffer with reaction time for gel-glasses: a) S60; b) S70; c)S80.....	69
3.9	Concentration of ions with reaction time in Tris and SBF solutions for gel-glass S60: a) P; b) Ca; c)Si.....	72
3.10	FTIR spectra of gel-glass powders after reaction in SBF for 20 hours.....	75
4.1	Nitrogen adsorption isotherms (a), and pore size distribution (b) of gel-silica glasses with different average pore radius.....	85
4.2	FTIR reflection spectra of gel-silica glass 85S before (a) and after reaction in SBFpH7.25 for 6 (b), 8 (c), 12 (d) and 24 (e) hours.....	89
4.3	FTIR reflection spectra of gel-silica glass 90S before (a) and after reaction in SBFpH7.25 for 5 (a), 7 (b) and 10 (d) days .....	90
4.4	FTIR reflection spectra of gel-silica glass 1S1.2/600 before (a) and after reaction in SBFpH7.25 for 15 (b), 25 (c), and 30 (d) days.....	91
4.5	Induction time for HA nucleation as a function of gel-glass composition .....	93
4.6	FTIR reflection spectra of gel-silica glass 1S1.2/600 before (a) and after reaction in SBF Ca200ppm for 16 (b), 20 (c), 48 (d) hours.....	95
4.7	Induction time for HA nucleation as a function of calcium concentration in SBF solution for gel-silica glass 1S1.2/600 .....	96
4.8	FTIR reflection spectra of gel-silica glass 1S1.2/600 after reaction in SBFpH7.25 and SBFpH7.4.....	97
4.9	FTIR reflection spectra of gel-silica glass 1S5.3/600 before (a) and after reaction in SBFpH7.25 for 4 (b), 6 (c), and 9 (d) days .....	98

4.10	Calcium and phosphorous concentrations as a function of immersion time in SBF for gel-silica glasses of various pore sizes .....	100
4.11	Induction time for HA nucleation on gel-silica glasses as a function of pore size, pore volume, and pore size x pore volume .....	101
4.12	FTIR reflection spectra of gel-silica glass 1S1.2/400 before (a) and after reaction in SBFpH7.25 for 9 (b), 15 (c), and 25 (d) days .....	102
4.13	FTIR reflection spectra of different materials before and after reaction in SBF pH7.25/Ca=200ppm. a) Quartz, 30 days; b) Slide Glass, 30 days; c) Gel-glass 1S1.2/600, 2 days; d) Vycor 10 days...	104
4.14	SEM micrographs showing morphology of hydroxyapatite formed on gel-silica glass 1S1.2/600 after immersion in SBF for 30 days: a) 1000x; b)10.000x.....	105
4.15	SEM micrographs showing morphology of hydroxyapatite formed on gel-silica glass 1S1.4/600 after immersion in SBF for 26 days: a) 1000x; b)10.000x.....	106
4.16	SEM micrographs showing morphology of hydroxyapatite formed on gel-silica glass 1S1.6/600 after immersion in SBF for 10 days: a) 1000x; b)10.000x.....	107
4.17	SEM micrographs showing morphology of hydroxyapatite formed on gel-silica glass 1S2.1/600 after immersion in SBF for 7 days: a) 1000x; b)10.000x .....	108
4.18	SEM micrographs showing morphology of hydroxyapatite formed on gel-silica glass 1S3.1/600 after immersion in SBF for 7 days: a) 1000x; b)10.000x .....	109
4.19	SEM micrographs showing morphology of hydroxyapatite formed on gel-silica glass 1S5.3/600 after immersion in SBF for 6 days: a) 1000x; b)10.000x .....	110
6.1	FTIR spectra of experimental bioactive glass powders after reaction in Tris buffer for 20 hours.....	147
6.2	SEM micrographs of specimens capped with melt	



derived glass 45S5 Bioglass (a) and melt derived  
glass (b), time period: 60 days..... 153

6.3 SEM micrographs of specimens capped with gel-  
glasses 54S(a) and 77S(b); time period: 60 days.... 155

Abstract of Dissertation Presented to the Graduate School  
of the University of Florida in Partial Fulfillment of the  
Requirements for the Degree of Doctor of Philosophy

BIOACTIVE GEL-GLASSES:  
PROCESSING AND REACTION MECHANISMS

By

Marivalda de Magalhães Pereira

April 1994

Chairman: Larry L. Hench

Major Department: Materials Science and Engineering

A sol-gel method to produce  $\text{CaO-P}_2\text{O}_5\text{-SiO}_2$  three component bioactive glasses using all alkoxide components in the gel synthesis was developed. By use of the all-alkoxide method, monolithic, transparent, homogeneous gel-glasses were obtained. The heterogeneity level in terms of calcium ion distribution, measured by electron microprobe analysis, decreased from as much as 35% when calcium nitrate was used as a precursor to 1% when all alkoxide components were used.

Characterization of the gel derived glasses was conducted using FTIR reflection spectroscopy, X-ray diffraction, thermal analysis and nitrogen adsorption analysis. The gel-glasses studied, with compositions in the range 60-80%  $\text{SiO}_2$ , were amorphous, porous materials with a surface area ranging from 250 to 450  $\text{m}^2/\text{g}$ .

The bioactivity of the all-alkoxide derived gel-glasses, defined by the rate of hydroxy carbonate apatite (HCA) formation on the surface of the glasses, was measured by FTIR reflection spectroscopy. All three compositions form an HCA layer within 8 hours in both test solutions used, Tris buffer and simulated body fluid (SBF), indicating that they are bioactive. The thickness of the HCA layer grows rapidly in SBF.

The mechanism of HCA formation on pure silica substrates was investigated and the effects of surface chemistry and texture on the nucleation process were established. The texture of the substrate has a direct effect on the nucleation rate. The induction time for HCA nucleation increases as pore size and pore volume decrease. It is proposed that the HCA nucleation occurs inside the pores and that the number of pores and the diffusion of ions into the pores are the variables that control the nucleation rate. The concentration of silanol groups on the silica surface does not control the rate of HCA nucleation, and evidence does not support involvement of silanol groups on the nucleation process.

## CHAPTER 1 INTRODUCTION

### 1.1 Bioactive Materials

The development of biomaterials has gained major importance over the past 30 years. A broad range of biomaterials--including metals (stainless steels, Ti and Ti alloys, Co-Cr alloys), polymers (polymethylmetacrylate-PMMA, polypropylene-PP) and ceramics (calcium phosphate ceramics, glasses and glass-ceramics)--is used in surgical implants. At present, approximately 40 biomaterials are used in as many as 50 prosthetic devices developed in modern medical and dental surgery (Hen80). In particular, the use of ceramics in medicine has increased significantly during the past two decades (Hen84, Duc87, Hen93b), and it is anticipated that the use of bioceramics will increase dramatically during the next 10 years. A recent review on the state of the science and clinical applications of bioceramics is presented in the book *An Introduction to Bioceramics* (Hen93b).

The potential of ceramics as biomaterials relies upon their compatibility in the physiological environment. According to the type of biomaterial-tissue interface developed, bioceramics are classified in three groups:



nearly inert, surface-active and resorbable (Hen80, Hen82). Inert bioceramics, typically oxides or carbon-based materials, undergo little or no chemical change during long-term exposure to the physiological environment. Tissue response to inert bioceramics involves the formation of a very thin (up to several micrometers) fibrous capsule around the implant material. Inert bioceramics may be attached to the physiological system through mechanical interlocking, by tissue ingrowth into undulating surfaces. Resorbable bioceramics, typically Ca and P based, are designed to degrade gradually over a period of time and be replaced by the natural host tissue. They are typically used as scaffolds or space fillers. Surface-active bioceramics "elicit a specific biological response at the interface of the material which results in the formation of a bond between the tissue and the material" (Hen84). These materials are referred to as bioactive ceramics.

The concept of a bioactive synthetic material capable of bonding with tissues originated with the work of Hench and colleagues in the early 1970s (Hen71, Hen74). It was discovered that certain glass compositions in the system  $\text{SiO}_2\text{-P}_2\text{O}_5\text{-Na}_2\text{O-CaO}$  (Bioglasses<sup>®1</sup>) could bond with bone when implanted. Later work by Wilson and Nolletti showed that certain compositions of the bioactive glasses also bond with soft tissues (Wil81, Wil90). The bond forming mechanism involves a series of controlled surface reactions in which a

---

<sup>1</sup>Bioglass<sup>®</sup> -Registered trademark University of Florida, Gainesville, FL.

biologically active calcium phosphate layer is produced from species leached from the bulk glass. Bioactive glasses were also examined by a team of researchers in Finland in the system  $\text{SiO}_2\text{-Na}_2\text{O-CaO-P}_2\text{O}_5\text{-B}_2\text{O}_3\text{-Al}_2\text{O}_3$  (And90b, Kan90, And91). They also identified the calcium phosphate surface layer that serves as the bonding zone between the glass and bone.

Bioactive glasses are used primarily in nonload-bearing applications due to their relatively low tensile strength. This observation has led to the development of bioactive glass-ceramics with improved mechanical properties. Multiphase glass-ceramics can be produced through nucleation and crystallization of their virginal glasses under controlled thermal treatment.

A series of bioactive glass-ceramics, termed Ceravital<sup>®2</sup> was developed by Brömer and others in Germany (Bro73, Bro77). Ceravital<sup>®</sup> compositions fall into the  $\text{SiO}_2\text{-P}_2\text{O}_5\text{-Na}_2\text{O-K}_2\text{O-MgO-CaO}$  system and are composed of apatite and a glassy matrix. The polycrystalline phase enhances the mechanical strength of the material, but not enough to allow its use in load-bearing applications. A Japanese group led by Professors Yamamuro and Kokubo developed a glass-ceramic material based on the  $\text{SiO}_2\text{-P}_2\text{O}_5\text{-Na}_2\text{O-K}_2\text{O-MgO-CaO}$  system, known as A-W glass-ceramic (Kok85, Nak85, Kok86). This kind of material is a microcomposite of apatite and wollastonite, both distributed in a glassy matrix. A-W can be used in load bearing applications because of the high strength resulting

---

<sup>2</sup>Ceravital<sup>®</sup> -Registered trademark Leitz W, Germany.

from its microstructure. A third group of glass-ceramics was developed by Vogel and Holand (Vog86, Hol93) containing phlogopite (mica) and apatite crystalline phases. These materials are somewhat machinable because of the presence of a micaceous crystalline phase, phlogopite. All three groups of glass-ceramics were shown to form a bond with bone (Hol85, Nak85, Gro88, Oht91).

Besides glasses and glass-ceramics, bioactive materials include synthetic hydroxyapatite (HA) which also forms an interfacial bond with bone (LeG93). Jarcho et al. (Jar76) and Tracy and Doremus (Tra84) reported that the bonding of sintered HA ceramic to bone is achieved by a direct chemical bond between the apatites in the ceramic and in the bone. HA can be prepared as dense or macroporous forms and has been used as a biomaterial for bone repair, augmentation and substitution (LeG93, Sho93).

A common characteristic of all bioactive materials is the formation of a hydroxy carbonate apatite (HCA) layer on their surface when implanted. The HCA phase is equivalent in composition and structure to the mineral phase of bone. It is that equivalence that is responsible for interfacial bonding (Hen91a). However, the time dependence of bonding, the strength of the bond, the mechanism of bonding, the thickness of the bonding zone and the mechanical strength and fracture toughness differ for the various bioactive materials.



## 1.2 Sol-Gel Processing of Bioactive Glasses

Bioactive ceramics are made in many different phases and forms. They can be polycrystalline (hydroxyapatite), glass (Bioglass®), glass-ceramic (A-W glass-ceramic), or composites (polyethylene-hydroxyapatite). They can be used as bulk materials in implants, as powders to fill space while the natural repair processes occur, as a coating on substrates, or as a second phase in a composite. The phase and/or form used depends on the properties and function required. To produce these materials many different processing techniques are used.

The specific group of bioactive materials focused on in this work, bioactive glasses, is conventionally produced by a melting and casting process. The glass components, usually in the form of oxides or carbonates, are mixed and then melted and homogenized at high temperatures, 1250-1400°C. The liquid is either cast forming the desired shape or poured into a liquid medium where it solidifies and fractures into small fragments, called a frit. Recently, R. Li et al. used a sol-gel processing technique to produce a new generation of bioactive gel-glasses (Li91b).

Sol-gel processing is a chemically based method for producing ceramics and glasses at much lower temperatures than the conventional methods. This technique has gained intense research interest in the last decade, and a large amount of literature describing the history, theory,

processing details and applications is available (Bri90, Hen90b). Basically, sol-gel processing can be divided into two main categories: a) destabilization of an organic salt containing one or more metal ions in aqueous solutions in which the only liquid present is water, and b) controlled hydrolysis and polycondensation of alkoxide precursors in nonaqueous solutions that contain solvents other than or in addition to water. The second method was used in the development of bioactive glasses in the system  $\text{SiO}_2\text{-CaO-P}_2\text{O}_5$  (Li91a).

Seven steps are involved in making gel-glasses by the sol-gel method (Hen90b). The sequence of processing steps is illustrated in Figure 1.1.

(1) Sol preparation. A liquid precursor is mixed with water and undergoes simultaneous hydrolysis and polycondensation reactions. As sufficient bonds are formed in a region, colloidal particles (sub micrometer) form, constituting the sol.

(2) Casting. As the network develops the viscosity increases. Prior to completion of network formation the sol can be applied as a coating, pulled into a fiber, impregnated into a composite, formed into powders, or cast into a mold with a precise shape and surface features.

(3) Gelation. At completion of network formation a solid object, called the gel, is formed. It consists of an interconnected 3-D network of particles holding an interstitial liquid that is a mixture of alcohols and water.

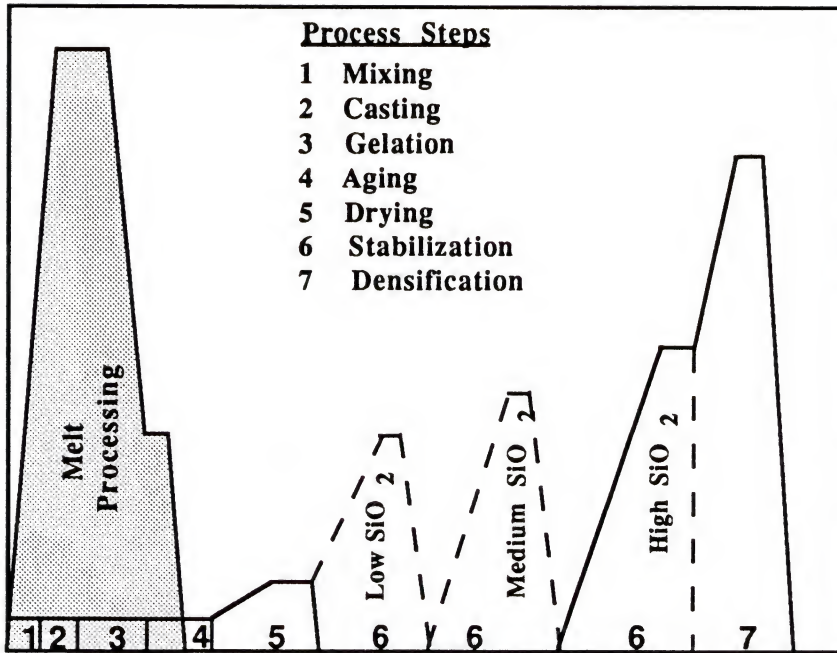


Figure 1.1 Processing steps in making bioactive gel-glasses by the sol-gel method.



The sol becomes a gel when it can support a stress elastically.

(4) Aging. Aging involves holding the gel in its pore liquid for several hours at 25-80°C. This leads to localized solution and reprecipitation of the solid network, which increases the thickness of the interparticle necks and the density and strength of the gel.

(5) Drying. During drying, the liquid is removed from the interconnected pore network and the wet gel experiences progressive shrinkage, hardening and stress development. Gels dried under ambient pressure and relatively low temperatures are termed xerogels. The surface area of these gels is very large, 200-800 m<sup>2</sup>/g, and the pore sizes can be varied from 1.0-12 nm. Because of the very small pore sizes large capillary stresses can arise during drying. If the gel is dried at high temperature and pressure, above the critical temperature ( $T_c$ ) and critical pressure ( $P_c$ ) of the liquid, there is no interface between liquid and vapor, so there is no capillary pressure and relatively little shrinkage. Gels made by this method, referred to as supercritical drying, are called aerogels. They have very low densities and strengths.

(6) Stabilization. Chemical stabilization of a dried gel is necessary to control the environmental stability of the material. The stabilization of silica gels is accomplished by thermal treatment in the range 500-900°C, where surface silanols (Si-OH) are desorbed and 3-membered

silica rings are eliminated. Stabilization also increases the density, strength and hardness of the gels.

(7) Densification. Densification is completed in the range 900-1150°C. It is essentially a sintering process by which the pores of a dry gel are eliminated. This last step is not performed on gels intended for bioactive applications.

The use of the sol-gel method to produce ceramics and glasses is based on the potential advantages offered by this process over conventional glass techniques, namely, higher purity and homogeneity and lower processing temperatures. In terms of production of bioactive glasses, a very important advantage of the sol-gel process is the ability to control the surface chemistry and texture of the material, both important features in controlling the rate of HCA formation on the gel glasses and their bioactivity (Li92b). This process extends the compositional range of bioactivity and increases the rate of HCA formation.

In using the procedure described by Li (Li91a) to synthesize the gel derived powders, the author determined that the material is often not homogeneous. The heterogeneity is apparent through variations in the diffuse reflectance infra-red spectra obtained with a Fourier Transform IR Spectrometer (FTIR). Figure 1.2 shows the range of FTIR spectra obtained from random samples of a batch of powder of nominal 58S composition (58% SiO<sub>2</sub>, 38% CaO, 4% P<sub>2</sub>O<sub>5</sub> weight %). The large variations of intensity in the

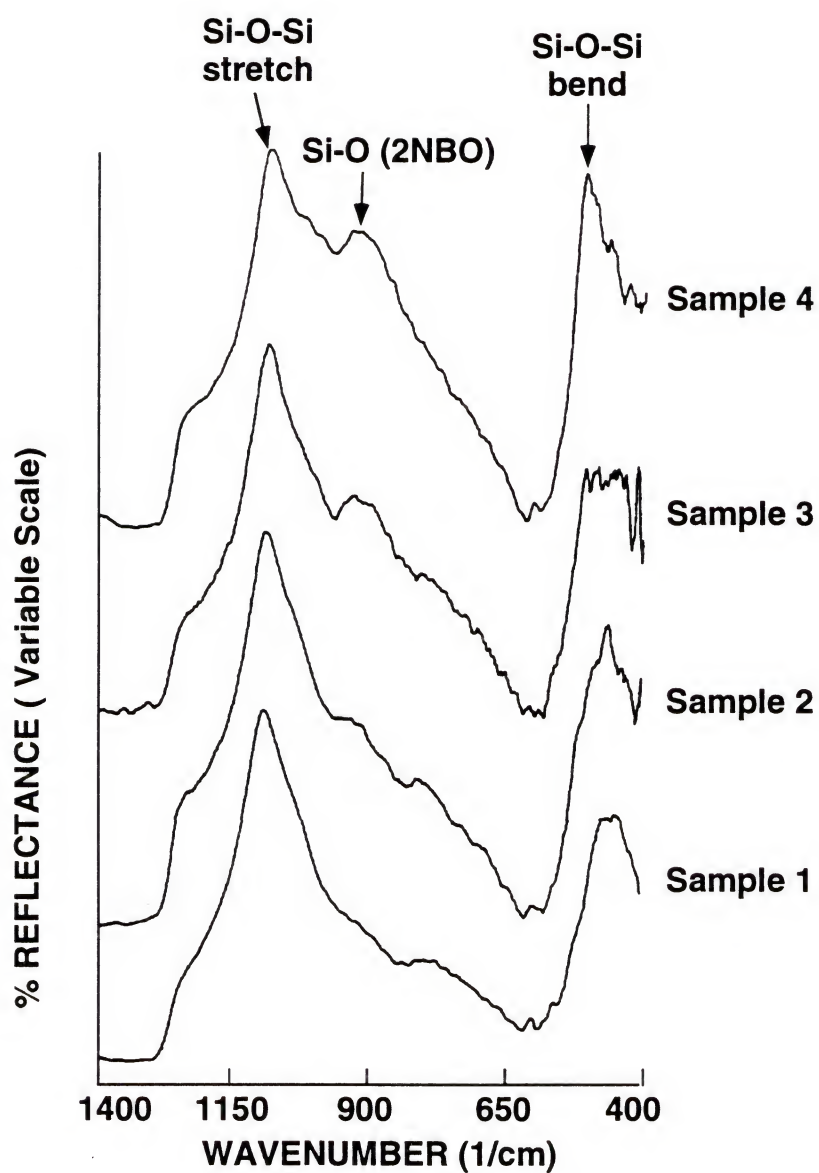


Figure 1.2 FTIR reflection spectra of 58S sol-gel derived glass.

800-950  $\text{cm}^{-1}$  region are due to variations in Si-O-Ca vibrational modes in the 4 samples. Variability in the FTIR spectra predicts a large uncertainty in the rate of bioactivity of the material, based upon previous correlation of composition with the rate of HCA formation (Ogi80, Hen88a, Kim92). Thus, one of the potential advantages of sol-gel processing, high homogeneity even at the molecular level, is lost in the processing.

### 1.3 Calcium Phosphate Formation on Bioactive Glasses

The bonding between glass and bone has been described in several papers (Hen88a, Gro88). The basis for bone bonding is the reaction of the glass with the surrounding solution. A sequence of interfacial reactions, which begins immediately after the bioactive material is implanted into the body, leads to the formation of a hydroxyapatite layer and establishment of interfacial bonding. Hench (Hen90a) summarizes the sequence of interfacial reactions as follows:

1. rapid exchange of  $\text{Na}^+$  or  $\text{K}^+$  with  $\text{H}^+$  or  $\text{H}_3\text{O}^+$  from solution and formation of silanols ( $\text{SiOH}$ )
2. loss of soluble silica, in the form of  $\text{Si}(\text{OH})_4$ , to the solution, resulting from breaking of Si-O-Si bonds and formation of silanols
3. polycondensation of silanols to form a hydrated silica gel layer



4. migration of  $\text{Ca}^{2+}$  and  $\text{PO}_4^{3-}$  groups to the surface through the silica layer
5. formation of a  $\text{CaO-P}_2\text{O}_5$ -rich film on the top of the silica-rich layer
6. growth of a  $\text{SiO}_2$ -rich layer by diffusion-controlled alkali ion exchange
7. growth of amorphous  $\text{CaO-P}_2\text{O}_5$  film by incorporation of soluble calcium and phosphates from solution
8. crystallization of the amorphous film by incorporation of  $\text{OH}^-$ ,  $\text{CO}_3^{2-}$  or  $\text{F}^-$  anions from solution to form a mixed hydroxyl, carbonate, fluorapatite layer (HCA)
9. adsorption of biological moieties in the HCA layer
10. action of macrophages
11. attachment of stem cells
12. differentiation of stem cells
13. generation of matrix
14. crystallization of matrix.

The development of both the silica-rich layer and HCA at the implant interface was detected on Bioglass® (Pan74, Cla76, Kim89), on other bioactive glasses derived from Bioglass® (And90b), and on the glass-ceramic Bioverit® (Hol85). A calcium phosphate layer was also seen to connect the implant with bone in the glass-ceramics Ceravital® and A/W (Kit87, Oht91, Neo92). In all cases, the bone bonding of glasses and glass-ceramics was established with the involvement of a calcium phosphate layer on their surfaces.

This layer was observed in vivo as well as in vitro (Kim89, Kok90b, And91, Kok92).

The rate of tissue bonding to bioactive glasses appears to depend on the rate of HCA formation, which depends on the glass composition (Ogi80, Kim92). The compositional factor most important in the HCA formation is the silica content, which establishes the compositional boundary between bonding and nonbonding bioactive glasses. No apatite formation or bone bonding can be observed on glasses when their silica content increases beyond around 60% (Hen77, Wal77, Ogi80, Hen90a). Phosphate-free glasses as well as glass-ceramics in which the phosphate is bound in a stable, relatively insoluble apatite phase are bioactive (Wal77, Ohu91). Kokubo and coworkers have shown that the minimum melt derived glass compositional system for bioactivity is  $\text{CaO-SiO}_2$  with a compositional limit of about 60 mole %  $\text{SiO}_2$  (Ohu91, Oht92b).

Another important compositional factor in bone bonding behavior is the inhibitory role of  $\text{Al}_2\text{O}_3$  (Hen88a, And90a, Ohu92). The amount of alumina that inhibits bone bonding depends on glass composition, but it is generally in the order of 1.0-1.5 weight percent. Gross and coworkers have shown that the same effect occurs for other multivalent cations such as  $\text{Ta}_2\text{O}_5$  (Gro85, Gro88). Additions of more than 1.5 to 3% multivalent ions usually make the glass inactive.

The dependence of bioactivity on the silica content is directly related to its effect on the reactions occurring on

the glass surface. The dissolution rate decreases greatly for compositions above 60%  $\text{SiO}_2$  because of the larger number of bridging oxygen bonds in the glass structure. This limits the hydration of the silica surface and repolymerization into a silica gel layer. At the same time, higher silica contents result in lower ion release and therefore lower concentrations of calcium and phosphate ions in solution. It is well established that higher concentrations of these ions in solution increase the rate of hydroxyapatite precipitation (LeG91, Li93a).

The compositional dependence of the rate of HCA formation was also seen on bioactive glasses produced by sol-gel processing (Li91b). In vitro studies on sol-gel derived powders in the system  $\text{SiO}_2\text{-P}_2\text{O}_5\text{-CaO}$  showed that the rate of HCA formation decreased as the  $\text{SiO}_2$  content increased, as observed for melt derived bioactive glasses. However, the compositional boundary was extended to 90%  $\text{SiO}_2$  and the rate of HCA formation was higher in sol-gel derived glasses than in melt derived glasses of the same silica content. The high bioactivity of the sol-gel derived powders was attributed to the large surface area and a large concentration of silanol groups on the surface of the microporous material.

The concentration of ions released from the bioactive glasses into the surrounding solution depends on both the composition of the glass and on the ratio of surface area/volume of solution. In the sol-gel derived glasses



there is a variation in texture simultaneous with a variation in composition. Therefore, in the evaluation of the rate of HCA formation on these glasses, the effects of composition and texture are superimposed. To separate these two parameters, R. Li et al. (Li92b) evaluated the effect of texture on the rate of HCA formation for a fixed composition of the gel-glasses, varying the texture by varying the treatment temperature of the gel. All the textural features (pore volume, pore size, surface area) decreased as temperature increased. The researchers observed a decrease in the rate of HCA formation as the temperature increased and related that directly to the effect of surface area and concentration of silanols on the nucleation of hydroxyapatite. However, as the concentration of ions in solution depends on the relation of surface area/volume, the effect observed may be related only indirectly to surface area, through its correlation with the concentration of released ions. Furthermore, all textural features varied simultaneously, and no attempt was made to isolate each variable.

Textural effects, apparent on sol-gel derived glasses, may also be important in the control of the rate of HCA formation on melt derived glasses. As discussed before, the reactions occurring on the surface of these glasses leads to the formation of a silica gel layer, on top of which HCA precipitates. The only attempt to characterize the textural features of the film formed on bioactive glasses when

exposed to aqueous solutions was done by Hench and Walker (Hen77, Wal77). They showed that the ability of a bioactive glass composition to bond with bone is dependent on the ability of that glass to react in aqueous solution to form a highly porous surface film, which in turn depends upon the glass composition. An increase in either the  $\text{SiO}_2$  content or the  $\text{CaO}$  to  $\text{Na}_2\text{O}$  ratio reduced the ability of the resulting glass to form such reaction films.

A useful experimental in vitro approach to evaluate the isolated effects of texture and concentration of ions in solution on the rate of hydroxyapatite formation on sol-gel derived glasses is to analyze its formation on pure silica gels having variable textures, controlled by thermal history, soaked in solutions with various ionic concentrations.

#### 1.4 Calcium Phosphate Formation on Pure Silica Substrates

The silica-rich gel layer apparently plays an important role in the formation of calcium phosphate on bioactive glasses since such precipitation generally follows the development of the silica layer. In spite of the general agreement with respect to the role of the silica layer on the nucleation of hydroxyapatite, a broadly accepted molecular mechanism is yet to be proposed. Thus, studies involving the formation of calcium phosphate on pure silica

substrates should provide a scientific basis for a general mechanism of apatite induction.

Heterogeneous deposition of calcium phosphate from solutions containing  $\text{Ca}^{2+}$  and  $\text{HPO}_4^{2-}$  ions was observed on the surface of colloidal silica particles by Adair et al. (Ada93) by use of scanning electron microscopy (SEM) with energy dispersive spectroscopy (EDS) and electrophoretic mobility determinations. They showed that calcium phosphate heterogeneously deposited on the surfaces of the silica particles at relative supersaturations considerably less than the supersaturation required for homogeneous deposition from solution. A decrease in the incubation time for calcium phosphate precipitation in the presence of two types of silica particles, with different surface areas and sizes of the particles, was observed by Damen and Cate (Dam89). The precipitation reaction was followed by measurement of the concentration of free  $\text{Ca}^{2+}$ . A decrease in incubation time also occurred for solutions containing silicic acid. However, stimulation of calcium phosphate precipitation could only be achieved by use of a solution that contained silicic acid largely in polymeric form. The X-ray diffraction analysis of the calcium phosphate phase revealed spectra that corresponded to that of hydroxyapatite. The results of these studies indicate that the surface of silica rather than soluble silicate species is involved in the heterogeneous precipitation of hydroxyapatite.



In a series of studies, P. Li and colleagues (Li92a, Li93a, Li93c-f) showed that an apatite layer could be formed on pure silica gels soaked in a simulated body fluid solution containing  $\text{Ca}^{2+}$  and  $\text{HPO}_4^{2-}$  at  $\text{pH}=7.4$ . No precipitation was detected on either quartz or dense silica glass. The induction of calcium phosphate formation and bone bonding on a porous silica substrate had been reported earlier by Hench and Walker (Hen77, Wal77). They observed bone bonding with Vycor®, which is essentially a very porous form of silica.

In the studies on pure silica gels, P. Li et al. showed that the apatite layer formed in vitro as well as in vivo (Li93a). The rate of formation was shown to depend on the concentration of ions in solution (Li93f) and on the sintering temperature of the silica gel (Li93c). The bonding ability of the silica gels was attributed to the large concentration of hydroxyl groups on the surface of the gel. The experimental evidence the authors use to support this hypothesis is the decrease of the rate of hydroxyapatite formation as the heat treatment temperature of the gels increases. However, as is well known, heat treatment affects not only the surface chemistry, i.e. the concentration of silanols (Zhu87), but also the texture of the gels (Hen88b). No data on the texture of the silica gels or the change of texture with temperature were presented in P. Li's work.

Thus a more detailed evaluation of the role of surface chemistry and texture of silica gels on the calcium



phosphate formation is necessary for the complete understanding of the mechanism of apatite nucleation.

### 1.5 Objectives

The use of sol-gel processing opens the field of bioactive glasses towards two major directions: 1) the production and use of bioactive glasses with variable and controlled surface reactions to match the requirements of specific implant conditions; 2) the study of the parameters that control the formation of hydroxyapatite on sol-gel derived glasses as a way of providing the scientific basis for understanding bioactivity. This work is an effort to improve both areas.

An overview of the field of bioactive materials and the sol-gel method has been described in the previous sections. Chapter II presents a specific review on parameters that control the homogeneity of multicomponent sol-gel derived glasses. A method for preparing bioactive gel-glasses with improved homogeneity is presented along with the characterization and homogeneity analysis of these gels. The bioactivity of the gel-glasses, in both bulk and powder form, is evaluated through the formation of hydroxyapatite in vitro in Chapter III. Chapters IV and V focus on the analysis of the parameters that affect hydroxyapatite formation on silica substrates. The effect of composition and texture of the silica substrate on the rate of apatite

nucleation is investigated in Chapter IV. Chapter V presents a general review of the mechanisms of hydroxyapatite formation using results of this work as well as the literature concerning the subject. The in vivo response of sol-gel derived bioactive powders is presented in Chapter VI. Finally, the general conclusions of this study are presented in Chapter VII.

CHAPTER 2  
HOMOGENEITY OF BIOACTIVE SOL-GEL  
DERIVED GLASSES IN THE SYSTEM  $\text{CaO-P}_2\text{O}_5\text{-SiO}_2$

2.1 Introduction

Sol-gel processing of ceramics and glasses has become an area of intense research interest with regard to both scientific issues and potential commercial applications. Much of the interest is due to inherent advantages compared to more conventional processing techniques, primarily a potentially higher purity, greater homogeneity and lower processing temperatures associated with the method (Hen90b, Mac82). Applications for sol-gel processing developed to date include preparation of films, powders, fibers and bulk glasses (Dis83, Bri90).

Among the sol-gel applications developed is the synthesis of bioactive powders in the system  $\text{CaO-P}_2\text{O}_5\text{-SiO}_2$  (Li91a). In using the procedure described by R. Li et al. to synthesize the gel derived powders, the author determined that the material is often not homogeneous, as shown in the previous chapter (Figure 1.1). Thus, one of the potential advantages of sol-gel processing, high homogeneity even at a molecular level, is lost in the processing.

In this chapter a quantitative evaluation of the degree of heterogeneity in the powders is documented. After reviewing the factors that affect the homogeneity of multicomponent gels, particularly in the system  $\text{CaO-P}_2\text{O}_5\text{-SiO}_2$ , alternative procedures for producing glasses in this system are developed and the resulting improvement in homogeneity is described.

## 2.2 Homogeneity of Multicomponent Gels

The sol-gel process can be divided into three main stages (Muk84):

Stage 1: gel preparation stage. At this stage, reactants are allowed to react and polymerize in the presence of a solvent to produce a sol that subsequently transforms into a wet gel at the gel point.

Stage 2: postgelation stage. This stage, beginning after the gel point is reached, includes all phenomena occurring with gels undergoing thermal treatment before the gel-to-glass transformation: aging; evaporation of solvent, water, and volatiles; structural and microstructural changes; and dehydroxylation.

Stage 3: sintering and/or fusion stage. At this stage the gel-to-glass transformation occurs either by sintering or by melting at high temperatures.

High homogeneity can be inherited in a multicomponent gel derived glass if the gel-to-glass conversion can be



accomplished without considerably changing the cation distribution achieved at the gel stage (Muk84). Thus the homogeneity is basically defined by stages 1 and 2 of the processing.

### 2.2.1 Gel Preparation Stage

At the gel preparation stage the degree of homogeneity of a multicomponent gel is strongly influenced by various processing parameters: 1) nature, structure and chemical reactivities of reactants; 2) nature of solvents and solubility of reactants in solvent; 3) concentration of water and sequence of addition; 4) pH of the reaction medium; 4) time and temperature of reactions.

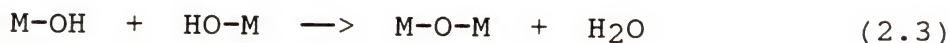
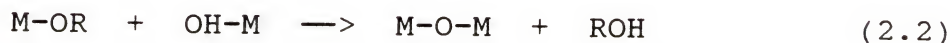
#### Nature, structure and chemical reactivities of reactants

When preparing multicomponent gels, two kinds of precursors can be used: metal alkoxides and inorganic or organic salts (Joh85, Gug88). The reactivity of a precursor not only depends on its chemical nature but also on the applied reaction conditions.

Metal alkoxides provide a convenient source of inorganic monomers that in most cases are soluble in common solvents. When mixed with water the liquid alkoxide precursor undergoes hydrolysis reaction, as schematically represented below:



Once hydroxides are formed a condensation reaction can occur leading to the formation of hydroxides or hydrated oxides:



Reactions (2.1) to (2.3) may simultaneously occur so that it is impossible to describe the process by separate and independent hydrolysis and condensation reactions.

The rate of the metal alkoxide reaction with water can greatly affect the homogeneity of a gel. If one component hydrolyzes much more rapidly than the others, the polymerized clusters of that component can form and the chemical homogeneity attained in the solution is lost.

Heterogeneities due to different hydrolysis rates can be avoided in several ways:

(1) The component alkoxides can be partially prehydrolyzed and subsequently mixed (Tho74, Yol79). In this process alkoxides are added in the reverse order of their respective reactivities. The idea is that the newly added, unhydrolyzed alkoxides, will condense with partially hydrolyzed sites on the polymeric species formed by the preceding hydrolysis steps.

(2) Use of alkoxides with similar rates of hydrolysis. The hydrolysis rate depends not only on the metal cation but

also on the type of alkoxy group involved. Aelion showed that for silicon alkoxides the rate of hydrolysis decreases with increasing size of the alkyl groups (Ael50).

(3) The solution can be slowly hydrolyzed by restricting the availability of water, generally by use of atmospheric water vapor as the only water source (Hay80, Agr90).

(4) Control of hydrolysis rates of highly reactive alkoxides by using chelating organic ligands such as glycols, organic acids or  $\beta$ -diketones (Gug88).

Gels in the system  $\text{CaO-SiO}_2$  were produced by mixing calcium ethoxide and tetraethylorthosilicate (TEOS) and subsequently hydrolyzing the mixture with the addition of water (Hay80). Since calcium ethoxide hydrolyzes much faster than TEOS this method resulted in preferential precipitation of the hydrolyzed product, i.e.,  $\text{Ca(OH)}_2$ , during hydrolysis and therefore inhomogeneities occurred. When the alkoxide mixture was hydrolyzed by atmospheric moisture, a better homogeneity was observed for the final glass. In the system  $\text{P}_2\text{O}_5\text{-SiO}_2$ , NMR studies of sols prepared using TEOS and triethylphosphate show that the hydrolysis of the phosphorous alkoxide is much slower than the hydrolysis of the silicon alkoxide (Tia88). The reaction was carried out at pH 2.

Besides alkoxides, other compounds may be used to introduce cations in multicomponent oxide systems (Joh85, Gug88). If alkoxides are used for those components that form

the network of the gel, then other soluble metal salts can be used to introduce the modifier ions. The reasons for this choice are limited solubility in alcohol of some alkoxides, lower cost of inorganic salts, lack of commercial availability of some chemicals and difficulty of laboratory preparation of some alkoxides.

The most frequently used nonalkoxide precursors are inorganic and organic salts. In the systems  $\text{CaO-SiO}_2$  and  $\text{CaO-P}_2\text{O}_5\text{-SiO}_2$  calcium has been introduced both as calcium nitrate (Hay80, Li91b) and calcium acetate (Var87). Heterogeneity occurred when calcium nitrate was used (Hay80). Metal salts have been used also to introduce sodium and barium (Vil88, Tre88, Bri81). Generally, the only evaluation of the homogeneity of a system by most authors was the formation of precipitates from the solution versus formation of a clear transparent gel.

There are two main reasons for the heterogeneity observed when soluble salts are used in the gel preparation:

(1) Migration of ions during drying (Joh85). The liquid migrates to the surface by capillary action during drying. In doing so, soluble ions are carried to the surface leaving a gradient of composition in the dried body.

2) Tendency for crystallization during drying of the gel when using nitrates. Nitrate crystallization implies lost homogeneity and even after decomposition by thermal treatment alkaline or alkaline earth ions may remain heterogeneously distributed in the system. Calcium nitrate



was used to prepare gels in the systems  $\text{CaO-Al}_2\text{O}_3\text{-SiO}_2$  (Pan84),  $\text{CaO-SiO}_2$  (Hay80) and  $\text{CaO-P}_2\text{O}_5\text{-SiO}_2$  (Li91a). In all cases calcium nitrate formed in the gel and decomposed between 500 and 600°C.

#### Nature of solvents and solubility of reactants in the solvent

A general requirement for sol-gel processing is that precursors have to be soluble in the reaction media. Liquid-liquid immiscibility will lead to heterogeneities in the gel (Pra84). Calcium methoxide and calcium ethoxide are only slightly soluble in their parent alcohols (Pan84).

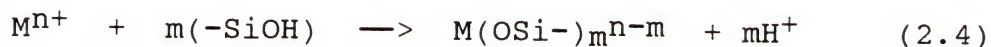
#### Concentration of water and sequence of addition

In multicomponent systems the amount ( $R$ =moles water/moles alkoxide) and sequence of addition of water can affect the homogeneity of the gels due to different hydrolysis rates for the different alkoxide components (Bri90). As discussed before, two means of controlling homogeneity are a very low hydrolysis rate, achieved by restricting the availability of water, or prehydrolysis of the slower reacting components with a later addition of the faster hydrolyzing component.

pH of the reaction medium

The effects of pH and different acid or base catalysts on the hydrolysis and condensation rates and final structure of the gel has been extensively studied for silicon alkoxides (Bri90). However, for multicomponent systems there are few systematic studies.

When soluble ions are present in the reacting solution pH can be an important factor. It is well known (Dug64) that the silanol group ( $-\text{SiOH}$ ) of the hydrated silica gel surface is weakly acidic, and therefore when the gel is mixed with an aqueous electrolyte some cation exchange is possible:



where M is the metal ion. The reaction is reversible in acidic solutions, but in alkaline solutions it appears to proceed towards the right. Therefore, low pH will not favor the incorporation of soluble alkali or alkaline earth ions within the silica gel network as it forms. Migration of ions and precipitation can occur during subsequent drying stages, which leads to heterogeneities.

On the other hand, the solubility of many compounds depends on pH. In solutions where calcium ions are present, high pH values can lead to precipitation of  $\text{Ca}(\text{OH})_2$  from the solution (Bae86). In the presence of phosphorous, calcium

phosphate compounds can also precipitate at high pH values (Bro81).

### 2.2.2 Postgelation Stage

In general it can be considered that the homogeneity derived at the gel stage determines the homogeneity of the final glass (Muk84). The changes occurring during the postgelation stage are not expected to change the homogeneity achieved by stirring. There is, however, one case where the cation distribution can be altered during the drying step. When soluble salts are used as precursors in sol-gel processing, soluble ions may remain in the liquid phase after gelation. As discussed earlier, migration of those ions to the surface and precipitation during drying lead to inhomogeneity in the dried gels.

One way of trying to increase the homogeneity in this case would be by inducing the introduction of the soluble cations into the network through pH control, as discussed before. Also the heterogeneity caused by the migration of soluble ions could be reduced by use of a very slow drying rate. As the liquid migrates by capillary action and evaporates at the surface, a gradient of soluble ions is created in the liquid phase. This gradient would cause a diffusion of ions in the opposite direction. If the evaporation is done at a sufficiently slow rate, sufficient time would elapse for the diffusion to occur, thereby

eliminating the concentration gradient. However, in both cases the source of potential heterogeneity in the system is not being eliminated. The modifications suggested are only minimizing its effect.

Based on the above analysis of the sources of heterogeneity in multicomponent gels, two approaches were taken to improve the homogeneity of  $\text{CaO-P}_2\text{O}_5\text{-SiO}_2$  gel derived bioactive glass powders.

(1) Use of calcium nitrate as  $\text{CaO}$  precursor. The degree of homogeneity of glass powders produced with the procedure developed by Li (Li91a) was determined. The change in homogeneity achieved by varying the rate of drying of the gels was established. Also, a different procedure was used in which the pH of the condensation step was changed.

(2) Use of calcium alkoxide as a source of  $\text{CaO}$ , which required development of an alternative procedure of gel processing.

## 2.3 Experimental Procedures

### 2.3.1 Materials

Tetraethyl orthosilicate (TEOS - Fisher Scientific, Pittsburgh, PA) and Triethylphosphate (TEP - Aldrich, Milwaukee, WI) were used as precursors for  $\text{SiO}_2$  and  $\text{P}_2\text{O}_5$  respectively. Calcium was introduced either as calcium nitrate or calcium methoxyethoxide 20% solution in



methoxyethanol (GELEST Inc., Tullytown, PA). Nitric acid or ammonia hydroxide were used to control the solution pH and ethanol was used as the solvent. All reactants were reagent grade.

### 2.3.2 Gel Preparation

Three compositions presented in Table 2.1 were investigated.

When using calcium nitrate, two methods for sol preparation were used. The first was the same procedure described by Li (Li91a) which is designated as "reference procedure (R)". The second calcium nitrate method is a modification of the reference procedure in which the hydrolysis step is carried out at a fixed pH and then modified for the condensation step by addition of either acid or base to vary the pH.

In the reference procedure, a certain amount of TEOS, which depends on the gel composition, water and nitric acid were mixed, under magnetic stirring, in a covered glass beaker. The amount of water used was that to give a molar ratio of water to alkoxides of  $R=8$ . The solution was immiscible at the beginning, but soon became clear. After an hour the TEP was added to the solution. Calcium nitrate was added after another hour of mixing. The solution was stirred for an additional hour, and then maintained quiet for half an hour. The resultant clear sol was cast in polyethylene

Table 2.1  
Nominal Compositions of Gel-Glasses  
(in mole %).

Sample	SiO <sub>2</sub>	CaO	P <sub>2</sub> O <sub>5</sub>
S60	60	36	4
S70	70	26	4
S80	80	16	4

containers and placed inside an oven, where the sol gelled and aged.

In the second method TEP, the slowest hydrolyzing alkoxide (Tia88), was hydrolyzed with addition of deionized water. The water to alkoxide molar ratio used was  $R=4$  and the pH of the solution was adjusted with nitric acid to  $pH=2$ . After stirring overnight TEOS was added and also hydrolyzed ( $R=4$ ,  $pH=2$ ). Calcium nitrate was added after one hour and the solution stirred for another hour. At this stage the final pH was adjusted with dropwise addition of a solution of water (enough to increase the water to alkoxide molar ratio to  $R=8$ ), ethanol and either  $HNO_3$  or  $NH_4OH$ , depending on the final pH desired. The use of a diluted solution was necessary because precipitation occurred upon addition of stronger basic solutions. There was a limitation on the highest pH attainable with this method since condensation rates increase strongly with pH. Gelation occurred instantly when a pH of about 5 was reached. A clear solution was obtained for pH values up to 4.3. The solution was cast in polyethylene containers and gelled at ambient temperature. Gelation time varied between 8 days to 2 hours for pH 1.6 to 4.3 respectively.

Two procedures were also used when the calcium alkoxide was used as the calcium precursor. In the first, all the alkoxides were mixed and stirred for two hours. The solution was cast in plastic containers and slowly hydrolyzed by using atmospheric water vapor. To maintain a better humidity

control the containers were put in a desiccator containing water and maintained at 25°C. A transparent light brown gel formed within 3 days. The gels were maintained in the desiccator for 4 more days to allow hydrolysis to proceed.

In the second procedure, TEP and TEOS were partially prehydrolyzed by adding water, and calcium methoxyethoxide was subsequently added. Several molar ratios of water to alkoxides were tried but for  $R > 2$  precipitation occurred when the calcium alkoxide was added. Also, if water was added after the addition of calcium alkoxide, precipitation occurred for any  $R$  value used in the prehydrolysis. The only viable way of obtaining a clear solution was a prehydrolysis of TEOS and TEP with low water ratio,  $R=1$ , subsequent addition of calcium alkoxide and completion of hydrolysis with atmospheric moisture. A transparent light-brown gel was formed within 3 days.

### 2.3.3 Postgelation Treatment

The calcium nitrate derived gels were aged at 60°C for 24 hours and dried according to the heating schedules presented in Figure 2.1. "A" is the drying schedule used in the reference procedure. "B" is the drying schedule used as a modification in the reference procedure. The calcium nitrate derived gels produced with different condensation pH values were also dried according to schedule B. The calcium alkoxide derived gels were also aged at 60°C for 24 hours



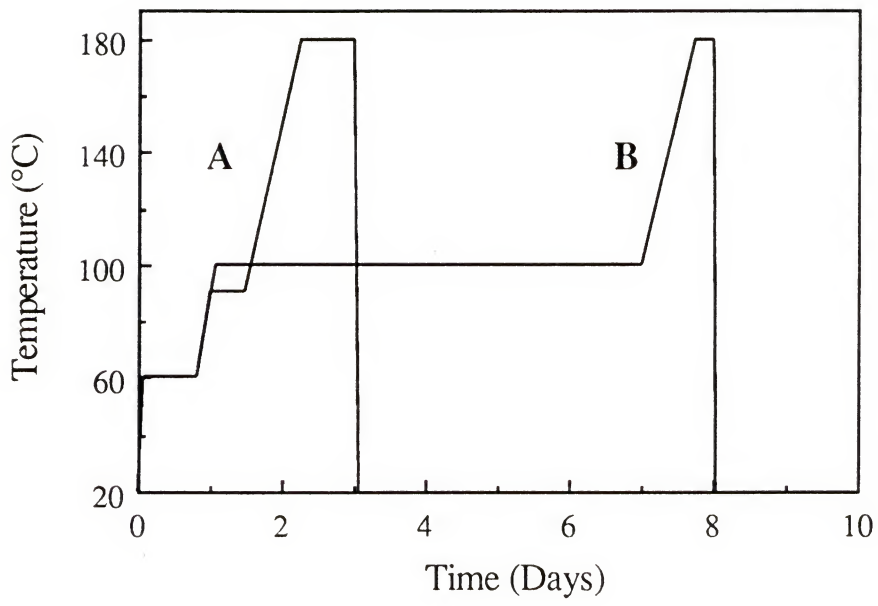


Figure 2.1 Drying schedules of gels.

and dried according to schedule A in Figure 2.1. The dried gels were subsequently treated at 700°C.

#### 2.3.4 Homogeneity Measurement

The homogeneity of the gel derived glasses was evaluated by electron microprobe analysis (EMP) and FTIR. Particles in the size range 500-710  $\mu\text{m}$  were embedded in acrylic resin, ground and polished with diamond paste prior to EMP analysis. Ten particles in three samples were analyzed for each composition. The electron beam spot size used in the analysis was 10  $\mu\text{m}$ . The ratio of the intensity parameter  $k$  measured for calcium and silicon was calculated:

$$r_k = \frac{K_{\text{Ca}}}{K_{\text{Si}}} \quad (2.5)$$

The standard deviation of this ratio ( $\text{SD}r_k$ ) was taken as a measurement of the degree of heterogeneity of the sample. To compare samples of different composition, and therefore with different  $r_k$ , results were normalized as:

$$\text{Heterogeneity Level (HL\%)} = \frac{\text{SD}r_k}{\text{mean } r_k} \times 100 \quad (2.6)$$

## 2.4 Results and Discussion

### 2.4.1 Gel Derived Glasses Prepared with Calcium Nitrate

When the soluble metal salt was used to prepare the gel, the resulting glasses had an appearance that varied from opaque white for the higher calcium concentration (36 mole %) to a translucent powder for the lower concentration (16 mole %).

Figure 2.2 presents the heterogeneity level determined through the EMP results for the three reference samples (S60R, S70R, S80R). Relative standard deviations of the  $r_k$  parameter of up to 35% were observed indicating a large heterogeneity in the calcium distribution. The first modification introduced in the above procedure was use of a slower drying rate (schedule B in Figure 2.1). The results are compared in Figure 2.2. No significant improvement was observed in the homogeneity, although a slight decrease in % HL was obtained for composition S70. Thus, the slow drying schedule was used in other experiments designed to improve further the homogeneity of the S70 composition.

The results obtained when the condensation reaction of the calcium nitrate based gels was carried out at different pH values are presented in Figure 2.3 for composition S70. The level of heterogeneity obtained was comparable to that of samples without an increase in pH. For the pH values used

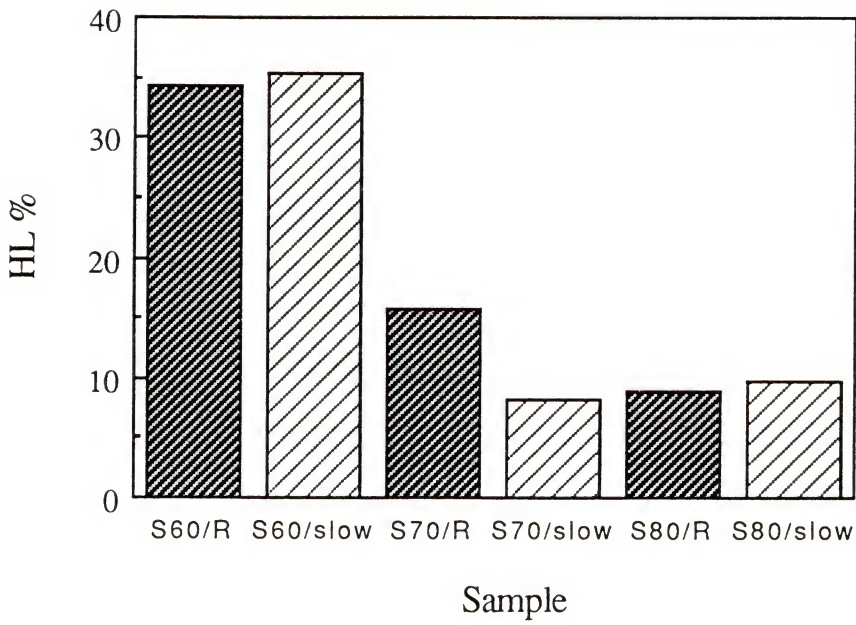


Figure 2.2 Heterogeneity level (HL) of calcium nitrate derived gels, reference procedure (R) and slow drying rate.



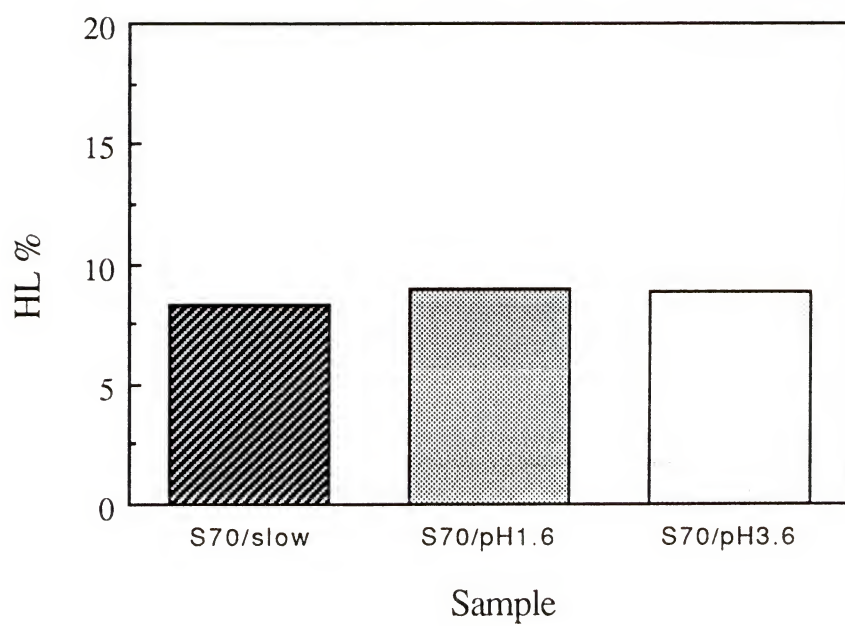


Figure 2.3 Heterogeneity level (HL) of calcium nitrate derived gels, varying condensation pH.

there was no significant improvement in the incorporation of calcium by the silicate structure during network formation. A basic pH may introduce significant changes but with the two-step procedure it is not possible to increase the pH of the condensation step above pH 5 without precipitation occurring.

Figure 2.4 illustrates the DTA curves obtained for composition S70 produced with the reference procedure and the procedure modified by higher pH and slower drying. In both cases an endothermic peak is observed at 570°C due to decomposition of calcium nitrate formed during drying of the gels (pure  $\text{Ca}(\text{NO}_3)_2$  decomposes at 561°C). It shows that the modifications introduced did not avoid the crystallization of calcium nitrate responsible for the poor homogeneity of the gel.

#### 2.4.2 Gel Derived Glasses Prepared with Calcium Alkoxide

Hydrolysis of the alkoxides with addition of water resulted in agglomeration. The calcium alkoxide hydrolyzes much faster than silicon alkoxide and preferential precipitation of the hydrolyzed product,  $\text{Ca}(\text{OH})_2$ , occurs leading to agglomeration.

Hydrolysis with moisture in the atmosphere resulted in transparent clear glasses for all three compositions tested. Even monolithic samples were obtained when a careful drying procedure was used. A Teflon<sup>®</sup> container with a very small

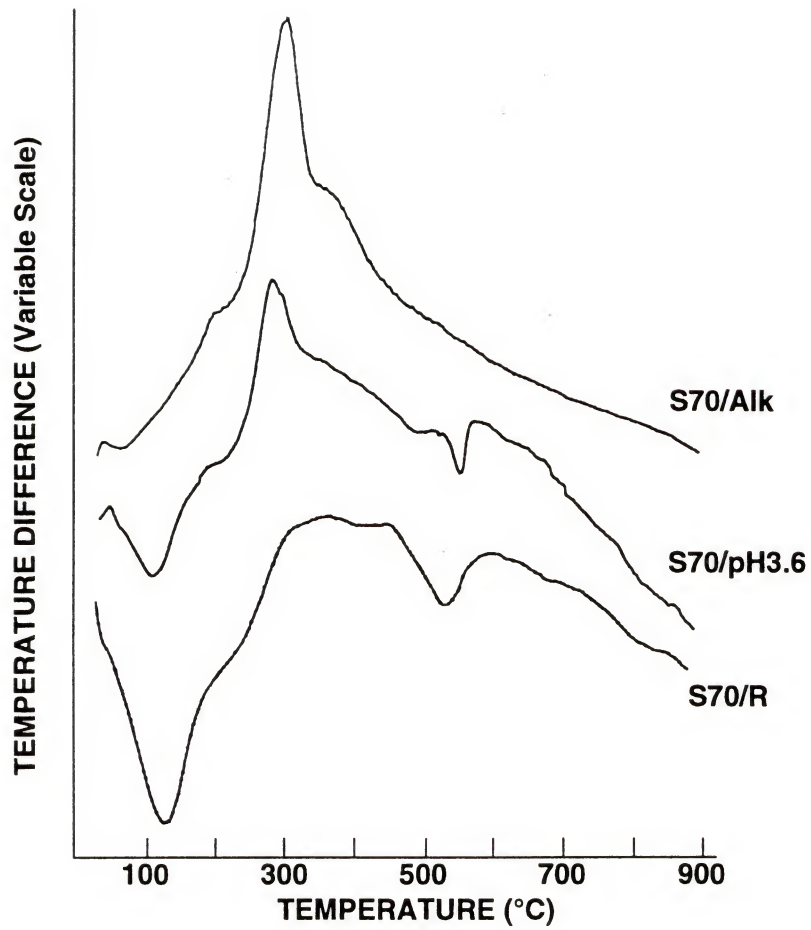


Figure 2.4 DTA curves for calcium nitrate and calcium alkoxide derived gels.

opening was used in this case. Figure 2.5 shows samples obtained by this procedure as well as samples produced when calcium nitrate was used as precursor. A prehydrolysis of TEOS and TEP with lower water ratio ( $R=1$ ) was possible but the hydrolysis was also only successfully completed with slow moisture adsorption.

The EMP heterogeneity level for samples obtained with the calcium alkoxide procedure are presented in Figure 2.6. The heterogeneity level is very low, ~1% or less, for all the compositions, indicating a very homogeneous distribution of calcium ions. The DTA analysis, illustrated by the top curve in Figure 2.4 for the composition S70, indicates that no reactions occur above 500°C for the alkoxide based gel.

FTIR analysis of randomly selected samples of the S60 calcium alkoxide derived gel-glass, following the 700°C thermal treatment, is given in Figure 2.7. The results show that the variability in Si-O-Ca vibrational modes characteristic of the calcium nitrate process (Figure 1.1) has been eliminated. Equivalent results were obtained for the S70 and S80 compositions.

A quantitative measure of bioactivity is the rate of formation of a hydroxy carbonate apatite (HCA) layer on a bioactive glass in a simulated body fluid (SBF) (Oht92, Fil93). Figure 2.8 shows the FTIR spectra of three samples of bioactive gel-glass S60 prepared by the new calcium alkoxide process following an in-vitro test. Samples were suspended in a SBF solution with the composition presented in



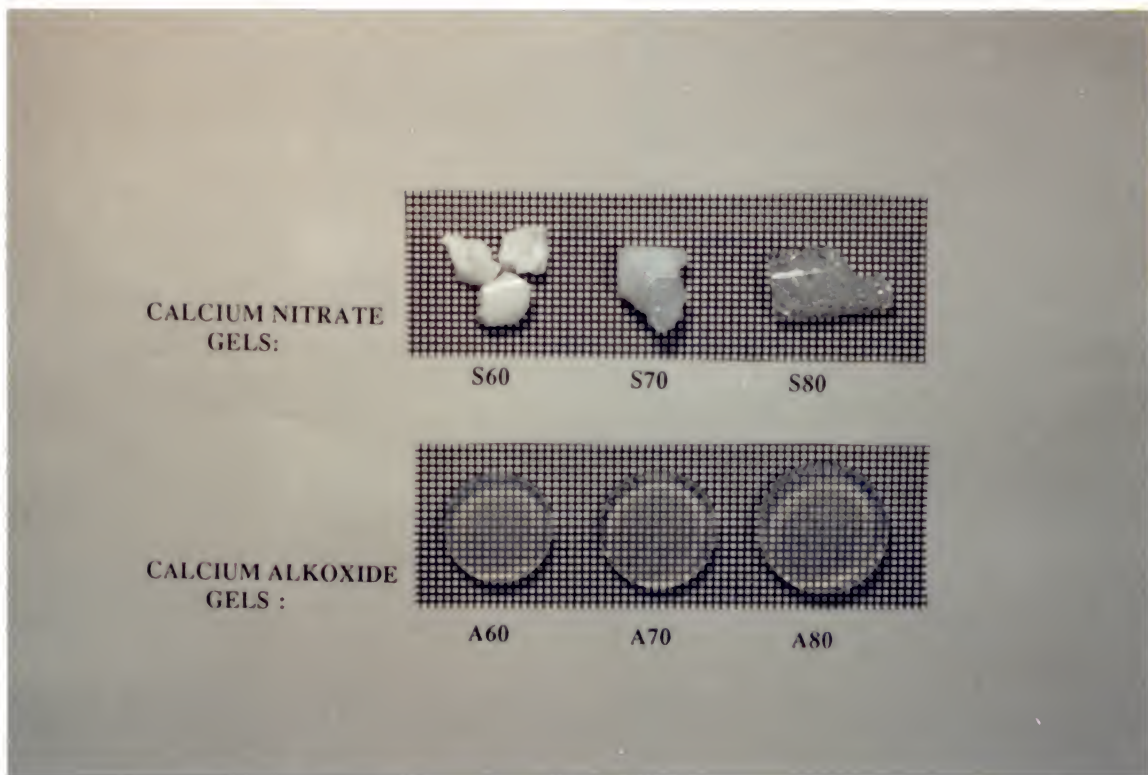


Figure 2.5 Calcium nitrate and calcium alkoxide derived gel-glasses.

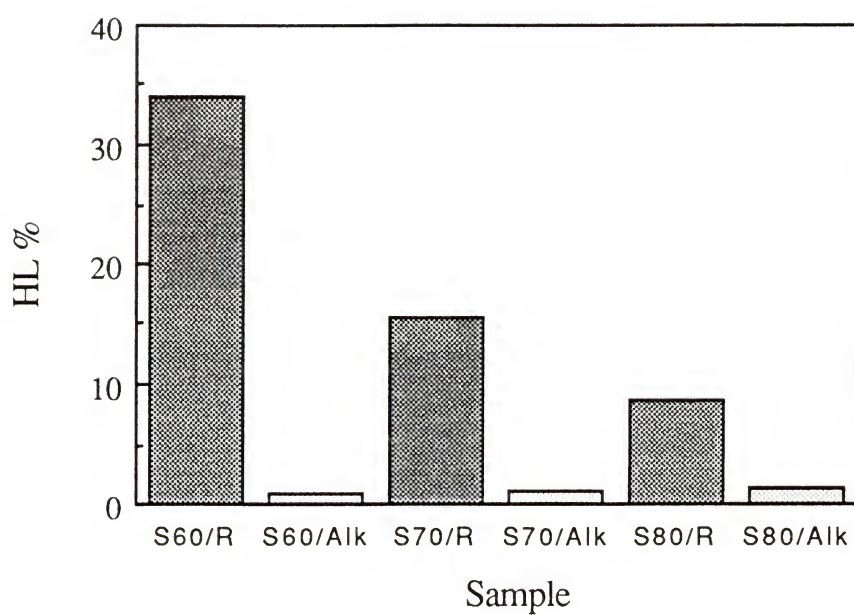


Figure 2.6 Heterogeneity level (HL) of calcium alkoxide derived gels.

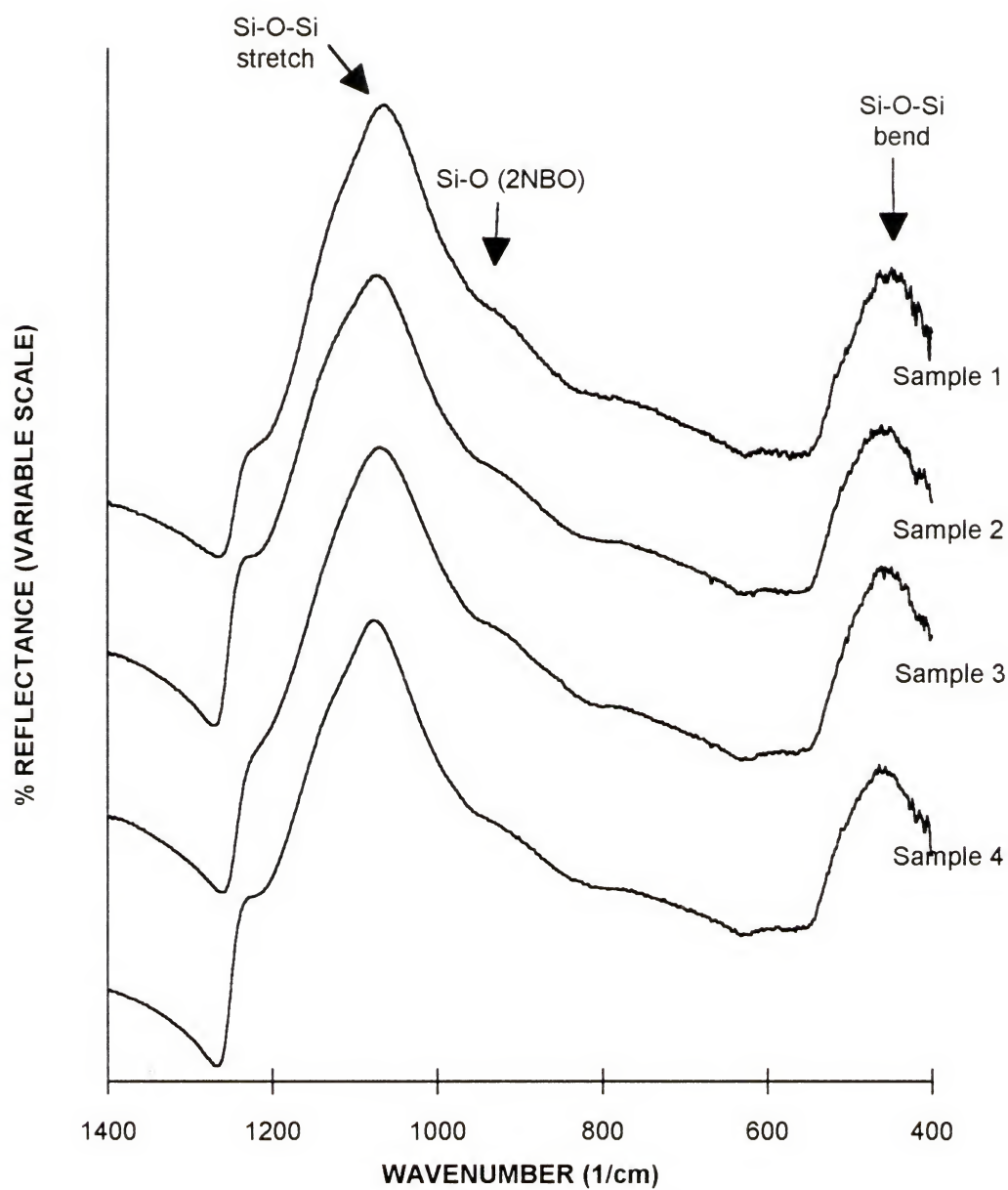


Figure 2.7 FTIR spectra of four randomly selected samples of S60 calcium alkoxide derived gel-glasses.

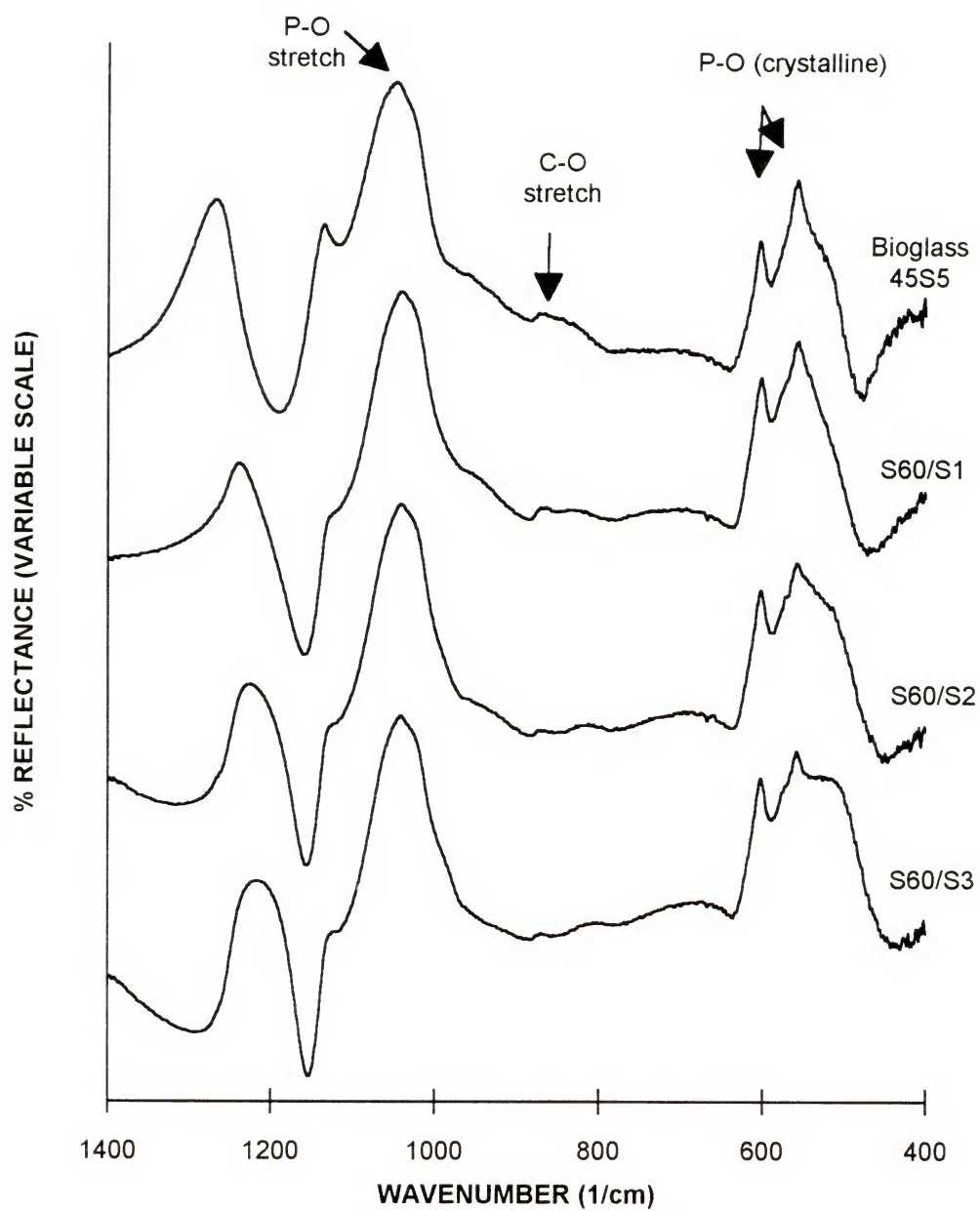


Figure 2.8 FTIR spectra of three samples of S60 calcium alkoxide derived gel-glasses and of 45S5 melt derived glass after reaction in SBF for 20hours.



Table 2.2 and pH 7.25 and maintained at 37°C for 20 hours. All three samples show nearly identical vibrational modes at 1042, 602, and 558  $\text{cm}^{-1}$  corresponding to the P-O stretching and bending modes of the crystalline hydroxy carbonate apatite (Fow74, LeG78).

The HCA layer obtained on the three component  $\text{CaO-P}_2\text{O}_5\text{-SiO}_2$  alkoxide derived glasses is equivalent to the HCA formed on four component  $\text{Na}_2\text{O-CaO-P}_2\text{O}_5\text{-SiO}_2$  melt derived glasses approved by the U.S. Food and Drug Administration for use as human implants. These results show a high level of bioactivity for the alkoxide derived glasses since there is a direct correlation between the in vivo behavior of bioactive glasses and its ability to form a HCA layer in an in-vitro test (Ogi80, Hen91b, Kok87).

## 2.5 Conclusions

1) Sol-gel derived powders in the  $\text{CaO-P}_2\text{O}_5\text{-SiO}_2$  system, obtained when using calcium nitrate as precursor, are heterogeneous in terms of calcium distribution. Decreasing the drying rate or altering the condensation pH up to 4.6 did not change the heterogeneity level significantly.

2) By use of all alkoxide precursors, monolithic, transparent gel-glasses can be obtained in the  $\text{CaO-P}_2\text{O}_5\text{-SiO}_2$  system with a low heterogeneity level of about 1%. A slow hydrolysis rate using atmospheric water is necessary.

Table 2.2  
Ion Concentration (mM) of SBF and Human Blood Plasma.

	$\text{Na}^+$	$\text{K}^+$	$\text{Mg}^{2+}$	$\text{Ca}^{2+}$	$\text{Cl}^-$	$\text{HCO}_3^-$	$\text{HPO}_4^{2-}$	$\text{SO}_4^{2-}$
SBF	142	5.0	1.5	2.5	147.8	4.2	1.0	0.5
Blood Plasma	142	5.0	1.5	2.5	103.0	27.0	1.0	0.5

3) The three component  $\text{CaO-P}_2\text{O}_5\text{-SiO}_2$  alkoxide derived gel-glasses all show a high level of bioactivity and develop a hydroxy carbonate apatite layer equivalent to four component  $\text{Na}_2\text{O-CaO-P}_2\text{O}_5\text{-SiO}_2$  melt derived glasses approved by U.S. Food and Drug Administration for use as human implants.

CHAPTER 3  
CALCIUM PHOSPHATE FORMATION ON  
SOL-GEL DERIVED BIOACTIVE GLASSES IN VITRO

3.1 Introduction

An alternative sol-gel method to produce  $\text{CaO-P}_2\text{O}_5\text{-SiO}_2$  three component glasses using all alkoxide components in the gel synthesis was described in the previous chapter. The resultant glasses present a much higher homogeneity than calcium nitrate derived gel-glasses. The all-alkoxide process also makes possible the production of monolithic samples not attainable with the previous method. It was also shown that the glasses form a hydroxyapatite layer when soaked in a SBF solution for 20 hours, indicating that the glasses are bioactive.

In the present chapter a more detailed characterization of the three component, all-alkoxide, sol-gel derived glasses and the in vitro formation of calcium phosphate at the surface of the glasses in the bulk and powder form is studied. The rate of HCA formation in two solutions, Tris Buffer and Simulated Body Fluid (SBF), is compared. A comparison with melt derived glasses is also presented.



### 3.2 Experimental Procedures

#### 3.2.1 Materials Preparation

Three glasses with the nominal compositions presented in Table 2.1 (Chapter I) were studied. The samples were prepared from tetraethylorthosilicate, triethylphosphate and calcium methoxyethoxide. After mixing the alkoxide components the sol was cast into polyethylene containers, loosely covered and placed inside a desiccator containing water. Hydrolysis of the alkoxides occurred with moisture from the ambient atmosphere and gelation occurred within three days. The gel was aged at 60°C and dried with a schedule ending at 180°C. The dried gels were heated in air at 700°C. The drying and partial densification schedules are presented in Figures 3.1 and 3.2.

The monolithic gel-glasses obtained were cut and used as bulk specimens for the in vitro bioactivity tests. Powders were prepared by grinding and sieving to a particle size range 90-710  $\mu\text{m}$ .

#### 3.2.2 Characterization Measurements

Thermogravimetric Analysis (TGA) and Differential Thermal Analysis (DTA) were conducted on dried gel powders by using a Dupont 951 thermogravimetric analyzer and 910 differential scanning calorimetric unit equipped with a

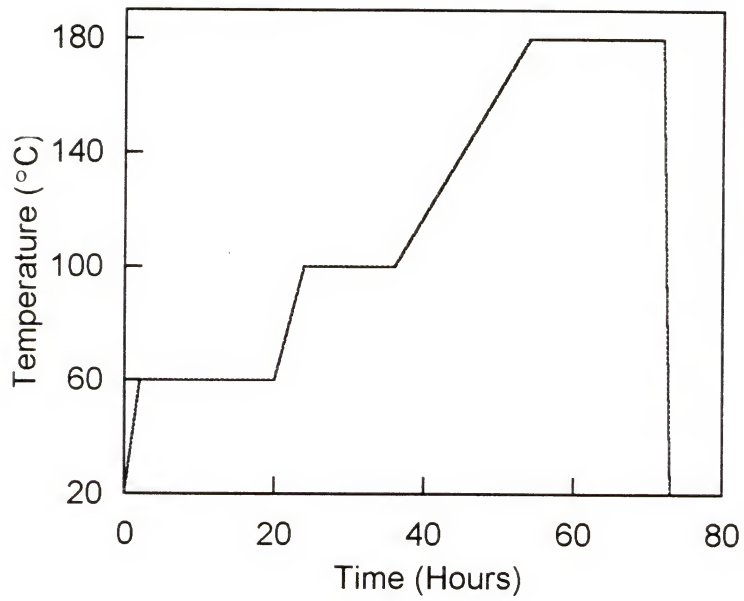


Figure 3.1 Drying schedule for calcium alkoxide derived gels.

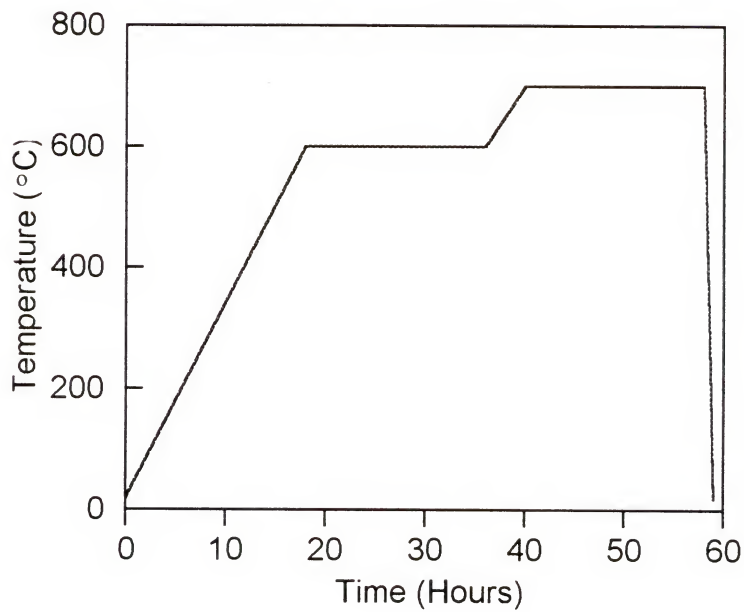


Figure 3.2 Partial densification schedule for calcium alkoxide derived gels.

differential thermal analyzer cell. The atmosphere was ambient air and the heating rate was 5°C/min.

The textural features (surface area, pore volume and pore radius) of the sol-gel derived glasses were measured with an automatic gas adsorption instrument, a Quantachrome Model Autosorb-6, using nitrogen gas as adsorbate. The structure was characterized by Fourier Transform Infrared Reflection Spectroscopy (FTIR) and by x-ray diffraction (XRD). A diffuse reflectance stage was used in the FTIR spectrometer Nicolet 20XB. The XRD range was from 5 to 85 degrees at a rate of 2°/min, using Cu-K radiation and operated at 40KV. Textural and structural characteristics were measured on gel-glasses treated at 700°C.

### 3.2.3 In Vitro Testing

Previous studies indicate that there is a direct correlation between the in vitro formation of a HCA layer on the glass surface and its ability to bond to bone (Ogi80, Kok87). Therefore, the rate of HCA formation was measured on monolithic samples of the three compositions after soaking in two solutions, Tris Buffer and Simulated Body Fluid (SBF), both used in the past to evaluate level of bioactivity. The SBF solution was prepared by dissolving reagent grade sodium chloride, sodium bicarbonate, potassium chloride, dibasic potassium phosphate, magnesium chloride, calcium chloride, and sodium sulfate in deionized water.

Both SBF and Tris Buffer solutions were buffered at pH 7.25 with hydrochloric acid and Tris hydroxymethyl aminomethane (THAM). The ion concentration of SBF is presented in Table 2.2 (Chapter II).

Samples were suspended in the solutions at 37°C by a nylon string. The ratio of geometric surface area (SA) to solution volume (V) was fixed at  $0.1 \text{ cm}^{-1}$  which corresponded to a ratio of weight to solution volume of  $0.012 \pm 0.002 \text{ g/cm}^3$ . Three samples were suspended for each condition. After soaking for various periods of time the specimens were removed from solution and dried in air.

The bioactivity kinetic study was performed using bulk samples since the tests are faster to perform and less affected by test variables (War89). For quality assurance (QA) purposes a one time bioactivity test was performed on powder samples as well. The test conditions used were similar to the QA test procedure developed for melt derived powders. Powders were dipped directly into a SBF solution in a glass container, which was mounted in an incubator shaker, with both speed and temperature control. The ratio of weight to solution volume was fixed at  $0.002 \text{ g/cm}^3$ . The temperature was maintained at 37°C and the speed of circular motion was kept at 175 rpm. This dynamic QA test procedure allows the solution to surround and react with powders continuously and uniformly.

The reacted surfaces were analyzed by FTIRS over the range of 400 to  $1400 \text{ cm}^{-1}$  and the solutions were analyzed



before and after reaction by Inductively Coupled Plasma (ICP) emission spectroscopy.

### 3.3 Results

#### 3.3.1 Characteristic Features of the Gel-Glasses

The three component  $\text{CaO-P}_2\text{O}_5\text{-SiO}_2$  sol-gel derived glasses produced with all alkoxide components and slowly hydrolyzed by atmospheric water were transparent homogeneous monolithic samples. They were light-brown after drying and clear after partial densification at  $700^\circ\text{C}$ .

Figure 3.3 shows the DTA and TGA curves for the S60 gel after drying at  $180^\circ\text{C}$ . The dried gel still contains a small amount of liquid which is usually a mixture of water, both physically and chemically adsorbed, and residual alcohol. The endothermic peak and the weight decrease observed in the temperature range  $80\text{--}120^\circ\text{C}$  corresponds to the evaporation of this liquid. A large exothermic peak is present in the DTA in the temperature range  $180\text{--}350^\circ\text{C}$  and corresponds to a large decrease in weight shown in the TGA curve. This peak was also observed for  $\text{CaO-SiO}_2$  gels produced from TEOS and calcium ethoxide (Joh85, Din90). It results probably from the oxidation of residual organic compounds present in the gel. The sol-gel preparation method used in this work, in which the hydrolysis conditions are not very severe, is likely to result in incomplete

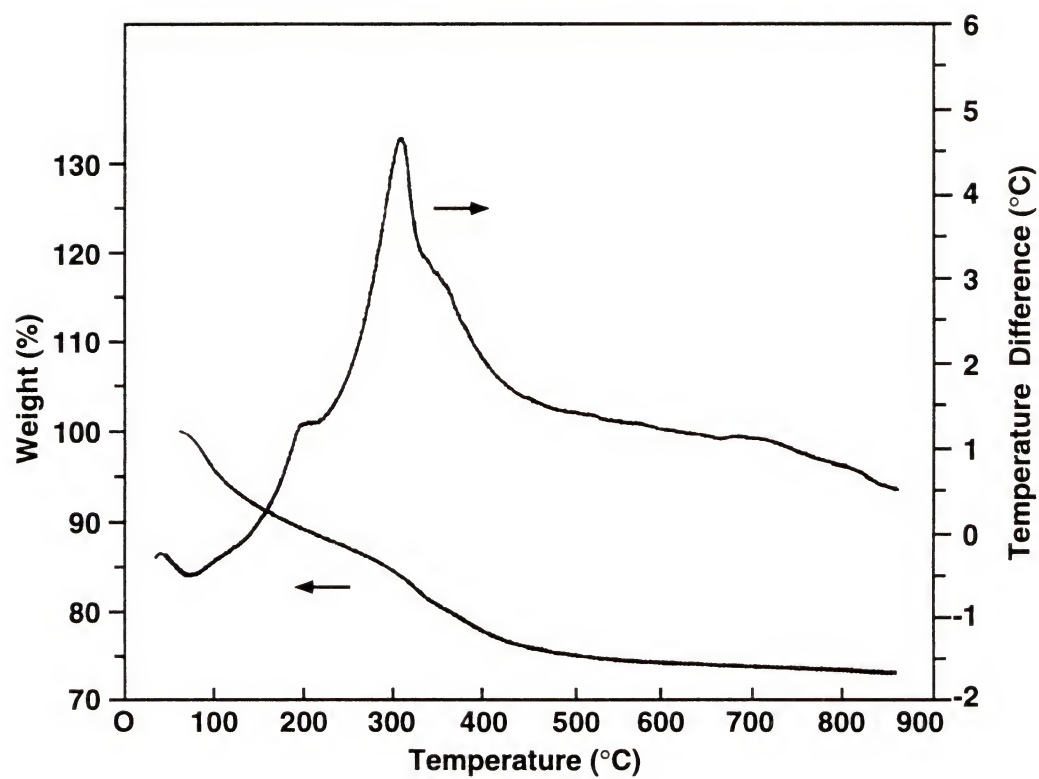


Figure 3.3 DTA and TGA curves for gel S60.

hydrolysis of the alkoxides, especially slowly hydrolyzing alkoxides such as triethylphosphate. The presence of residual organic compounds in the gels is also indicated by their light-brown coloration in the dried state, which disappears after a high temperature treatment. No other reactions are observed up to 900°C and the weight loss stabilizes at around 600°C.

The XRD spectra for the gel-glasses is presented in Figure 3.4. No diffraction lines are observed, only a broad peak characteristic of an amorphous silicate solid. The diffuse reflectance spectra are presented in Figure 3.5. The FTIR spectra show peaks at 1202, 1095 and 482  $\text{cm}^{-1}$ . The most intense 1095  $\text{cm}^{-1}$  band and the 1202  $\text{cm}^{-1}$  band correspond to TO (transverse optical) and LO (longitudinal optical) modes of the asymmetric Si-O-Si stretching vibrations, respectively. The 482  $\text{cm}^{-1}$  band is assigned to a Si-O-Si bending vibration mode (Bel70, Gas70). Composition S60 presents a shoulder at about 900  $\text{cm}^{-1}$  related to the Si-O-Ca vibrational modes. When CaO is added and its content increased, it disrupts the silicate glass network and creates more non-bridging oxygen. As a result a peak around 900 $\text{cm}^{-1}$  due to Si-O stretching vibrations with two non-bridging oxygen starts to appear.

Table 3.1 presents the textural characteristics of the gel-glasses after heat treatment at 700°C for 18 hours. The total pore volume and the surface area increased as the silica content increased. The same trend was observed on

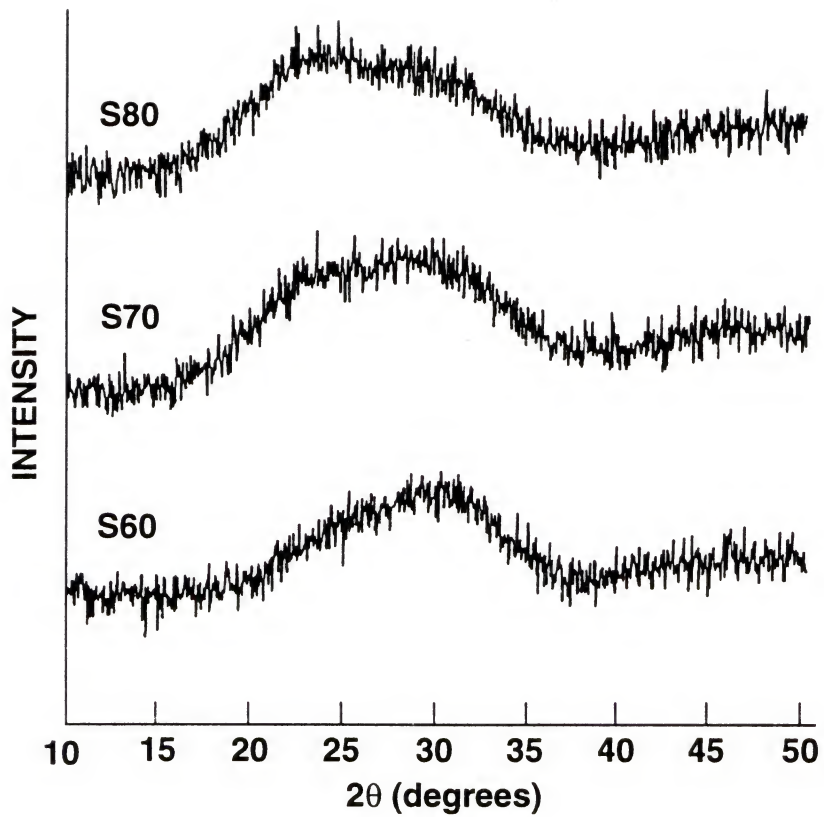


Figure 3.4 X-ray diffraction spectra for calcium alkoxide derived gel-glasses.



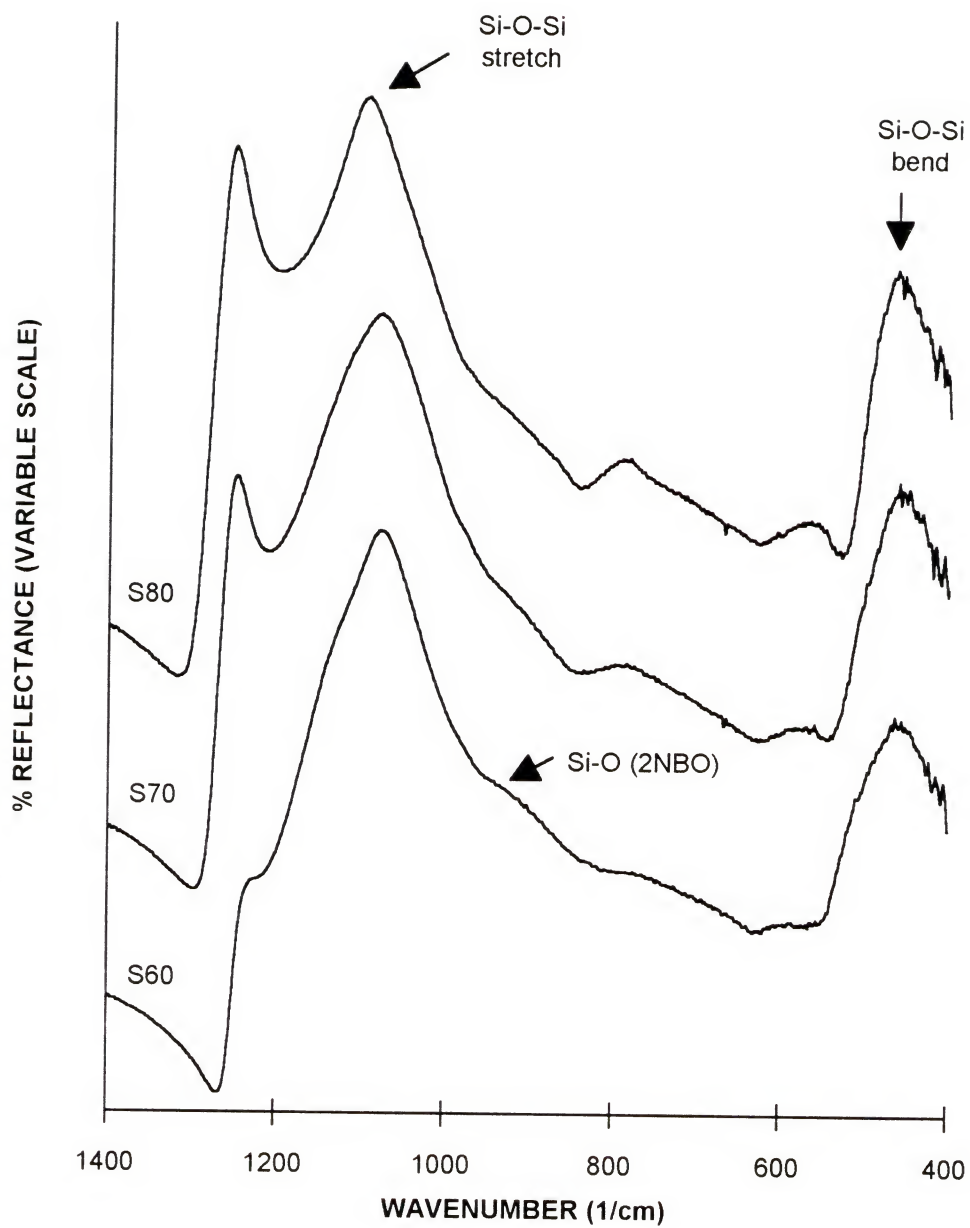


Figure 3.5 FTIR spectra of gel-glasses treated at 700°C.

bioactive gel-glasses produced with the calcium nitrate process (Li91a). The texture is very sensitive to gelation conditions. Lower pore volumes and diameters are obtained when the ambient conditions are changed to result in a lower hydrolysis rate. The textural characteristics for conditions in which gelation occurred in 5 days are presented in Table 3.2. Unfortunately, a more precise study of the textural variation with relative humidity was not possible, since a humidifying chamber with humidity and temperature control was not available.

### 3.3.2 In Vitro Calcium Phosphate Formation

Figures 3.6 and 3.7 show the diffuse reflectance spectra of the three compositions studied after in vitro reactions in Tris buffer and SBF for three periods of time. Only small differences are observed for the three gel-glass compositions studied. The peaks at 598 and 566  $\text{cm}^{-1}$  are assigned as P-O bending vibrations in the  $\text{PO}_4$  tetrahedra (Fow74, LeG78). These two peaks are characteristic of a hydroxy carbonate apatite (HCA) crystalline phase. In Tris Buffer the apatite peaks appear as early as 5 hours but the Si-O-Si bending peak is still present up to 360 hours (15 days) reaction. In SBF an amorphous calcium phosphate peak (at 600  $\text{cm}^{-1}$ ) is present in the early stages of reaction. Subsequent crystallization occurs and the HCA layer increases very rapidly as indicated by the elimination of

Table 3.1  
 BET Data for Bioactive Gel-Glasses.  
 Gelation Time = 3 days.

Sample	Surface Area (m <sup>2</sup> /g)	Pore Volume (cm <sup>3</sup> /g)	Pore Size (nm)
S60	286	0.44	3.0
S70	340	0.53	3.1
S80	423	0.63	3.0

Table 3.2  
 BET Data for Bioactive Gel-Glasses.  
 Gelation Time = 5 days.

Sample	Surface Area (m <sup>2</sup> /g)	Pore Volume (cm <sup>3</sup> /g)	Pore Size (nm)
S60	284	0.28	2.0
S70	325	0.27	1.6

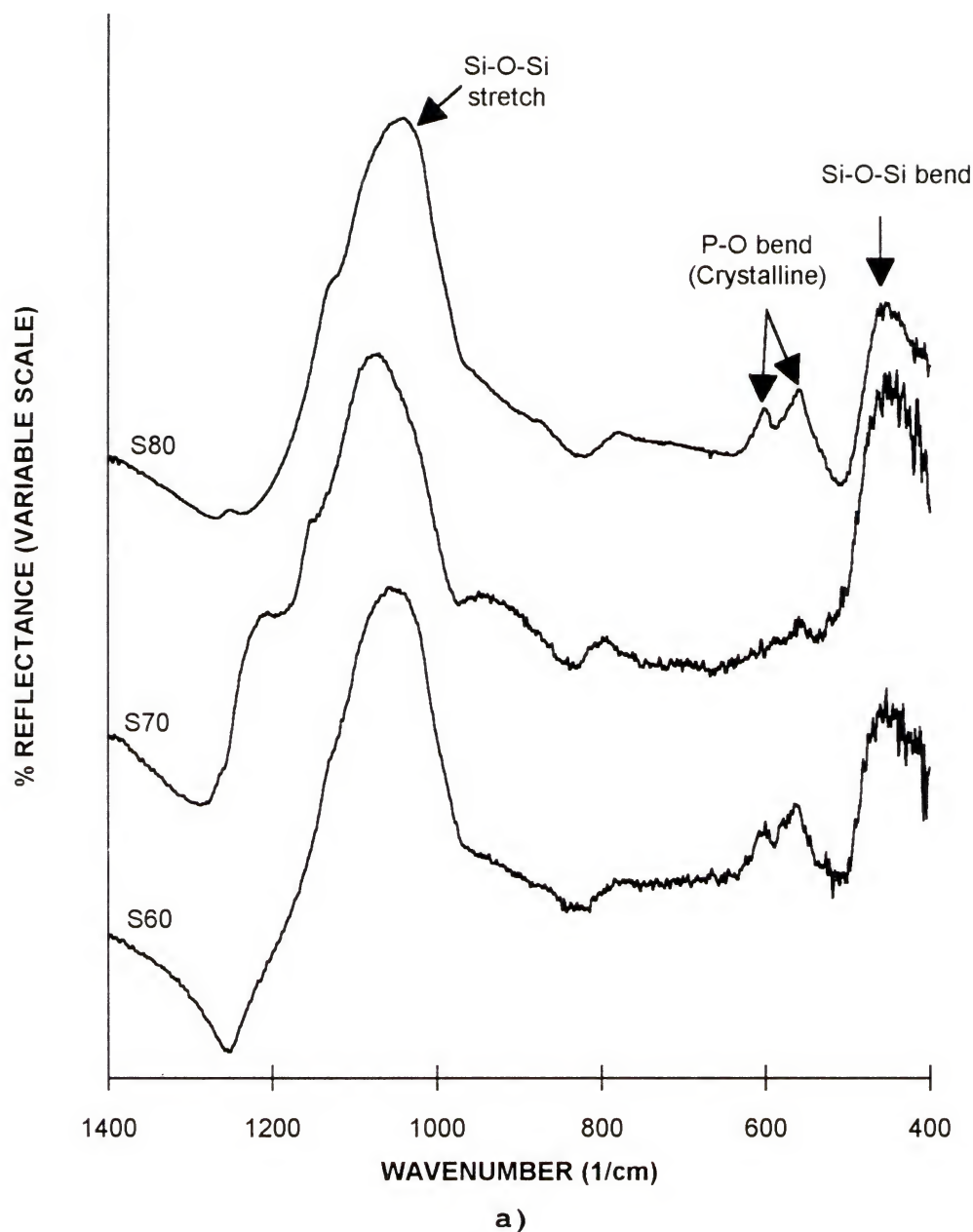


Figure 3.6 FTIR spectra of gel-glasses after reaction in Tris buffer for: a) 5 hours; b) 24 hours; c) 360 hours.



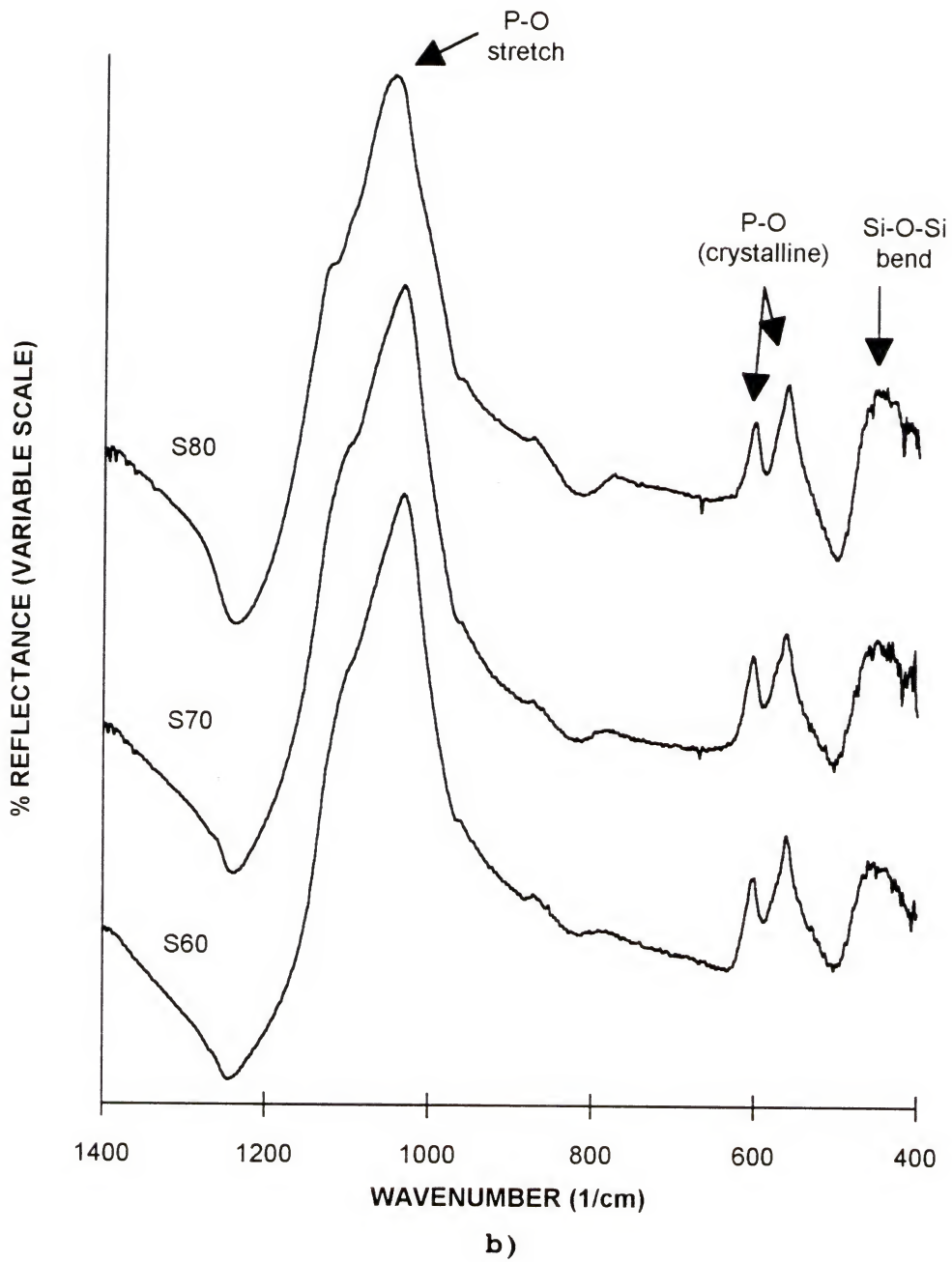


Figure 3.6--continued

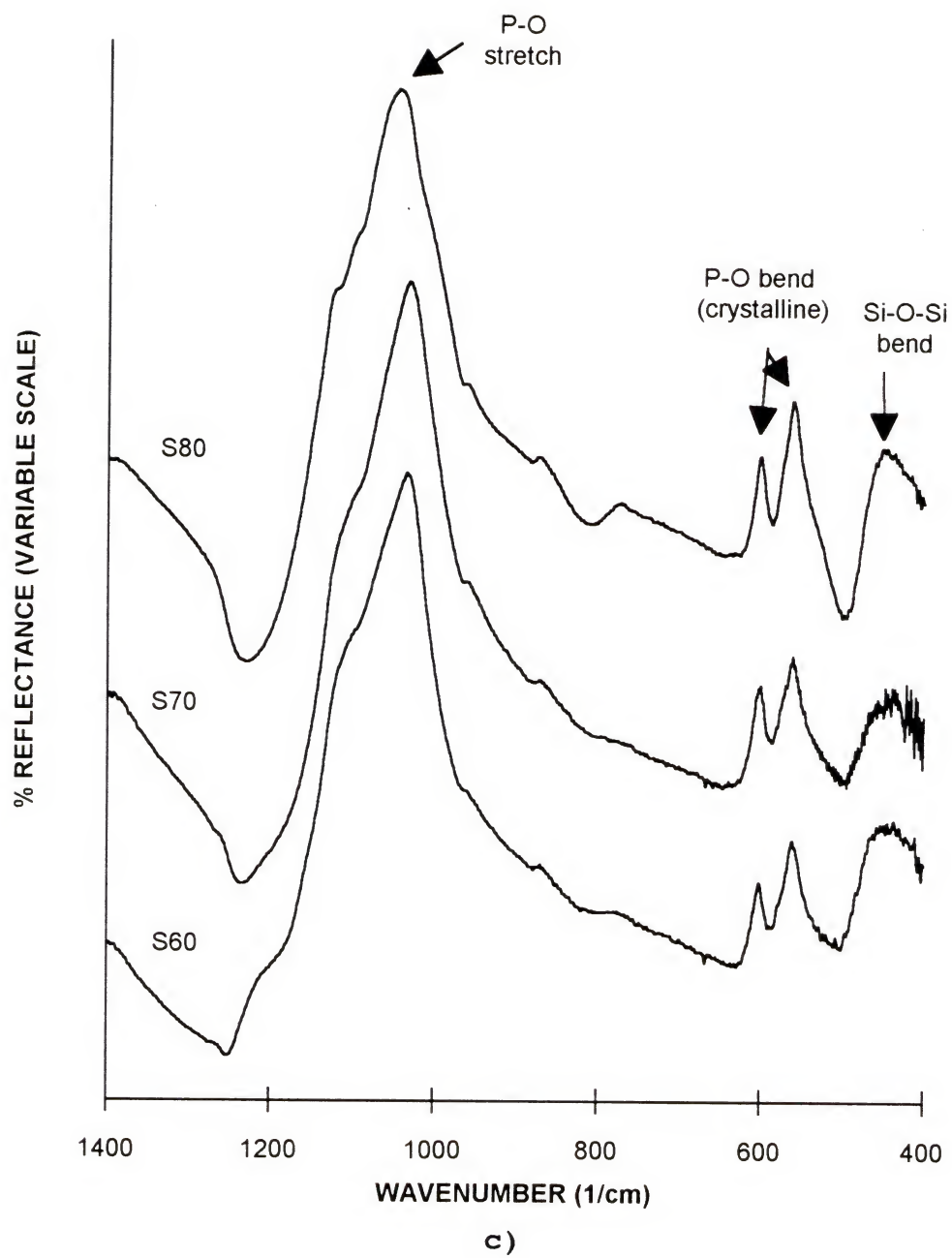


Figure 3.6--continued

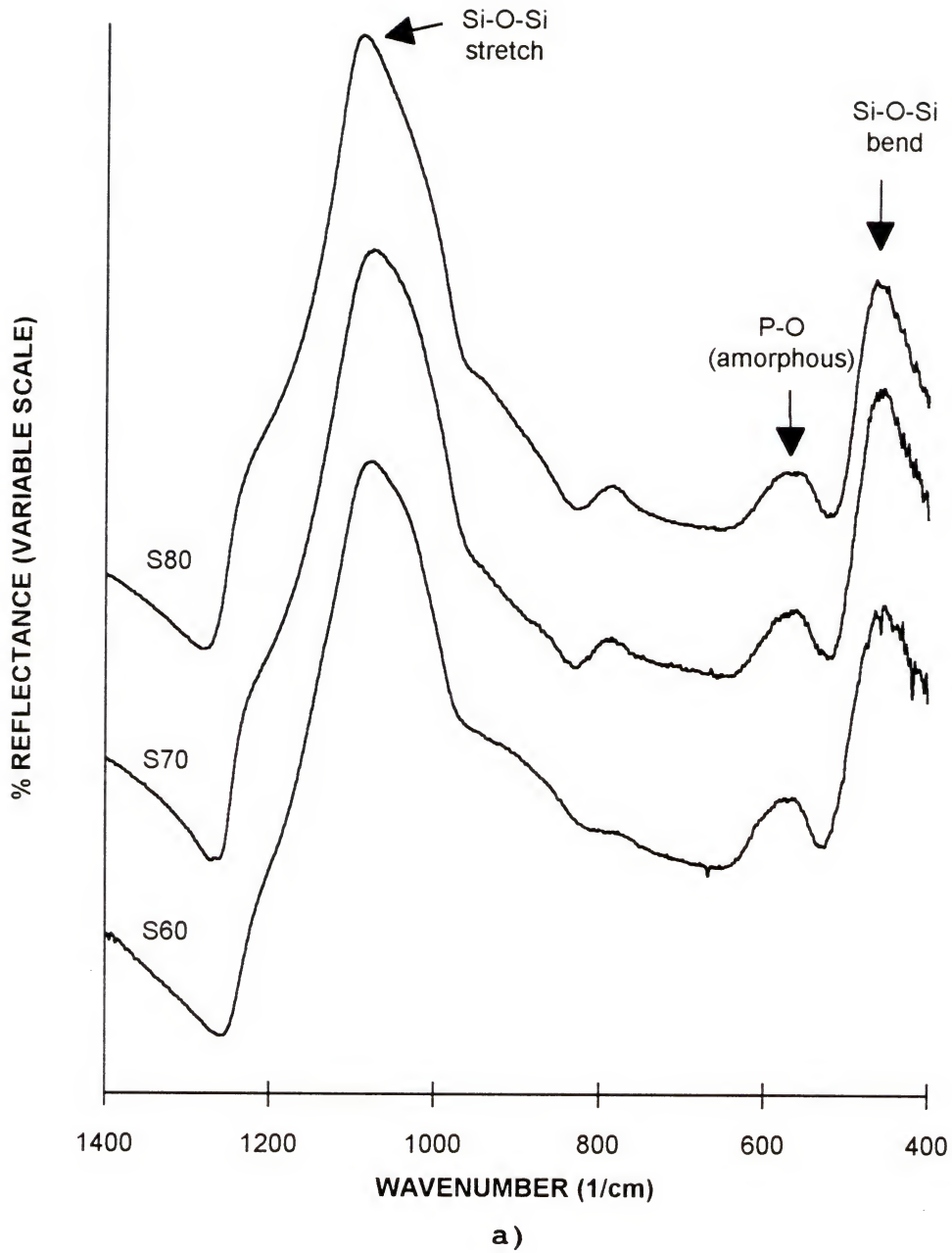


Figure 3.7 FTIR spectra of gel-glasses after reaction in SBF for: a) 5 hours; b) 12 hours; c) 20 hours.

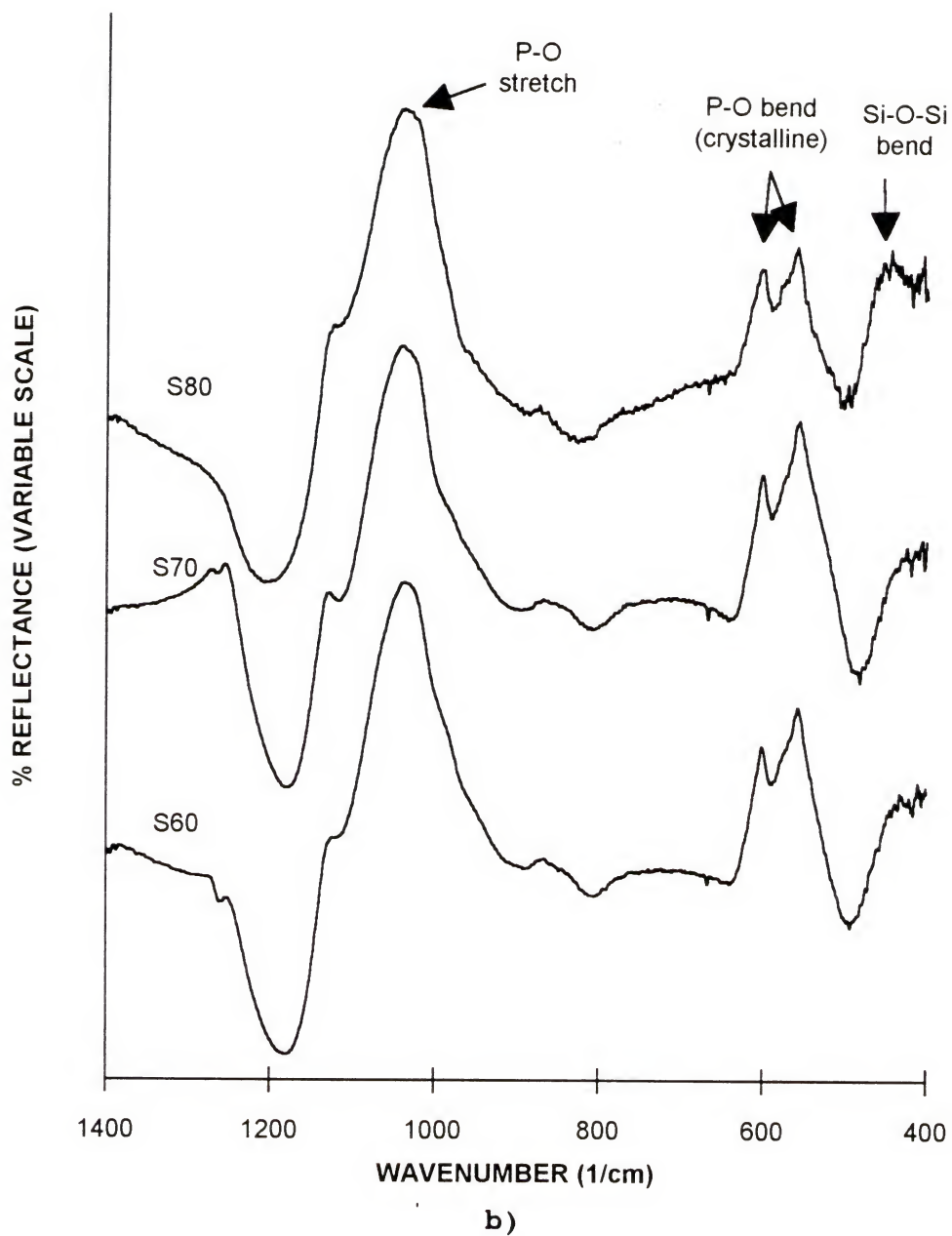


Figure 3.7--continued



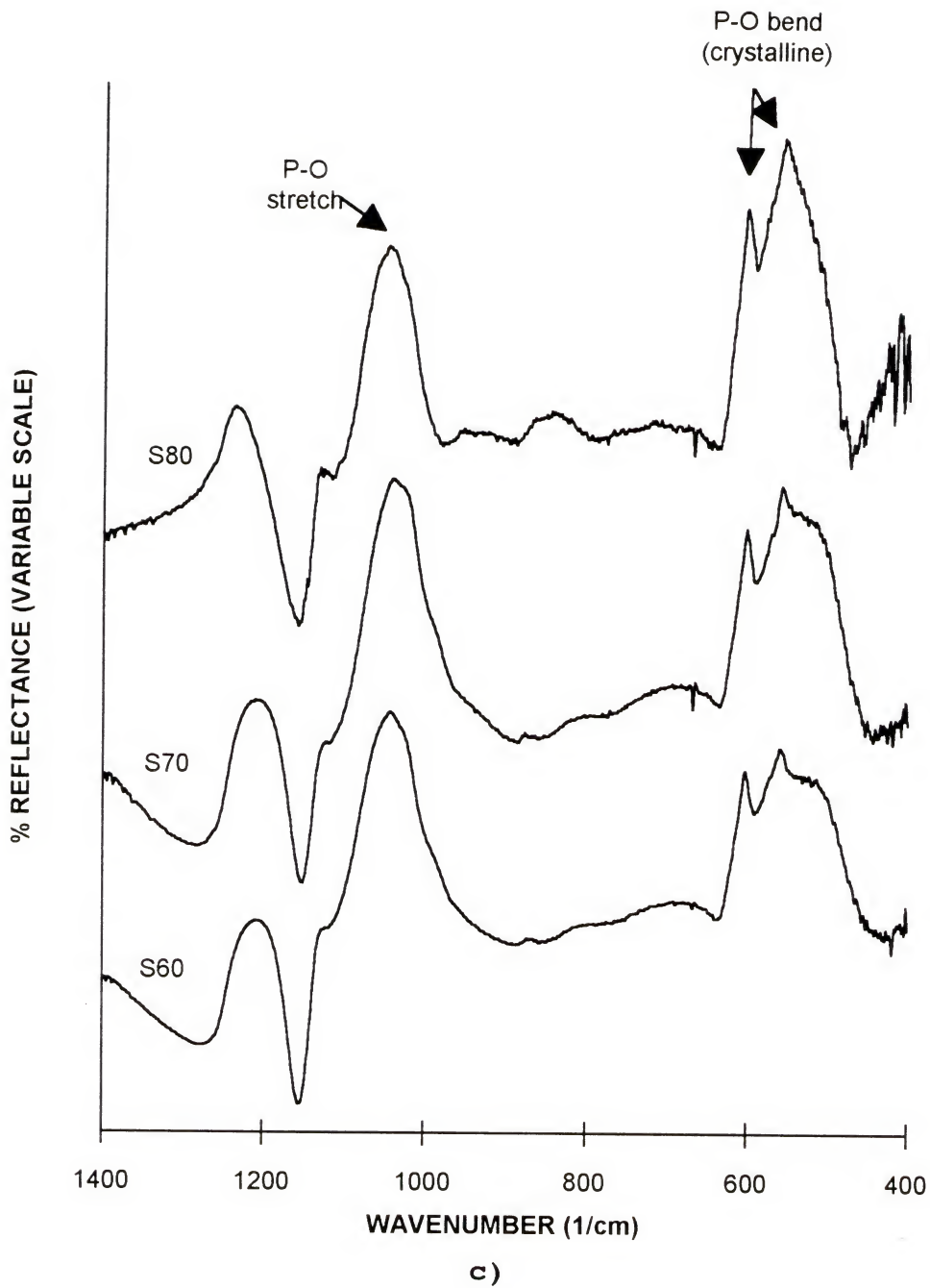


Figure 3.7--continued

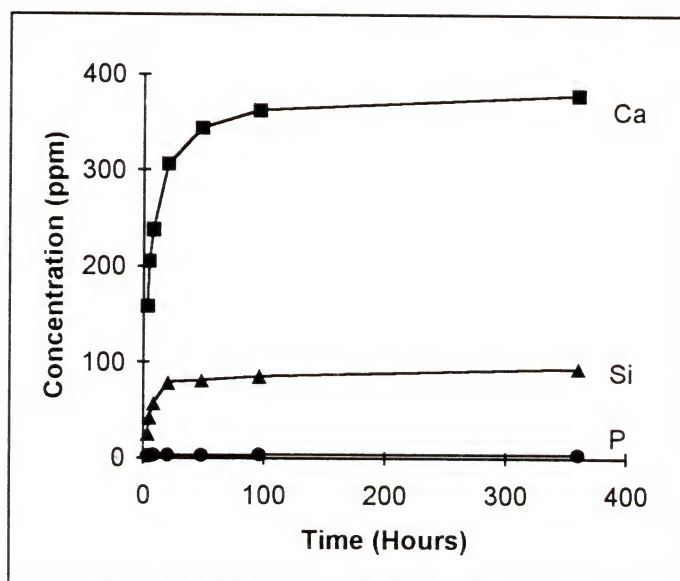
the Si-O-Si peak and the presence of a well crystallized HCA phase after 20 hours reaction (Figure 3.7).

The ion concentrations in solution after reaction in Tris buffer are presented in Figure 3.8. The Ca, Si, and P concentrations increase rapidly in the early stages of reaction and reach a constant level after 50 to 100 hours. Figure 3.9 presents a comparison of the ion concentrations in Tris buffer and SBF for composition S60. The P concentration reaches very low values in Tris buffer. In SBF the P level decreases with time from the initial value. The concentration levels of Ca and Si reached in solution are much lower in SBF than in Tris buffer.

The FTIR spectra for powder samples of the three compositions after reaction in SBF for 20 hours is presented in Figure 3.10. The peaks corresponding to the HCA crystalline phase are present for all three compositions.

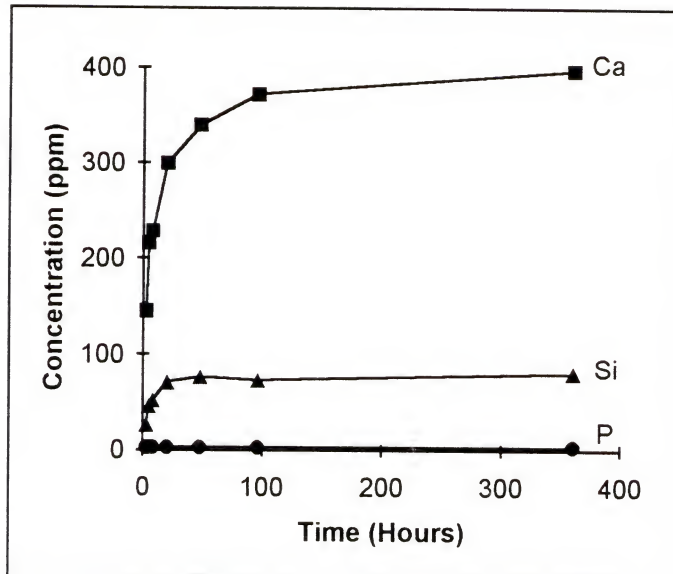
### 3.4 Discussion

The correlation between the in vitro formation of HCA and the in vivo bioactivity is well demonstrated for several bioactive glasses and glass-ceramics (Ogi80, Kok87). The results of the present study show that all the compositions tested of sol-gel derived glasses are able to induce formation of HCA both in Tris buffer and SBF, indicating that they are bioactive.



a)

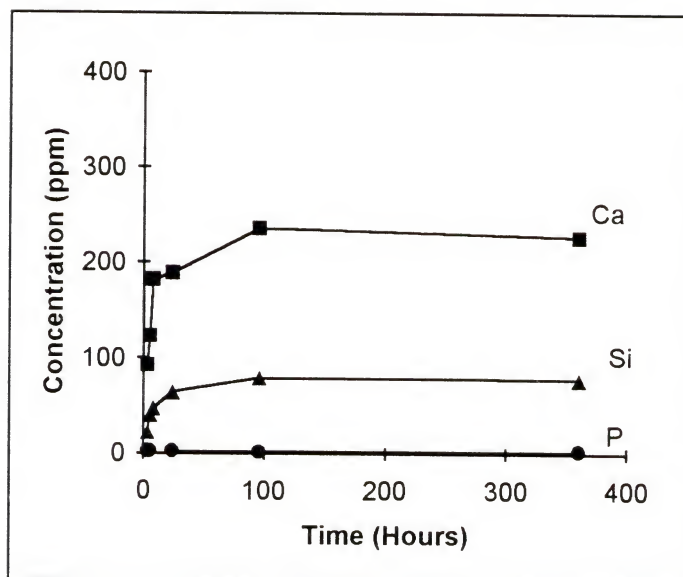
Figure 3.8 Concentration of Ca, P, and Si in Tris buffer with reaction time for gel-glasses:  
a) S60; b) S70; c) S80.



b)

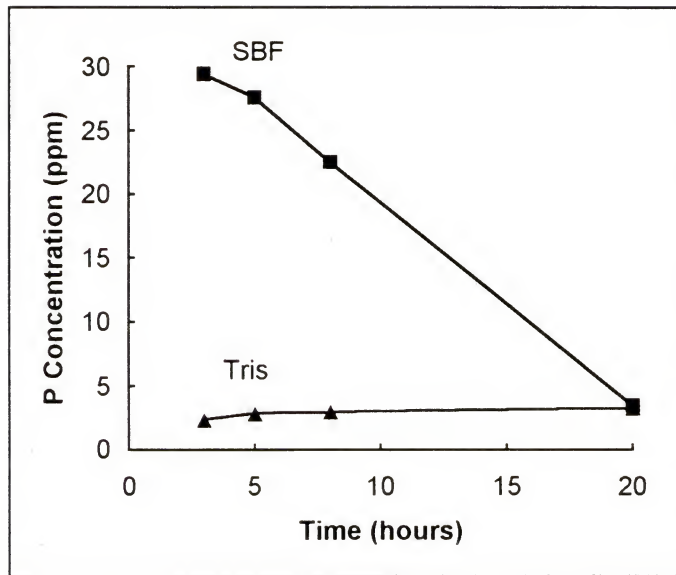
Figure 3.8--continued





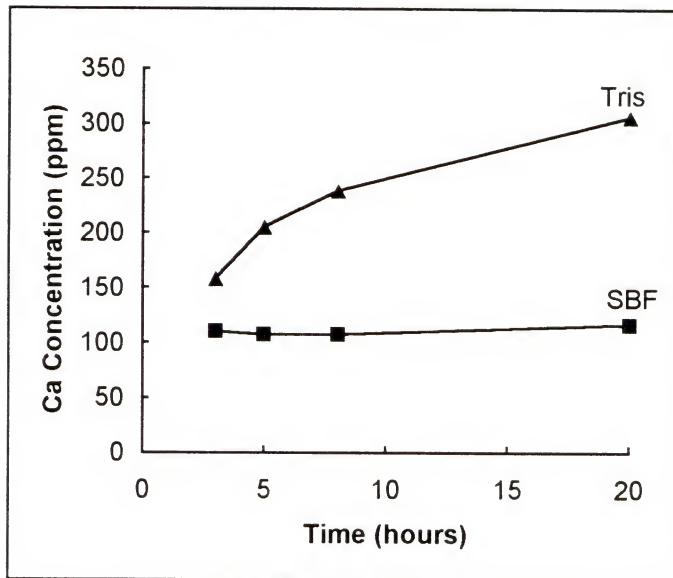
c)

Figure 3.8--continued



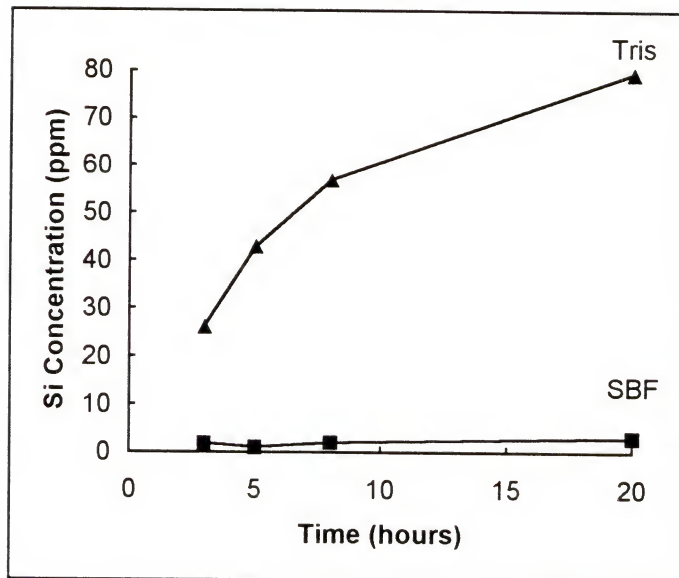
a)

Figure 3.9 Concentration of ions with reaction time in Tris and SBF solutions for gel-glass S60: a) P; b) Ca; c) Si.



b)

Figure 3.9--continued



c)

Figure 3.9--continued



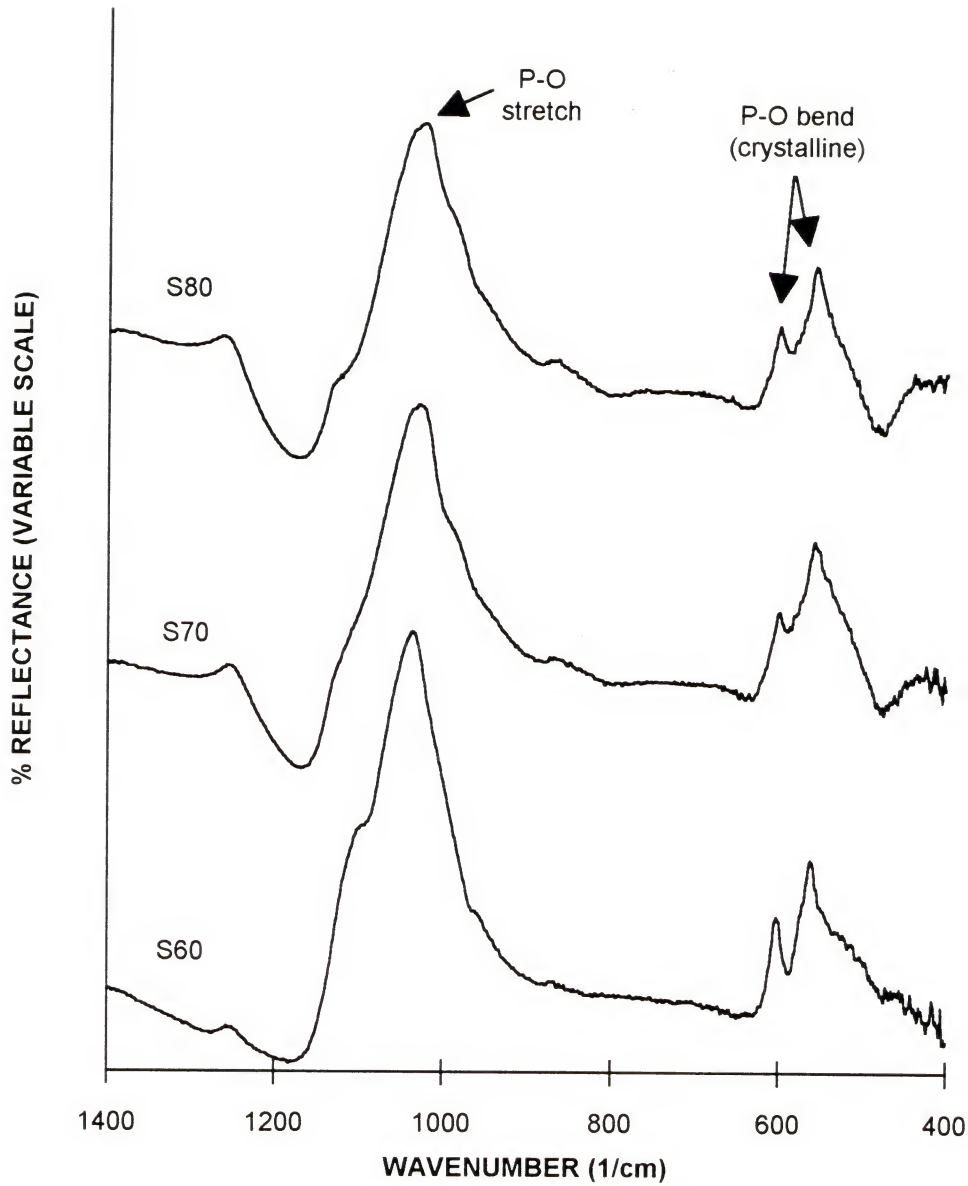


Figure 3.10 FTIR spectra of gel-glass powders after reaction in SBF for 20 hours.

Other studies have shown that pure silica gel is able to induce HCA formation when soaked in a SBF solution containing  $\text{Ca}^{2+}$  and  $\text{HPO}_4^{2-}$  ions (Li92a). The rate of HCA formation is dependent on pH and the concentration of ions in solution (Li93f). These studies show that the presence of a porous hydrated silica gel layer is necessary for the HCA nucleation. Pure silica glass, which has no porosity, does not nucleate HCA in SBF.

On melt derived glasses three reactions lead to the development of a porous hydrated silica gel layer: ion exchange, silica dissolution, and condensation of silanols to form siloxane bonded hydrated silica chains or rings (Hen88a, Hen92a). As the  $\text{SiO}_2$  content increases in melt derived glasses the rates of reactions decrease, reducing both the availability of  $\text{Ca}^{2+}$  and  $\text{HPO}_4^{2-}$  ions in solution and the ability to develop the silica gel layer on the surface. The result is the reduction and eventual elimination of the bioactivity of the melt derived glasses as the  $\text{SiO}_2$  content approaches 60% (Ogi80, Hen88a).

For gel derived glasses the bioactivity is maintained for compositions up to pure silica gels. A particular characteristic of sol-gel processing is the production of microporous materials (Hen90b, Bri90). Two consequences follow; the high surface area associated with the porous gels leads to a rapid increase in the concentration of  $\text{Ca}^{2+}$  and  $\text{HPO}_4^{2-}$  ions in solution in the case of glasses containing Ca and P in their compositions. For the

compositions studied, the Ca content in Tris buffer reaches a value approximately 6 times higher than for the corresponding melt derived compositions. Also, the texture produced by sol-gel processing results in a porous gel layer even with reduced ion exchange and dissolution rates as the  $\text{SiO}_2$  content increases. These two factors are responsible for the high rate of HCA formation and for the extension of the compositional bioactivity range in the sol-gel derived bioactive glasses.

Although HCA forms very rapidly on the glass compositions studied, the thickness of the layer does not increase much up to 15 days in Tris buffer, as indicated by the permanence of a Si-O-Si peak up to this time period. However, when soaked in SBF, crystalline HCA peaks completely substitute for Si-O-Si peaks after 20 hours. The ICP data show that the Ca content in Tris buffer is much higher than in SBF but the P content is low. The low P concentration is probably the limiting factor for the growth of the HCA layer on the surface of the glasses. In SBF the initial P level is high (31ppm) which allows growth of the HCA layer.

Another difference observed between the two solutions studied is that the Ca and Si contents reach higher values in Tris buffer than in SBF. A reason for this difference is that the fast nucleation and growth of the apatite layer on the glasses when soaked in SBF slows down the ion exchange and dissolution reactions. Also, the initial Ca

concentration in SBF is already 100 ppm which should decrease the driving force for the ion exchange reaction.

### 3.5 Conclusions

The three component  $\text{CaO-P}_2\text{O}_5\text{-SiO}_2$  alkoxide derived gel-glasses studied, with composition in the range 60-80%  $\text{SiO}_2$ , were amorphous, porous materials with a surface area ranging from 250 to 450  $\text{m}^2/\text{g}$ . All three compositions are able to induce the formation of HCA both in Tris buffer and SBF, indicating that they are bioactive. The thickness of the HCA layer grows rapidly in SBF. The low concentration of phosphorous released in solution is the limiting factor for the growth of the HCA layer in a Tris buffer solution.



CHAPTER 4  
EFFECT OF TEXTURE ON THE RATE OF  
HYDROXYAPATITE FORMATION ON SILICA GEL SURFACE

4.1 Introduction

Specific compositions of silicate glasses exhibit the property of bonding to living tissue and in particular to bone (Hen88a, Wil90). Most of the bioactive glasses (Hen84, And90a) and glass-ceramics (Gro85, Nak85) form a layer of a carbonate-containing hydroxyapatite and bond to the living bone through this hydroxy carbonate apatite (HCA) layer.

The first bioactive glasses contained  $\text{Na}_2\text{O}$ ,  $\text{CaO}$ ,  $\text{P}_2\text{O}_5$  and  $\text{SiO}_2$  in their composition (Hen71) and it was shown that there was a compositional dependency of the bioactivity defined as rate of bone bonding (Ogi80). Later it was shown that  $\text{CaO-SiO}_2$  glasses, free from  $\text{P}_2\text{O}_5$ , could also form the apatite layer on their surface (Oht91, Oht92a). This work extended the earlier study of Hench and Walker (Hen77, Wal77) that showed that a nearly pure silica glass bonded to bone if the porosity was greater than  $80 \text{ m}^2/\text{g}$ .

A silica-rich gel layer apparently plays an important role in the formation of calcium phosphate on bioactive glasses since such precipitation generally follows the development of the silica layer. In a series of studies, P.



Li and colleagues (Li92a, Li93a, Li93c-f) showed that the apatite layer could be formed on pure silica gels soaked in a simulated body fluid solution containing  $\text{Ca}^{2+}$  and  $\text{HPO}_4^{2-}$  ions. The rate of formation was shown to depend on pH and concentration of ions in solution (Li93f), and on the sintering temperature of the silica gel (Li93c). It was suggested that the silanol groups ( $-\text{SiOH}$ ) present on the surface of the silica gel are responsible for the apatite formation. This hypothesis had been previously suggested by other researchers in the field (Hen91a, Li91a). P. Li et al. claim that an experimental evidence that proves this hypothesis is the decrease of the rate of hydroxyapatite formation as the heat treatment temperature of the gels increases. However, as it is well known, heat treatment affects not only the surface chemistry, i.e., the concentration of silanols (Zhu87), but also the texture of the gels (Hen88b). No data on the texture or its change with temperature was presented in this work.

In the present chapter it is analyzed the time required for crystalline hydroxyapatite (HA) to be formed on sol-gel derived pure silica glasses with different textures when soaked in solutions containing  $\text{Ca}^{2+}$  and  $\text{HPO}_4^{2-}$  ions. The porous gel-silica substrates used in this study are similar to the type VI gel-silica glasses developed for optical applications (Hen88b, Hen93a). The concentration and pH effect on the rate of HA nucleation are also studied by

varying the solution condition and by analyzing gel-glasses with different compositions.

## 4.2 Experimental Procedures

### 4.2.1 Preparation of Sol-Gel Derived Glasses

Two glass compositions in the system  $\text{CaO-P}_2\text{O}_5\text{-SiO}_2$  (Table 4.1) were produced using the calcium nitrate sol-gel process described in Chapter II. The heterogeneity level of the two compositions is below 10 % (Figure 2.2). To prevent cracking and produce monoliths small samples were cast (6 mm thickness x 10 mm diameter) and the drying was carried in Teflon containers with a very small opening and a slow drying rate. The dried gels were heated to 600°C and maintained at temperature for 3 hours. The 85S gel-glasses were translucent and the 90S were transparent. The texture of the gel-glasses, measured using an automated isothermal nitrogen sorption instrument, is presented in Table 4.2.

Pure silica gels with various textures were prepared by acid hydrolysis and polycondensation of tetramethoxysilane (TMOS). To produce gels with average pore radius of 1.2 nm, TMOS was hydrolyzed with deionized water and nitric acid. For larger pore size gels the hydrolysis was catalyzed by a mixture of dilute nitric and hydrofluoric acids (Hen88b, Hen92b). The solutions were cast, gelled at ambient temperature and aged at 70°C. The drying was carried out

Table 4.1  
Nominal Compositions of Gel-Glasses  
(in mole %).

Sample	SiO <sub>2</sub>	CaO	P <sub>2</sub> O <sub>5</sub>
85S	85	11	4
90S	90	6	4
1S	100	-	-

Table 4.2  
BET Data of Gel-Glasses Treated at 600°C.

SAMPLE	Surface Area (m <sup>2</sup> /g)	Pore Volume (cm <sup>3</sup> /g)	Pore Size (nm)
85S	504	0.47	1.8
90S	582	0.41	1.4
1S1.2	616	0.38	1.2

slowly, with a schedule ending at 180°C. The dried gels were heated to treatment temperature in ambient air at a rate of 100°C/h and maintained at temperature for 3 hours. The texture, surface defects and changes in pore network due to hydrolysis and thermal history, have been extensively characterized (Hen88b, Hen93a). The textural features of the gel-silica glasses, measured by N<sub>2</sub> adsorption isotherms, are presented in Tables 4.3 and 4.4. The adsorption-desorption isotherm hysteresis loops and the pore size distributions of gel-glasses with three different pore sizes are presented in Figure 4.1. The shape of the isotherms is similar for all glasses, and according to deBoer (Deb58) they are typically Type A hysteresis loops which are associated with cylindrical pores open at both ends.

#### 4.2.2 Soaking in Solutions

A simulated body fluid (SBF) was prepared by dissolving reagent grade sodium chloride, sodium bicarbonate, potassium chloride, dibasic potassium phosphate, magnesium chloride, calcium chloride, and sodium sulfate in deionized water, according to Kokubo et al. (Kok90c). The solutions were buffered at pH values 7.25 and 7.4 with hydrochloric acid and tris hydroxymethyl amino methane (THAM). The concentrations of ions in the SBF are shown in Table 4.5. Solutions with different calcium concentrations were prepared by adding calcium chloride to the SBF solution at



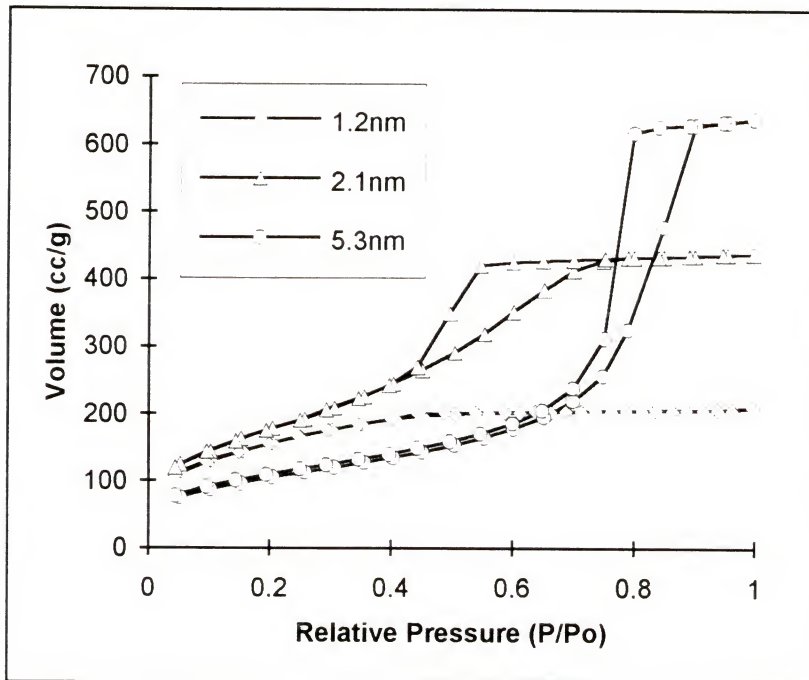
Table 4.3  
BET Data of Gel-Silica Glasses and  
Porous Vycor® Treated at 600°C.

SAMPLE	Surface Area (m <sup>2</sup> /g)	Pore Volume (cm <sup>3</sup> /g)	Pore Size (nm)
1S1.2/600	616	0.38	1.2
1S1.4/600	583	0.41	1.4
1S1.6/600	694	0.57	1.6
1S2.1/600	650	0.68	2.1
1S3.1/600	527	0.82	3.1
1S5.3/600	370	0.99	5.3
Vycor®	136	0.22	3.2

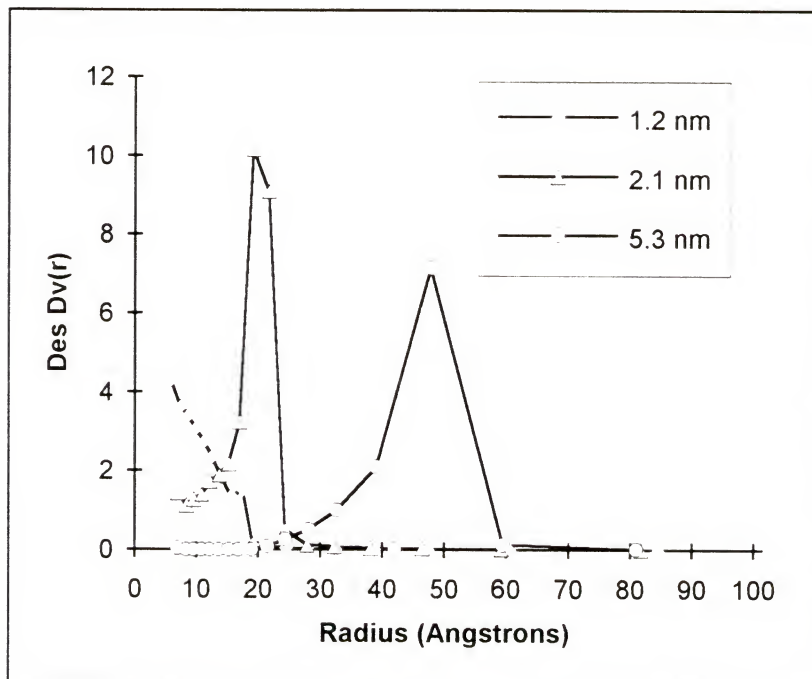
Table 4.4  
BET Data of 1S1.2 Gel-Silica Glasses Treated  
at 400, 600 and 800°C

SAMPLE	Surface Area (m <sup>2</sup> /g)	Pore Volume (cm <sup>3</sup> /g)	Pore Size (nm)
1S1.2/400	753	0.48	1.28
1S1.2/600	616	0.38	1.22
1S1.2/800	416	0.25	1.20





a)



b)

Figure 4.1 Nitrogen adsorption isotherms (a), and pore size distribution (b) of gel-silica glasses with different average pore radius.

Table 4.5  
Ion concentration (mM) of SBF and human blood plasma.

	Na <sup>+</sup>	K <sup>+</sup>	Mg <sup>2+</sup>	Ca <sup>2+</sup>	Cl <sup>-</sup>	HCO <sub>3</sub> <sup>-</sup>	HPO <sub>4</sub> <sup>2-</sup>	SO <sub>4</sub> <sup>2-</sup>
SBF pH7.25	142	5.0	1.5	2.5	147.8	4.2	1.0	0.5
SBF Ca150	142	5.0	1.5	3.75	150.3	4.2	1.0	0.5
SBF Ca200	142	5.0	1.5	5.0	152.8	4.2	1.0	0.5
Blood Plasma	142	5.0	1.5	2.5	103.0	27.0	1.0	0.5

pH=7.25. The initial Ca and P concentrations in SBF were measured in ten 1000ml solutions, as prepared. The concentrations were determined by Inductively Coupled Plasma (ICP) atomic emission spectroscopy. A variation of  $\pm 5\%$  was observed and the average Ca concentration (91 ppm) was lower than the nominal value (100 ppm). The phosphorus concentration (30 ppm) was very close to the nominal value (31 ppm).

The gel-silica samples were suspended in the solutions at 37°C by a nylon string. For comparison, specimens of porous Vycor<sup>1</sup> (textural features included in Table 4.3), borosilicate microscope slide glass and crystalline quartz were also suspended. At least three samples were suspended for each time period analyzed. The ratio of geometric surface area (SA) to solution volume (V) was fixed at 0.075 cm<sup>-1</sup>. For the gel-silica glasses this SA/V corresponded to a ratio of weight to solution volume of 0.0098-0.012 g/ml.

#### 4.2.3 Analysis of Surface Structure

After soaking for various periods of time the specimens were removed from solution and dried in air. The surfaces were analyzed by Fourier Transform Infrared Reflection Spectroscopy using a diffuse reflectance stage (DRIFTS) and by Scanning Electron Microscopy (SEM). Energy Dispersive X-

---

<sup>1</sup>Vycor - Registered trademark Corning Glass Works, Corning, NY.

ray Analysis (EDXA) was performed during SEM observation. The samples analyzed were coated with carbon.

#### 4.2.4 Ion Concentration Analysis

The concentrations of calcium and phosphorus in the SBF solutions were measured by Inductively Coupled Plasma (ICP) emission spectroscopy before and after immersion of the specimens.

### 4.3 Results

#### 4.3.1 Effect of Composition of Sol-Gel Derived Glasses on Hydroxyapatite Formation

Figures 4.2 to 4.4 show the FTIR spectra of the gel-glasses 85S, 90S and 1S1.2 treated at 600°C, before and after soaking in SBF pH=7.25 for several time periods. The spectra shown are representative of the reaction pattern of the materials but small variations were observed. Two factors may account for these variations: 1) the random character of the structure of sol-gel derived materials for which a distribution of values represent the textural features (Hen93a); 2) a small variation in the initial calcium and phosphorus concentrations in the SBF solutions.

Two peaks characteristic of a hydroxyapatite crystalline phase (Fow74, LeG78) are present at 598  $\text{cm}^{-1}$  and 566  $\text{cm}^{-1}$  in the spectra of all gel-glasses after reaction in

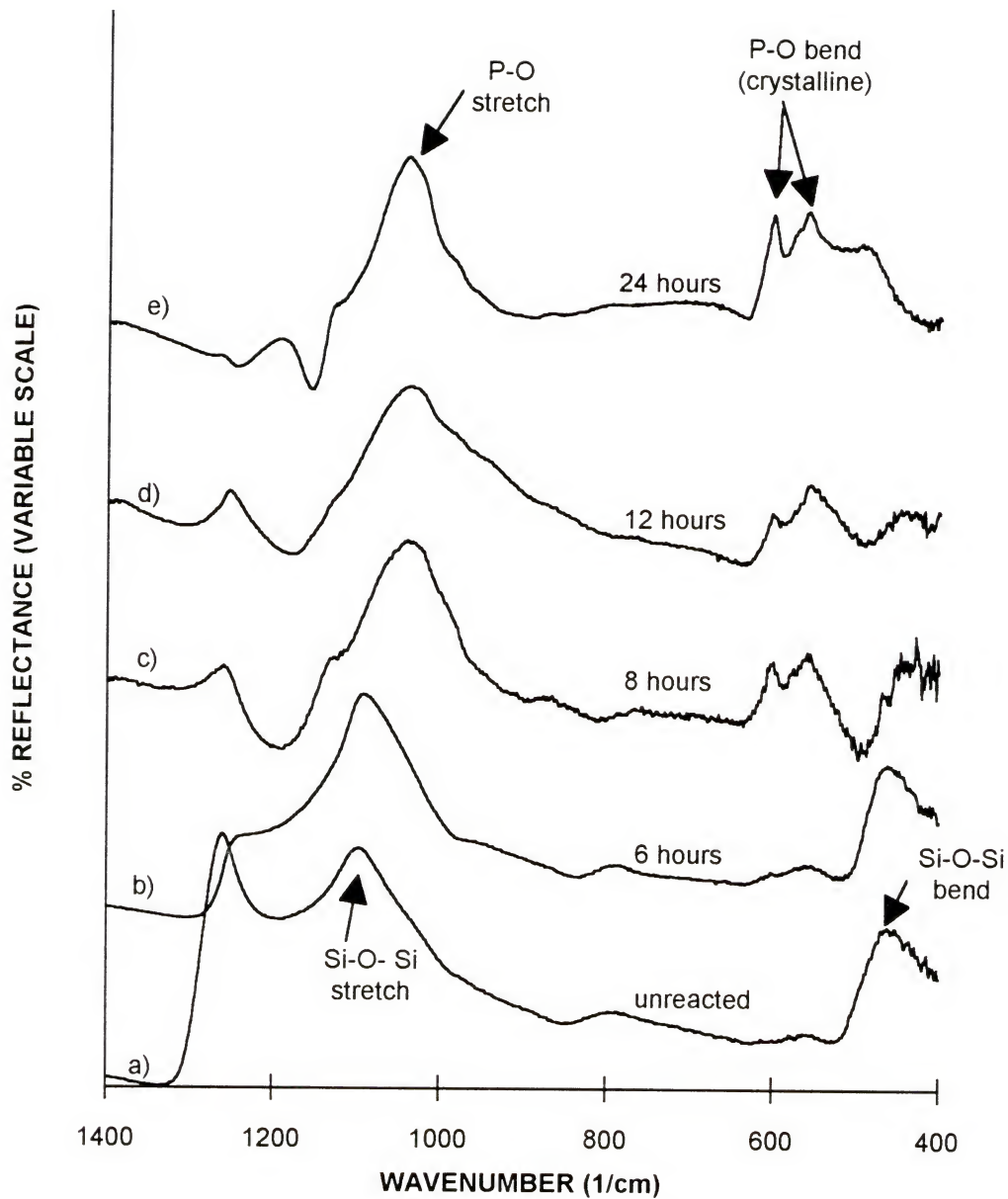


Figure 4.2 FTIR reflection spectra of gel-silica glass 85S before (a) and after reaction in SBFpH7.25 for 6 (b), 8 (c), 12 (d) and 24 (e) hours.



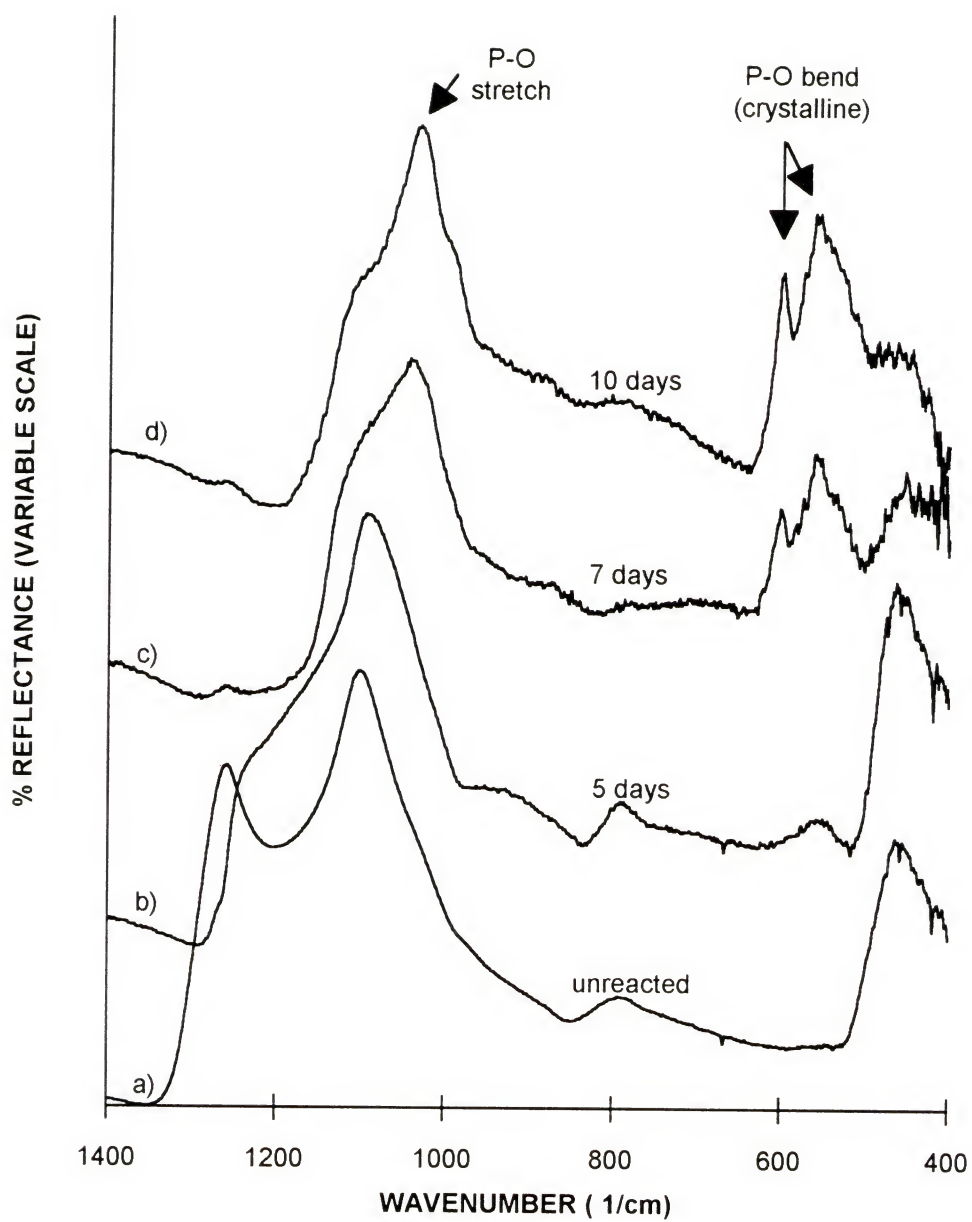


Figure 4.3 FTIR reflection spectra of gel-silica glass 90S before (a) and after reaction in SBFpH7.25 for 5(a), 7(b) and 10(d) days.

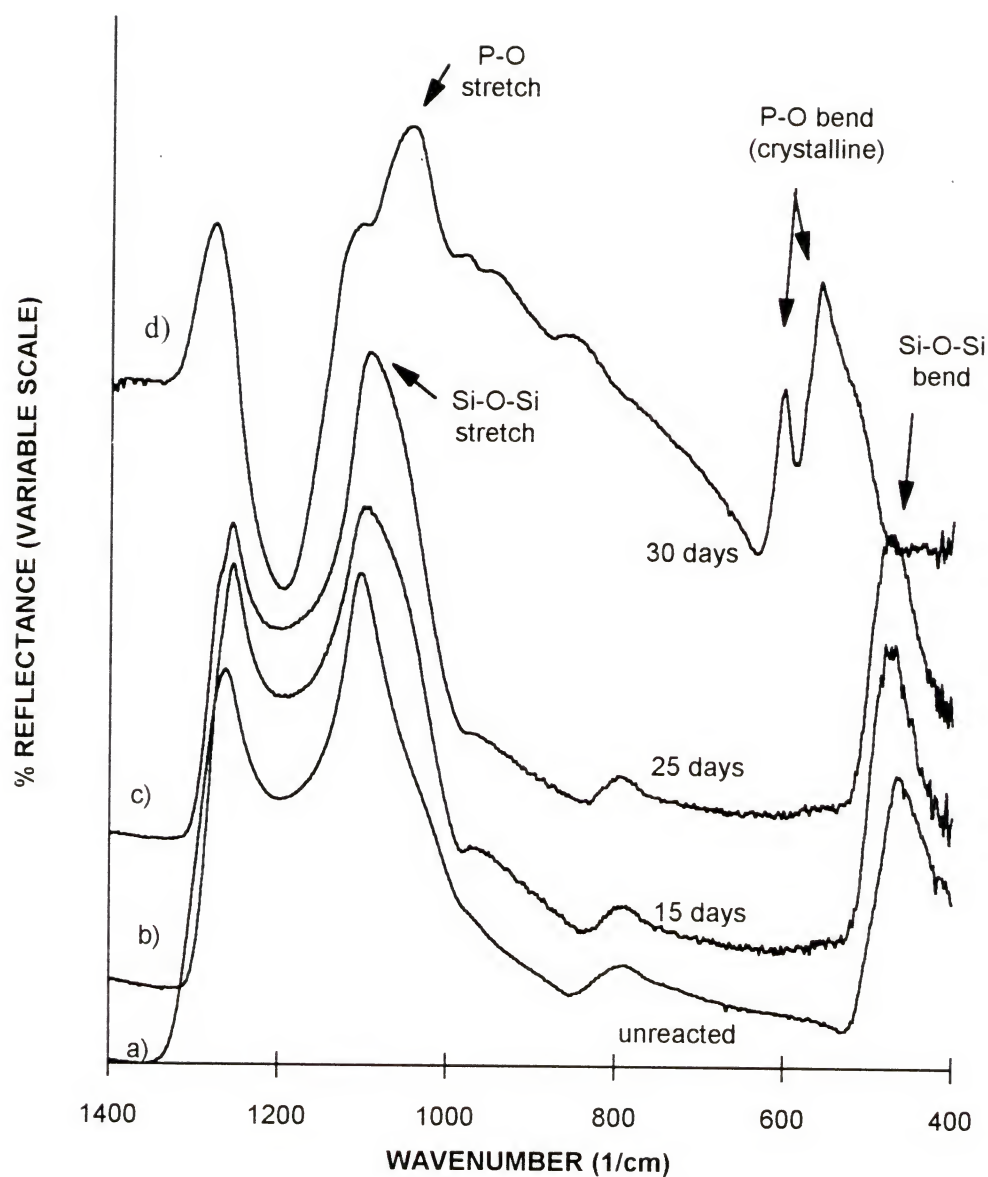


Figure 4.4 FTIR reflection spectra of gel-silica glass 1S1.2/600 before (a) and after reaction in SBFpH7.25 for 15(b), 25(c), and 30 (d) days.

the SBF solution for sufficient time. The immersion time necessary for detection of the HA phase varies for the different gel-glasses. Figure 4.5 presents a plot of the induction time for HA nucleation as a function of the silica content. As the silica content in the gel increases, the induction time for HA nucleation increases. The same trend has been observed before for both melt derived (Ogi80, Kim92) and sol-gel derived bioactive glasses (Li91b) with lower silica contents.

As a consequence of the variation in composition the texture of the gel-glasses varies as shown in Tables 4.1 and 4.2. Therefore the variation in the induction time depicted in Figure 4.5 is related to the effect of composition of the glasses: 1) on the dissolution of the glasses and the resultant increase in the calcium and phosphorus concentration in solution, or more specifically, at the glass-solution interface; 2) on the texture of the gel-glasses and its possible effect on the nucleation process; 3) on the difference in amount of ions released from the glasses due to the different surface areas associated with them.

The series of studies conducted on the pure silica gels, designed to separate the effects of ionic concentration and texture on the rate of HA formation are presented in the following sections.

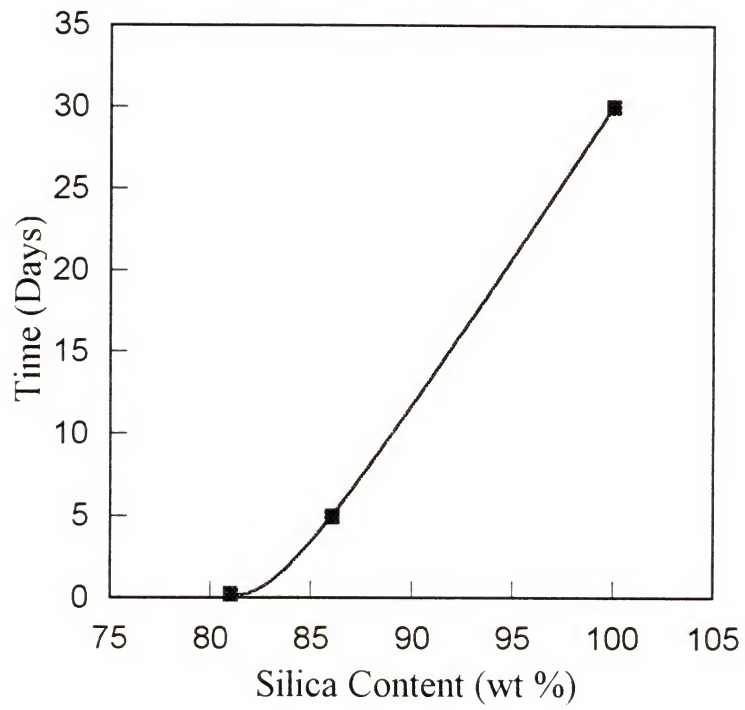


Figure 4.5 Induction time for HA nucleation as a function of gel-glass composition.

#### 4.3.2 Effect of Solution Parameters on the Hydroxyapatite Formation

SBF solution parameters affect the time for nucleation and crystallization of HA. Comparison of Figures 4.4 and 4.6 illustrate the effect of different calcium concentrations in the solution on the reflection spectra of the 1.2 nm pore size gel-silica glass treated at 600°C. Increasing the  $\text{Ca}^{2+}$  concentration from 2.5 mM to 5.0 mM reduces the HA induction time from 30 days to 16 hours or less. Figure 4.7 presents a plot of the induction time as a function of calcium concentration for this gel-glass. A large decrease in the time for HA formation is observed for higher calcium concentrations. The pH of the SBF solution has a similar effect as calcium concentration on HA formation. An increase in the pH leads to a decrease in the nucleation time as shown in Figure 4.8. Similar results were reported by P. Li et al. (Li93f).

#### 4.3.3 Effect of Texture on the Hydroxyapatite Formation

Figures 4.4 and 4.9 show FTIR reflection spectra of two 1S gel-glasses treated at 600°C (1.2 and 5.3 nm pore sizes), before and after soaking in SBF pH=7.25 for several time periods. The peaks characteristic of the HA crystalline phase are present in the spectra of all gel-silica glasses after reaction in the SBF solution for sufficient time. The immersion time necessary for detection of the HA phase



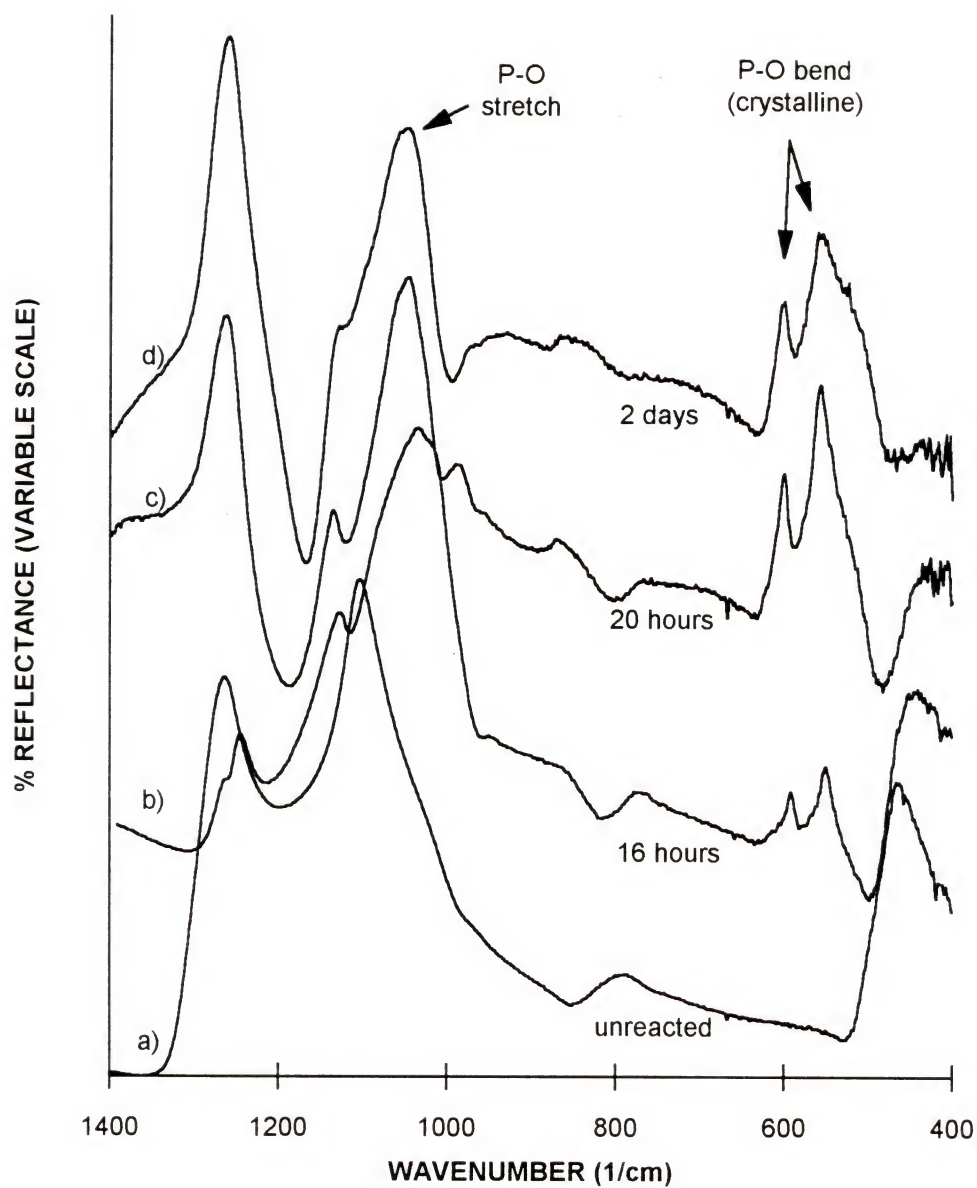


Figure 4.6 FTIR reflection spectra of gel-silica glass 1S1.2/600 before (a) and after reaction in SBF/Ca200ppm for 16 (b), 20 (c), and 48 (d) hours.

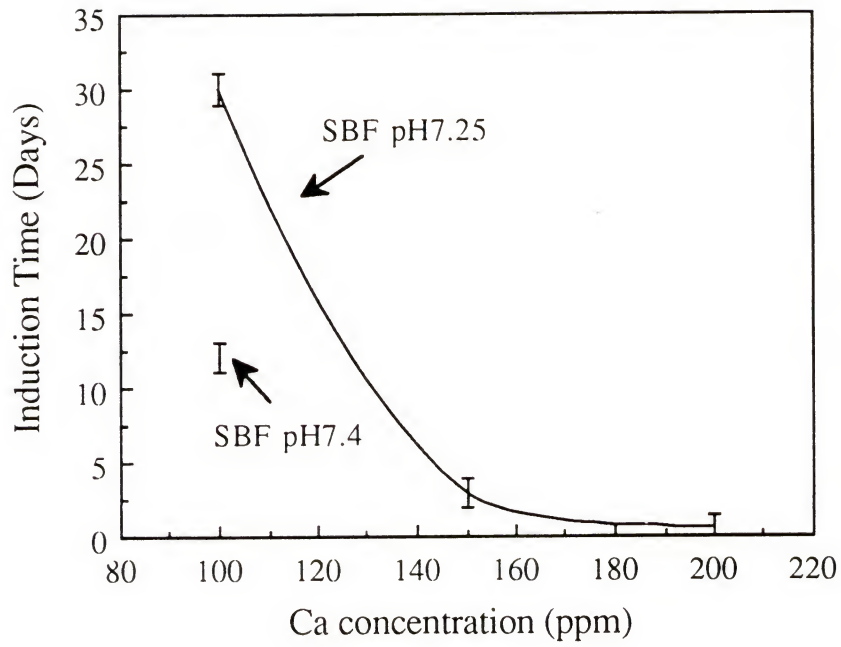


Figure 4.7 Induction time for HA nucleation as a function of calcium concentration in SBF solution for gel-silica glass 1S1.2/600.

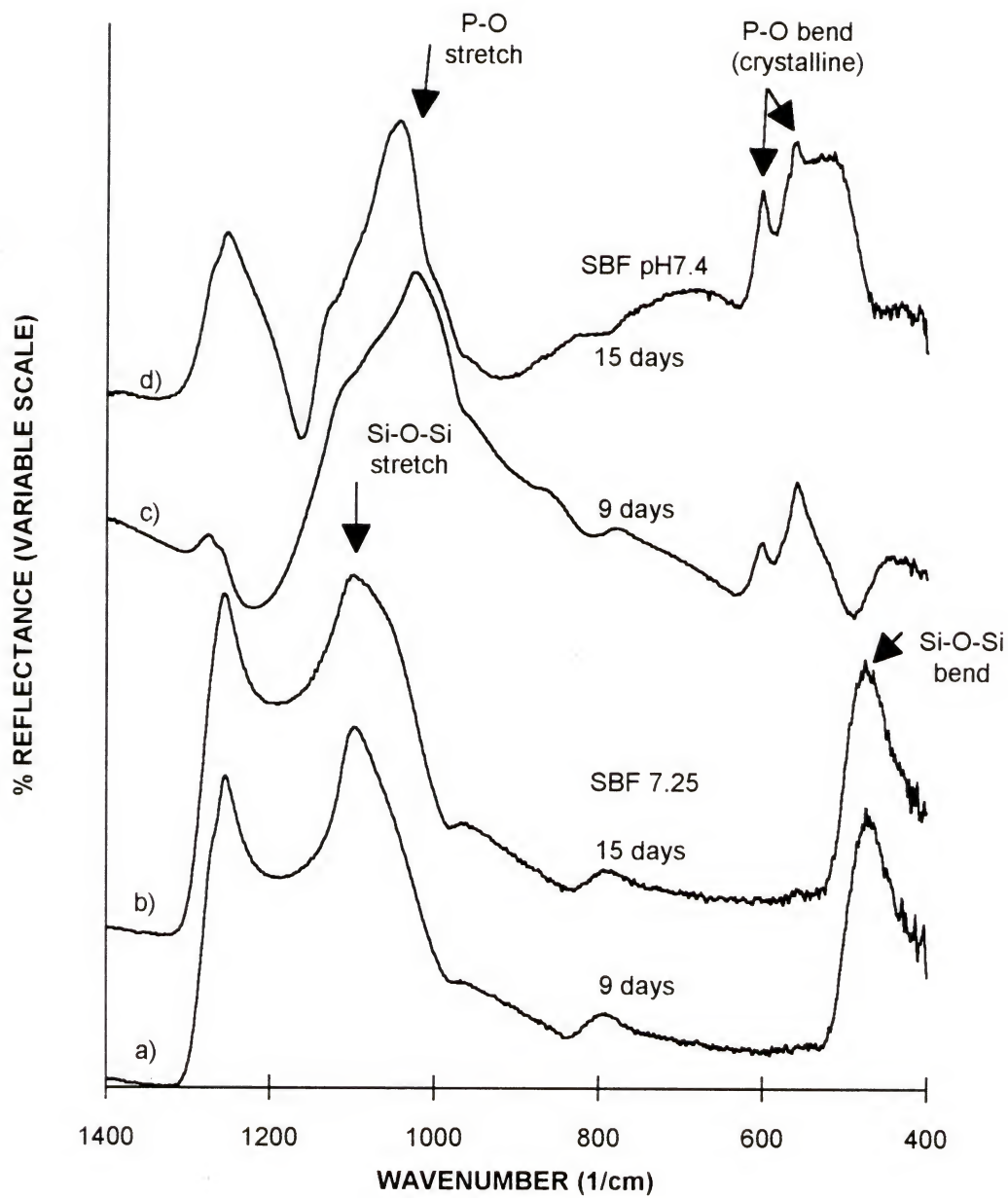


Figure 4.8 FTIR reflection spectra of gel-silica glass 1S1.2/600 after reaction in SBFpH7.25 and SBFpH7.4.

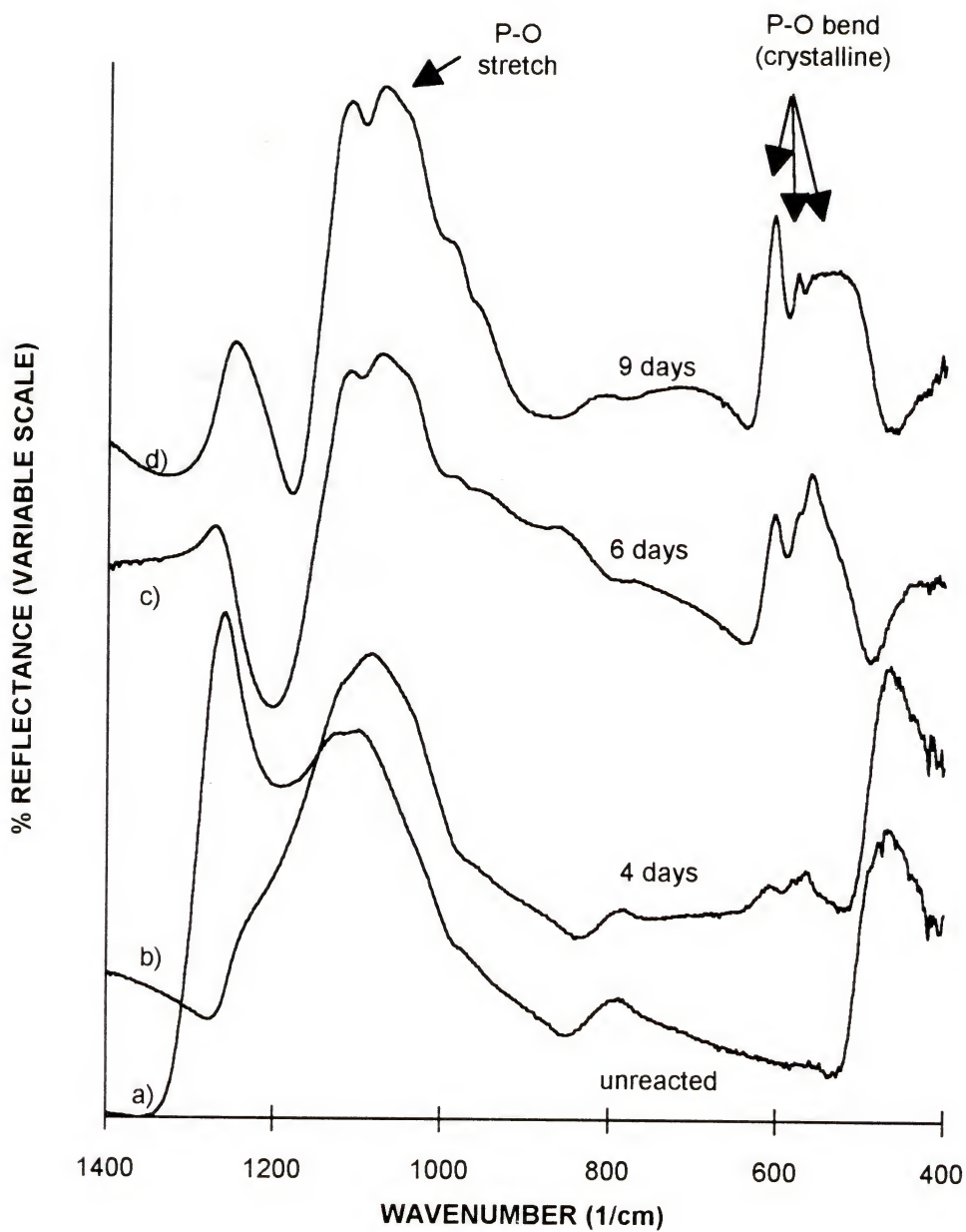


Figure 4.9 FTIR reflection spectra of gel-silica glass 1S5.3/600 before (a) and after reaction in SBFpH7.25 for 4 (b), 6 (c), and 9 (d) days.

varies for the different gel-glasses. The largest pore size material (5.3 nm) takes the shortest time, and the smallest pore size gel-silica (1.2nm) takes the longest.

The immersion time necessary for HA nucleation (induction time) can also be determined by solution analysis as described by P. Li et al. (Li93a). Figure 4.10 presents the calcium and phosphorus concentrations in solution as a function of the immersion time for different pore size gels. The induction time based on the decrease in the concentration of calcium and phosphorus in solution are in good agreement with the results obtained by FTIR. The induction time, based on the FTIR results, is plotted as a function of pore size and pore volume in Figure 4.11. As these two parameters do not vary independently for the gels considered here, a plot of induction time as a function of the product of pore volume and pore size is also presented (Figure 4.11c). The induction time for Vycor fits the data in this plot showing that the HA nucleation depends on both pore volume and pore size.

The 1.2 nm pore size gel was also treated at different temperatures 400, 600, and 800°C which alters the texture of the gel-glass. Table 4.4 shows that the surface area and pore volume decrease with increasing heat treatment temperature but the pore size is nearly unchanged. The FTIR spectra for samples treated at 400°C and exposed to SBF for various times are presented in Figure 4.12. No appreciable difference in time for HA formation is observed for the gel-



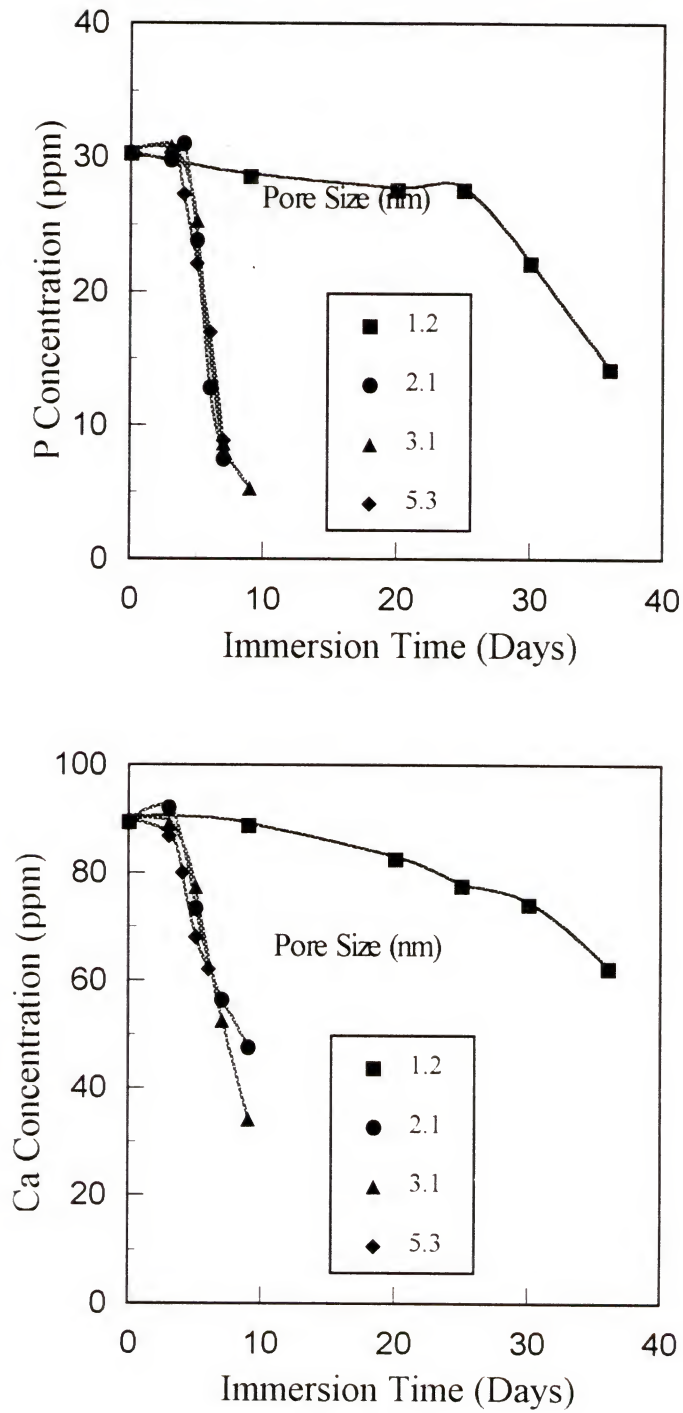


Figure 4.10 Calcium and phosphorous concentrations as a function of immersion time in SBF for gel-silica glasses of various pore sizes.

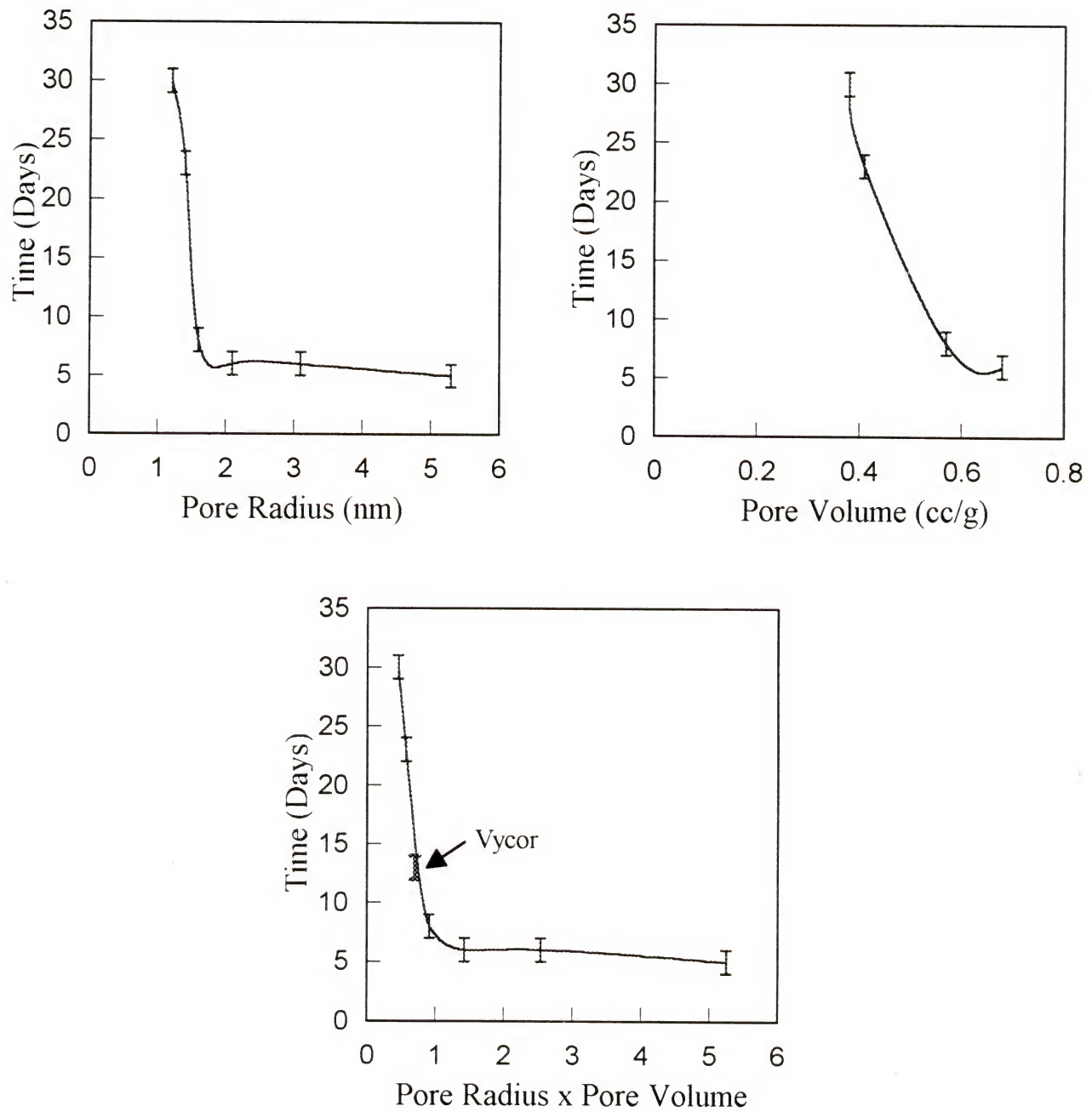


Figure 4.11 Induction time for HA nucleation on gel-silica glasses as a function of pore size, pore volume, and pore size x pore volume.

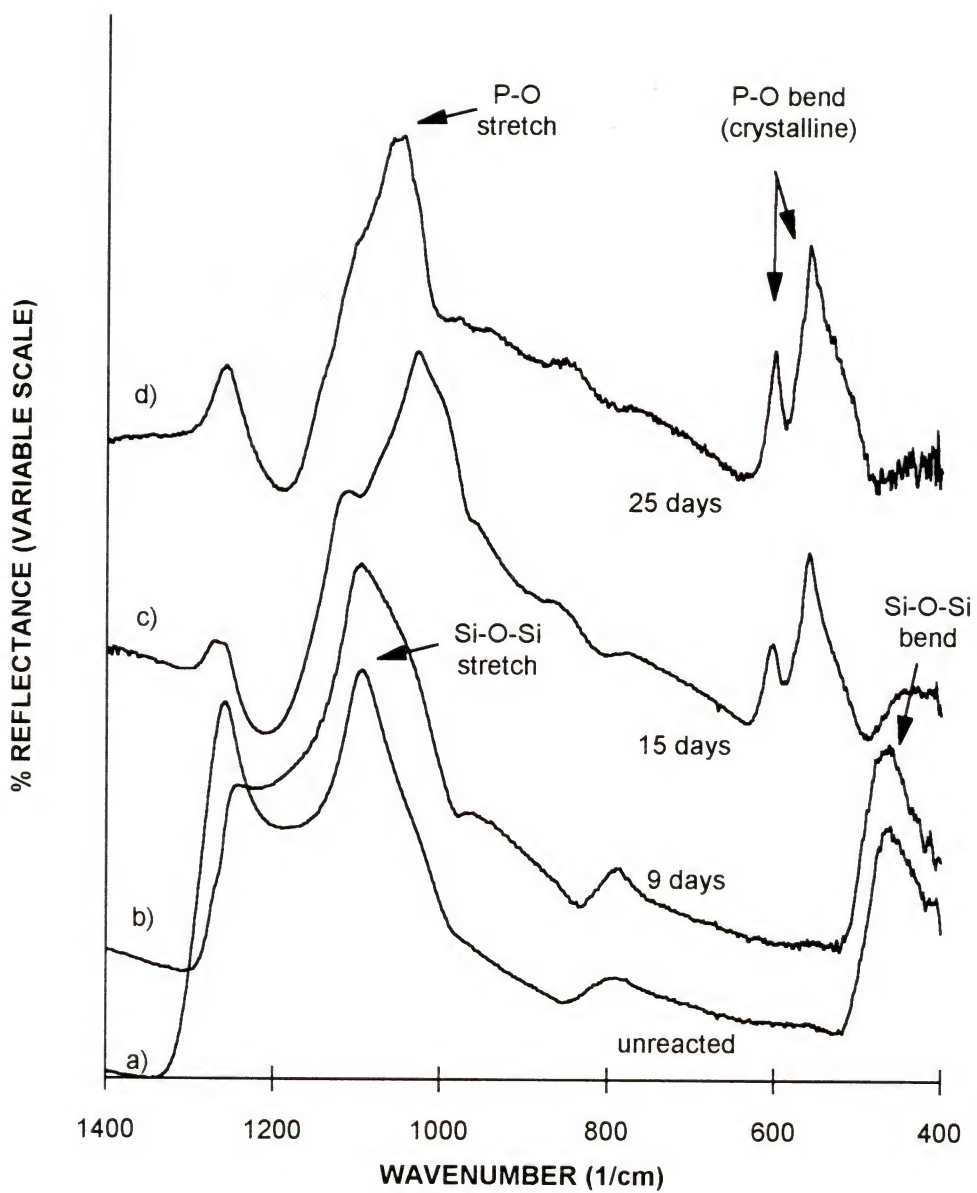


Figure 4.12 FTIR reflection spectra of gel-silica glass 1S1.2/400 before (a) and after reaction in SBFpH7.25 for 9 (b), 15 (c), and 25 (d) days.

silica glasses treated at 600 and 800°C. Faster apatite formation is however detected for the 400°C treated glass, i.e., less than 15 days for 400°C (Fig. 4.12) vs. 30 days for 600-800°C gel-glass (Fig. 4.4).

HA was also detected on porous Vycor after approximately 12 days immersion in SBF pH 7.25. In contrast to the porous gel-silica and Vycor substrates, no HA was detected on the surfaces of either quartz or microscope slide glass up to 30 days, even in the solution with the higher calcium concentration, as illustrated in Figure 4.13.

#### 4.3.4 Morphology of Hydroxyapatite Formed on Silica Gels with Different Textures

Figures 4.14 to 4.19 show SEM micrographs of the surfaces of pure silica gels with different pore sizes, after soaking in SBF for times that allowed the formation of hydroxyapatite. Different morphologies are observed depending on the pore size of the gel-glass. On the smaller pore size gel-glasses (1.2 and 1.4 nm, Figures 4.14 and 4.15) the hydroxyapatite developed in a flower-like configuration in which the flowers are formed by plates having hexagonal feature. HA formed on gel-glasses with pore radius above 1.6 nm presented similar morphology (Fig. 4.16 to Fig. 4.19). The HA precipitated as spherulites, the size of which increased as the pore size increased. The apatite growth habit in the spherulites appears to vary from a needle-like habit (Fig. 4.17) to a short-rod habit (Fig.

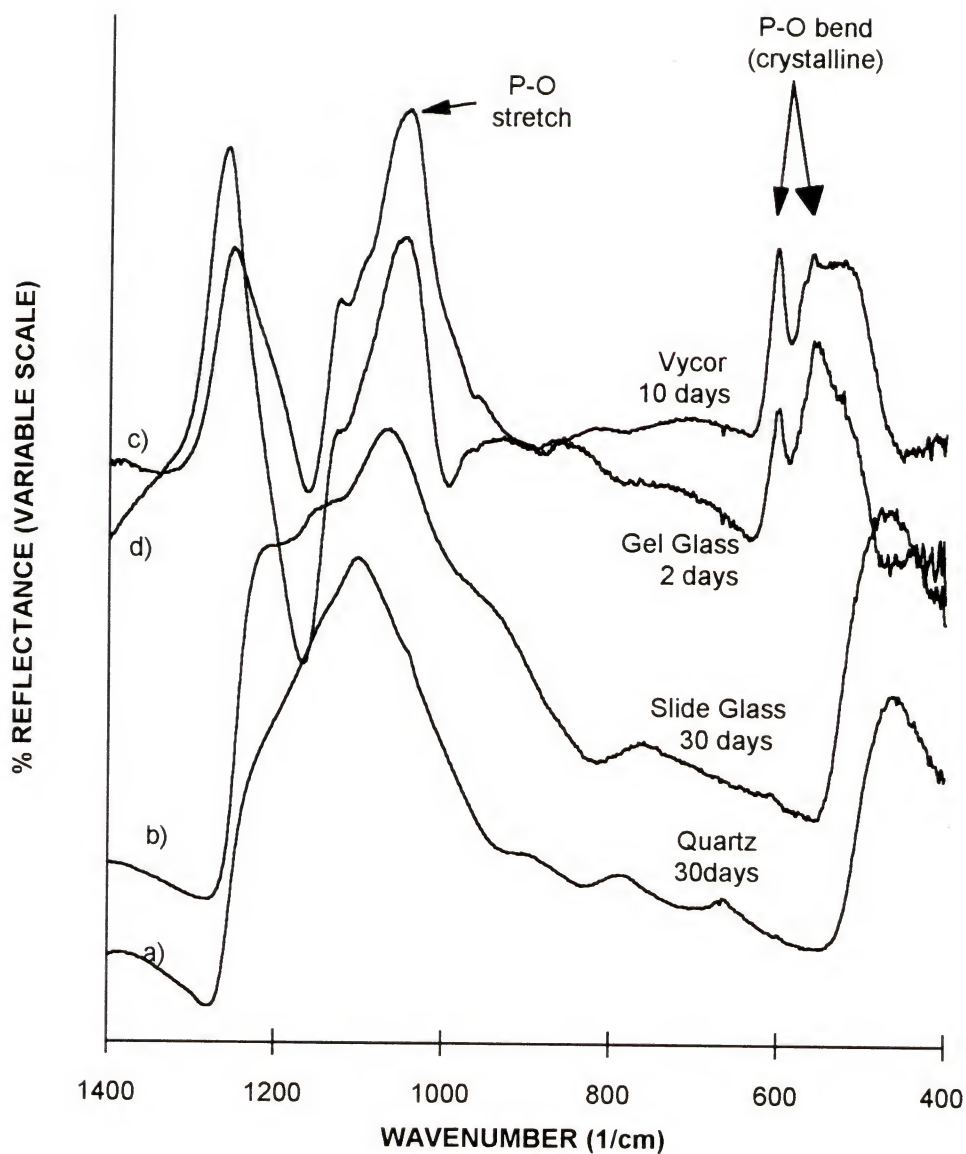
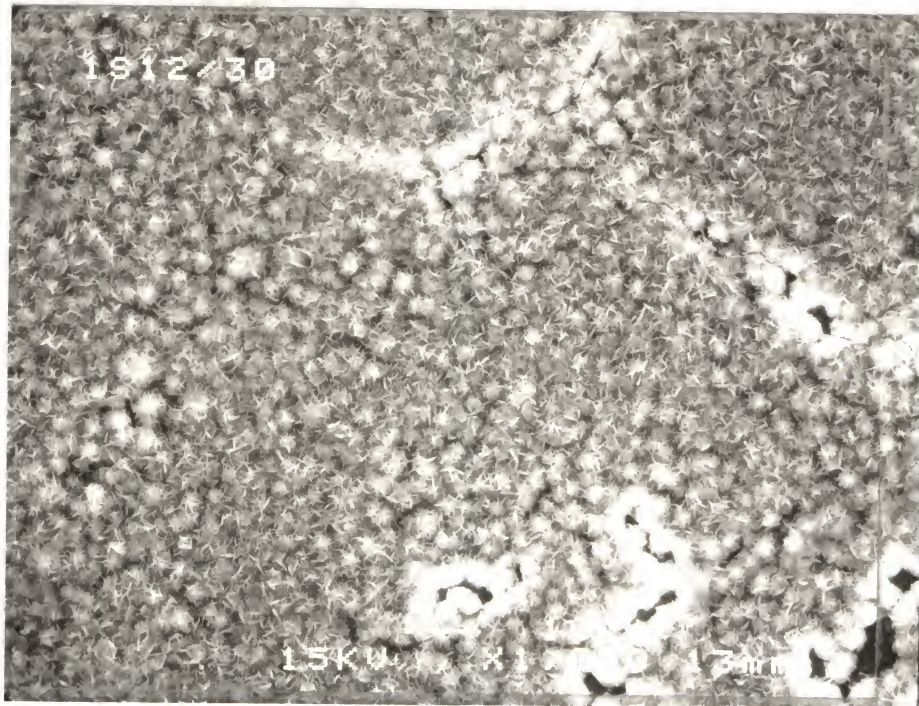


Figure 4.13 FTIR reflection spectra of different materials before and after reaction in SBF pH7.25/Ca=200ppm. a) quartz, 30 days; b) slide glass, 30 days; c) gel-glass 1S1.2, 2 days; d) Vycor 10 days.



a)



b)

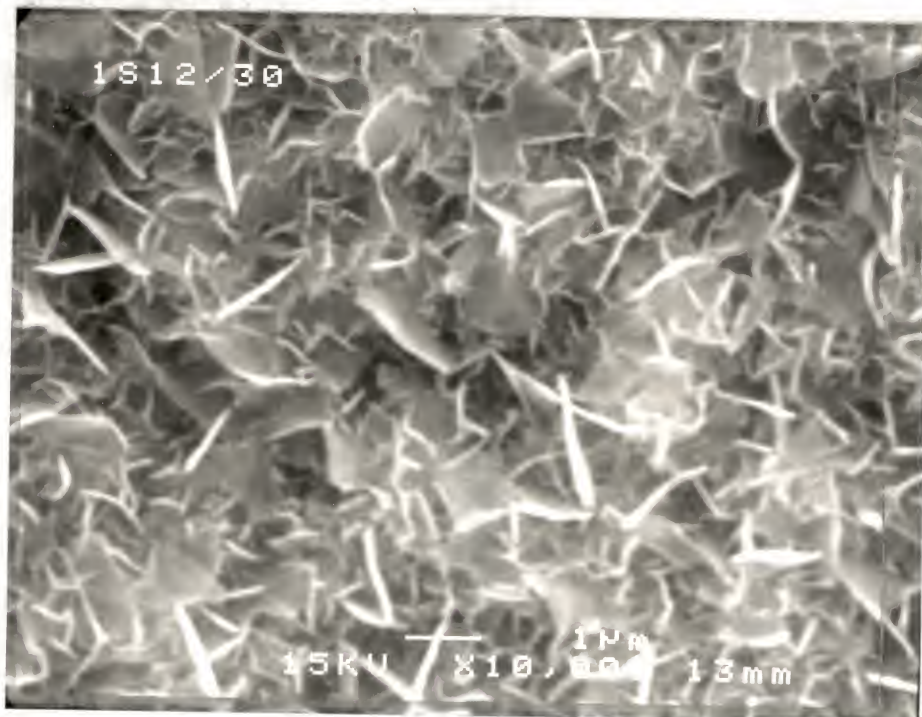
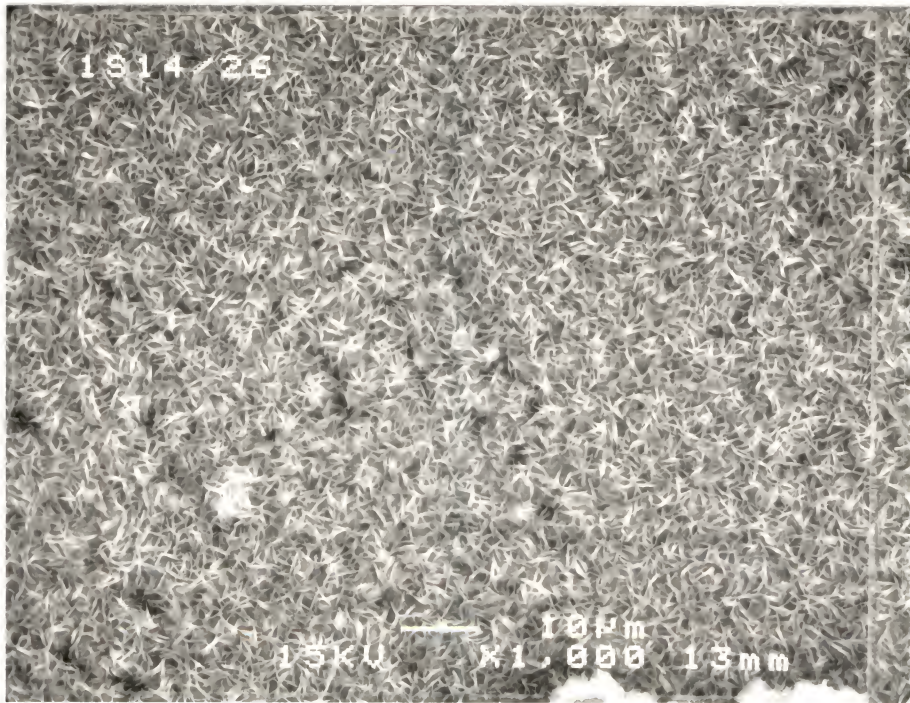


Figure 4.14 SEM micrographs showing morphology of hydroxyapatite formed on gel-silica glass 1S1.2/600 after immersion in SBF for 30 days: a) 1000x; b)10.000x.



a)



b)

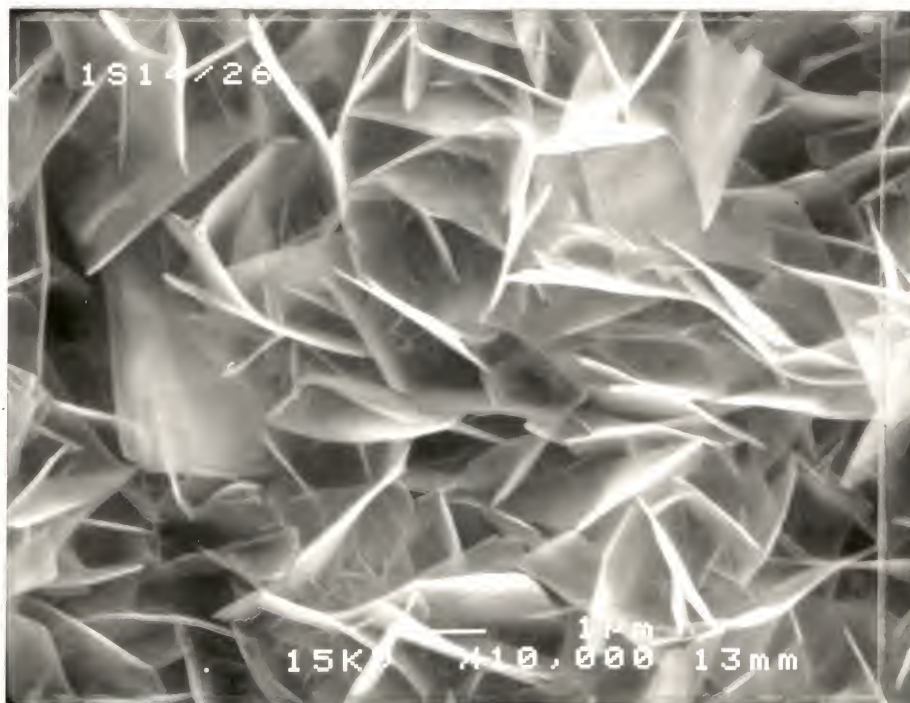


Figure 4.15 SEM micrographs showing morphology of hydroxyapatite formed on gel-silica glass 1S1.4/600 after immersion in SBF for 26 days: a) 1000x; b)10.000x.



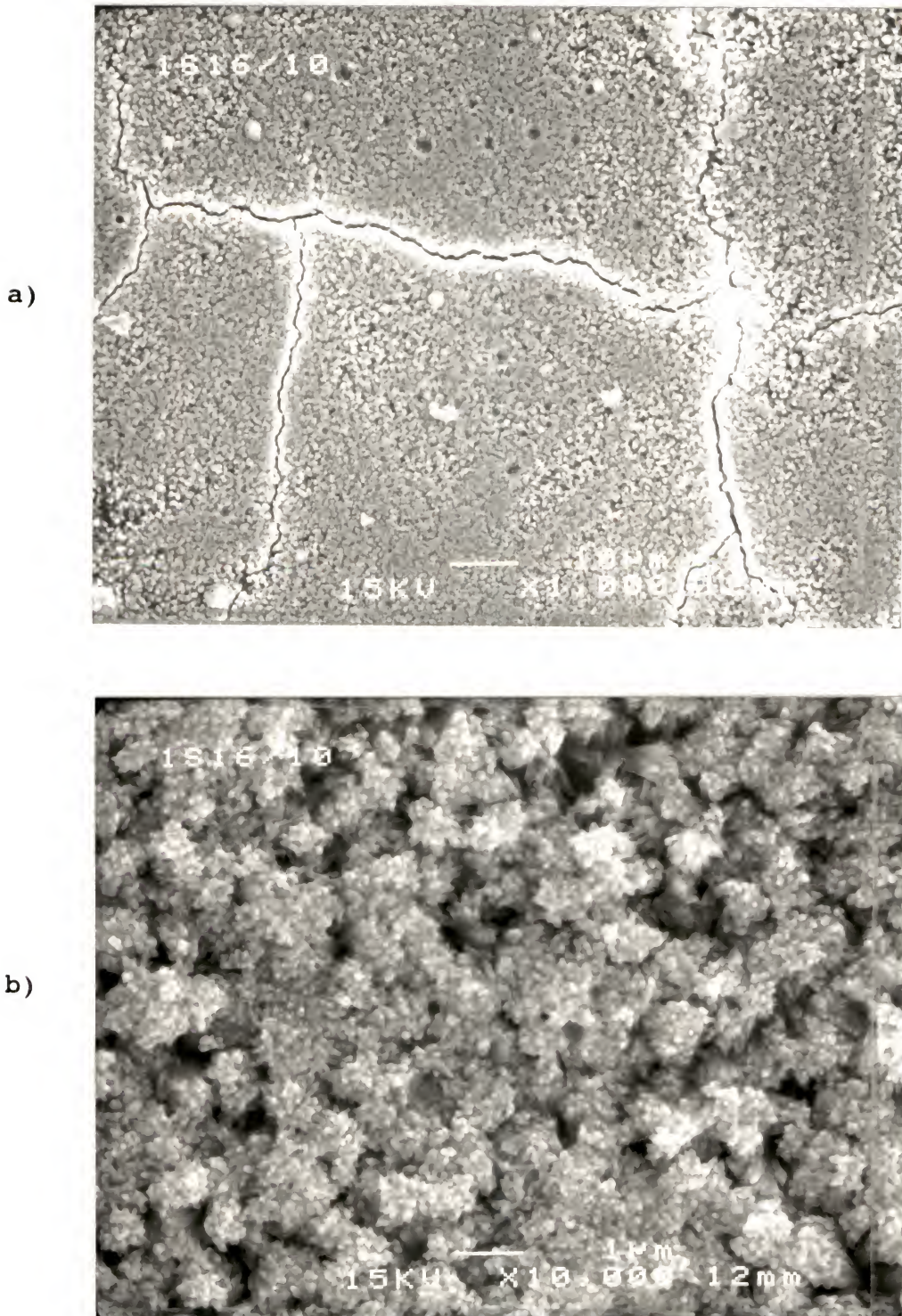
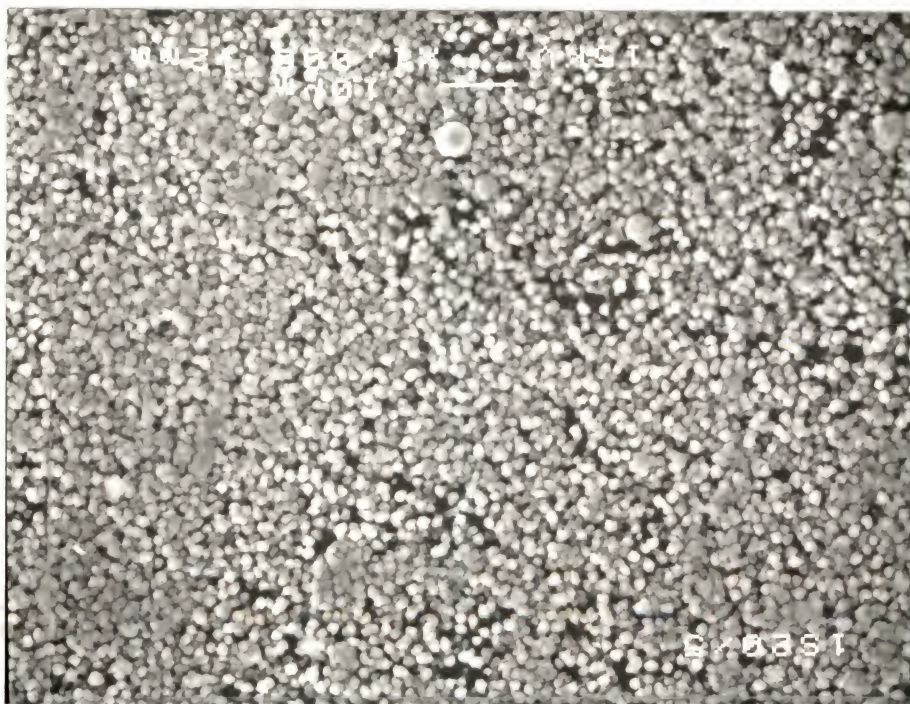


Figure 4.16 SEM micrographs showing morphology of hydroxyapatite formed on gel-silica glass 1S1.6/600 after immersion in SBF for 10 days: a) 1000x; b)10.000x.



a)



b)

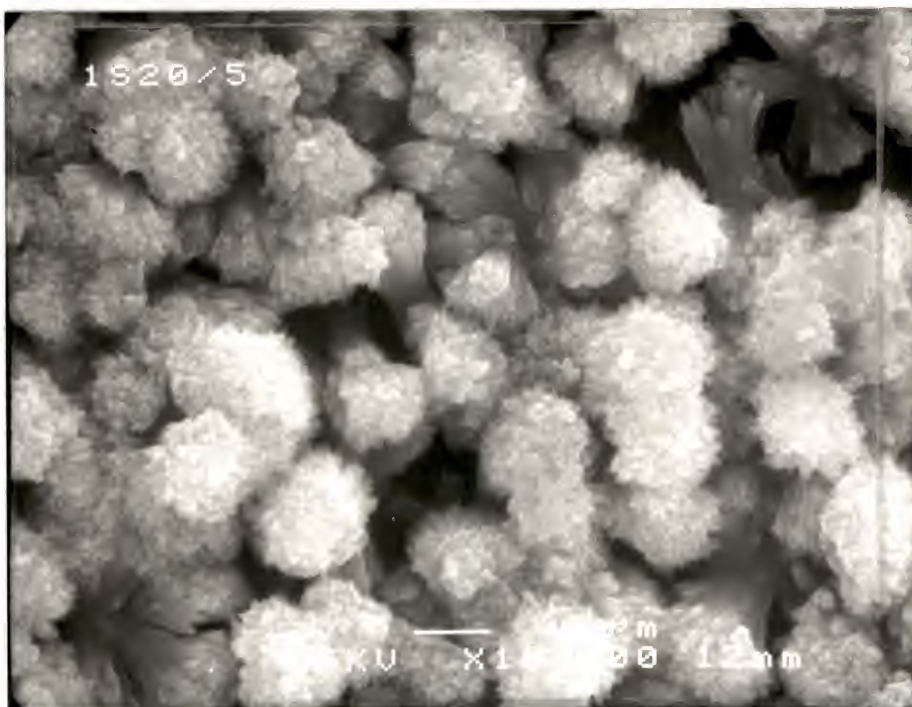


Figure 4.17 SEM micrographs showing morphology of hydroxyapatite formed on gel-silica glass 1S2.1/600 after immersion in SBF for 7 days: a) 1000x; b)10.000x.



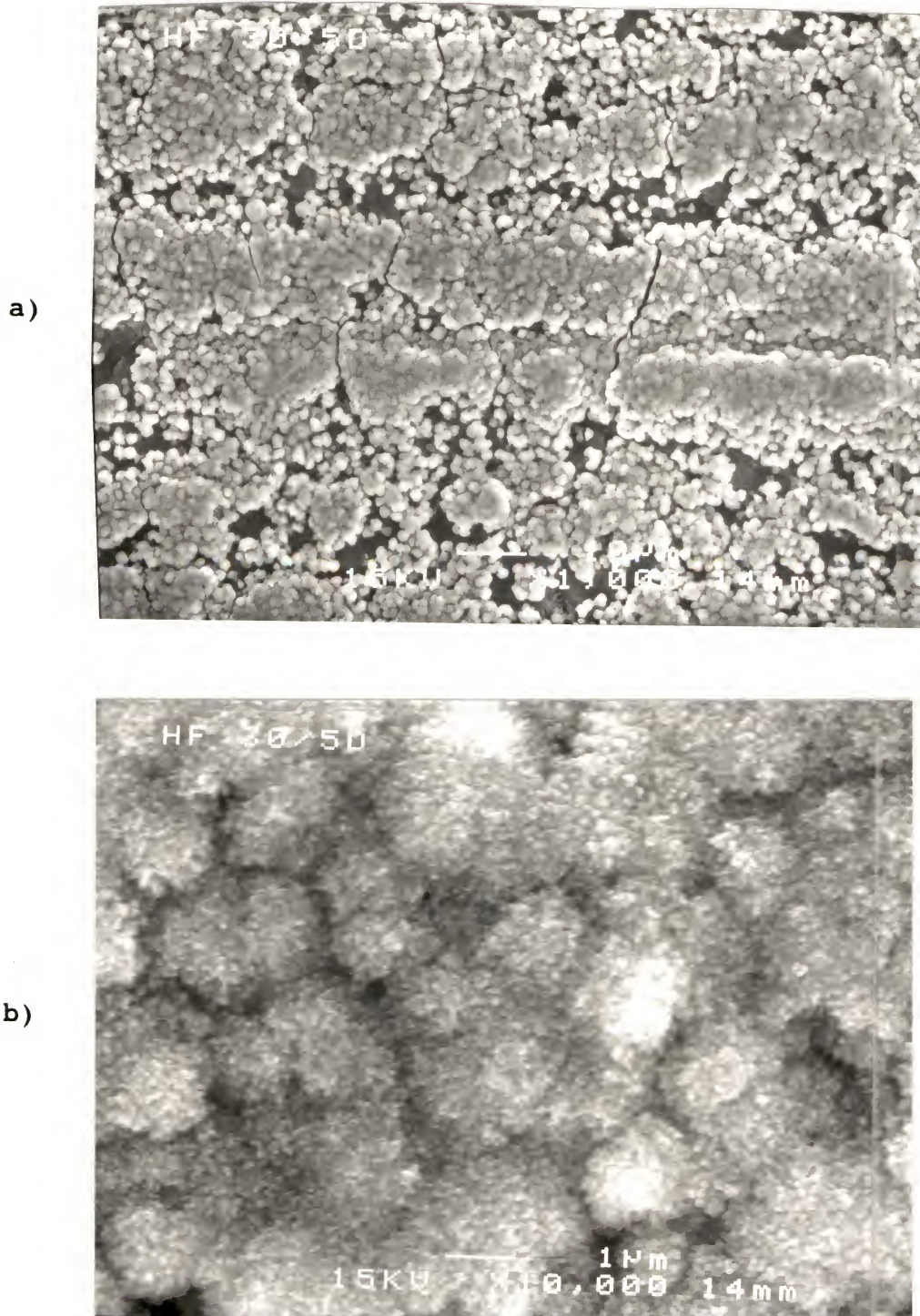
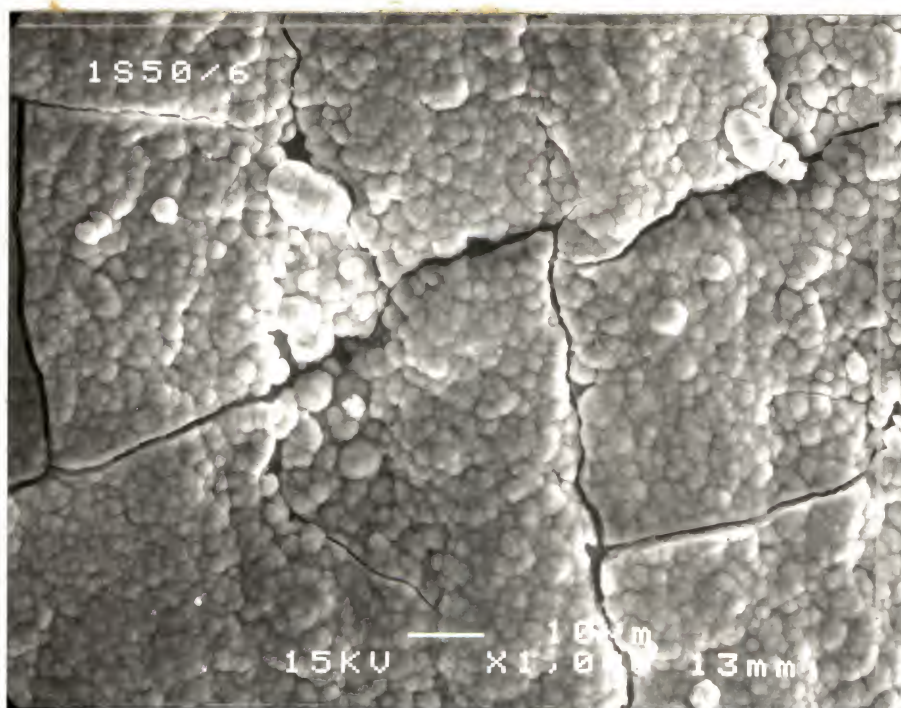


Figure 4.18 SEM micrographs showing morphology of hydroxyapatite formed on gel-silica glass 1S3.1/600 after immersion in SBF for 7 days: a) 1000x; b) 10,000x.



a)



b)

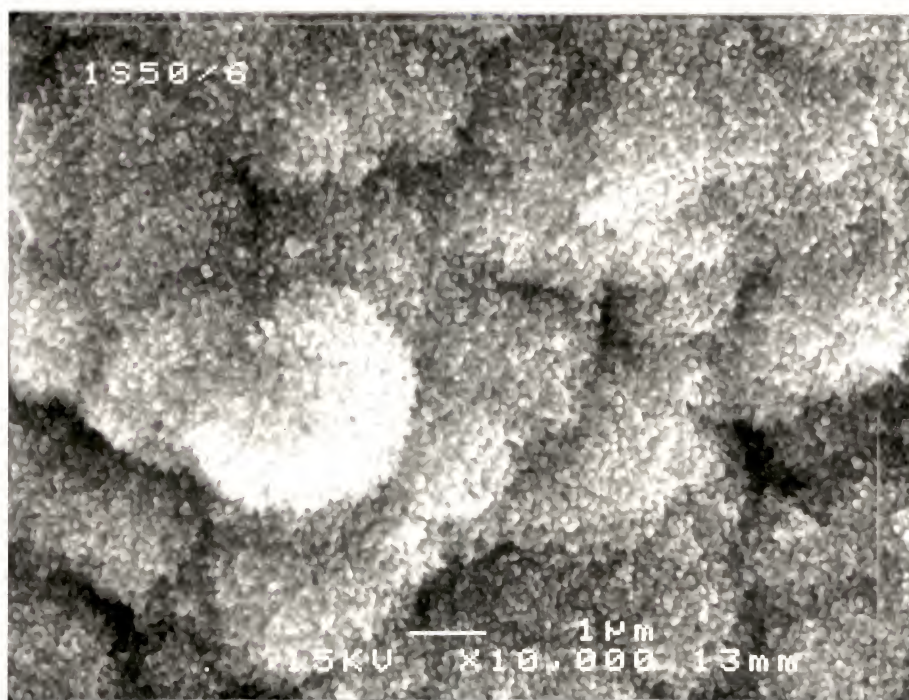


Figure 4.19 SEM micrographs showing morphology of hydroxyapatite formed on gel-silica glass 1S5.3/600 after immersion in SBF for 6 days: a) 1000x; b) 10,000x.

4.19) and is oriented in one specific direction, i.e., toward the surrounding fluid.

The different morphologies described above were also observed by P. Li et al. for hydroxyapatites precipitated on silica gel-glasses (Li93d). However, the variation in morphology was related to a variation in the pH of the solution, the concentration of calcium and phosphorus, and the presence of added fluorine.

#### 4.4 Discussion

The rate of precipitation of hydroxyapatite is strongly affected by the composition of the sol-gel derived glasses as shown in Figure 4.5. As discussed before, the compositional variation includes simultaneous variations in texture and glass dissolution rate, and consequently, in the final pH and ionic concentration of the surrounding fluid. The isolated effect of each of these parameters was studied on the pure silica gel system. The results show that both SBF solution parameters and the texture of substrates control the rate of heterogeneous precipitation of hydroxy carbonate apatite.

Both concentration and pH have a remarkable effect on the rate of apatite formation. The effect of the concentration of the species involved, in this case  $\text{Ca}^{2+}$  and  $\text{HPO}_4^{2-}$ , are apparent through nucleation theory. The nucleation rate per volume is given by:

$$(I_v)_{eq} = u n_s n^* \quad (4.1)$$

where  $u$  is the collision frequency of single molecules with the nuclei and  $n_s$  is the number of molecules on the periphery of the critical size nucleus  $n^*$ . An increase in the concentration increases the nucleation rate thus decreasing the induction time for nucleation, as observed in this work. The pH effect is also implicit in this theory since the thermodynamic barrier for nucleation is a function of the pH of the solution (Bro81).

At the concentration levels studied here, which are generally involved in bone formation at the surface of bioactive materials, heterogeneous precipitation of hydroxyapatite occurred on the surfaces of sol-gel derived porous silica and porous Vycor. It did not occur however on the surface of dense silicate glass or quartz substrates, even for the highest calcium concentration analyzed. These results confirm the importance of the porosity of the silica substrate on the heterogeneous nucleation of HA, as discussed by P. Li et al. (Li92a, Li93a).

The rate of HA formation depends on the texture (pore size and pore volume) of the porous silica substrate as shown in Figure 4.11. The variation in texture affects also the morphology of the precipitated HA. To understand these results the substrate related factors that possibly affect the nucleation of HA are discussed: 1) hydroxyl



concentration, 2) total amount of hydroxyl, 3) rehydration rate, 4) electric double layer, 5) restricted diffusion.

One of the hypotheses in the literature assumes that hydroxyl groups act as nucleation sites for HA formation. It is argued (RLi91b, PLi92) that the gel structure would have a higher concentration of hydroxyl groups on the surface, thus increasing the nucleation rate. Zhuravlev (Zhu87) determined the OH coverage of amorphous silicates for one hundred different samples of silicate particles and gels. He found that, in the fully hydroxylated state, the average hydroxyl coverage equaled  $4.9 \text{ OH/nm}^2$ , independent of the form or synthesis conditions of the amorphous silica. Presumably on such small length scales, there is no effect of surface irregularity (fractal surfaces) so that all forms of silica exhibit approximately the same hydroxyl coverage. For dehydroxylated surfaces the OH coverage decreased with thermal treatment temperature, varying from  $4.9 \text{ OH/nm}^2$  (fully hydroxylated) to  $0.2 \text{ OH/nm}^2$  ( $1000^\circ\text{C}$ ). For a given temperature the hydroxyl coverage was also independent of the textural characteristics and method of preparation.

Silica gels with different textures treated at the same temperature exhibit different HA induction times (Figure 4.11) although they present the same initial OH coverage according to Zhuravlev (Zhu87). Differently from Zuravlelv's results, Iler (Ile79) points out that on small negative radii of curvature, as present in small pores, there is more hydrogen bonding and dehydroxylation is more difficult.



Thus, the smallest pore size should have the highest OH coverage and the smallest HA induction time, opposite to results observed in this study. In either case, a difference in hydroxyl coverage does not explain the variation in induction time for different pore size gels treated at the same temperature.

The HA nucleation rate could be related to the total amount of OH rather than to the OH concentration on the surface. In this case the nucleation rate would be directly related to the surface area of the material. The data of this study show that this is not the case. The larger pore size gels have a lower surface area but are more reactive, i.e., exhibit a lower induction time for HA formation.

When the dehydroxylated silica substrate is put into an aqueous solution or water containing atmosphere, rehydration will occur until the fully hydroxylated equilibrium state is reached. The rehydration rate depends on the degree of dehydroxylation of the surface; the more completely the surface is dehydrated the longer is the time required for rehydration (You58, You60). According to Iler (Ile79) it is likely that rehydration occurs only next to a hydroxyl group and the hydroxylated area grows in patches as hydration proceeds along the boundary between hydroxylated and siloxane areas. Bunker et al. (Bun89) and Wallace et al. (Wal93) showed that the rehydration kinetics depends on the treatment temperature of silica gels and related the

rehydration rate to the presence and concentration of trisiloxane ring defects on the structure.

The studies reviewed above indicate that the initial hydroxyl coverage and subsequent rehydration rates decrease as temperature increases. The results of the present study show that HA nucleation rate is much higher on 1.2 nm gel-silica treated at 400°C than on the same gel treated at 600°C. P. Li et al. (Li93c) also showed that the induction time for HA nucleation increased with sintering temperature for gel-silica glasses sintered in the range 900-1200°C. These results support the hypotheses that the initial OH coverage and subsequent rehydration rate affect the rate of HA formation on gels treated at different temperatures. This argument however does not apply to different pore size gels treated at the same temperature.

In previous work, P. Li and Zhang (Li90) applied the concept of the electrical double layer to the analysis of the mechanism of HA precipitation on silica substrates. They pointed out that cations present a higher activity in the electrical double layer developed around the negatively charged surface of silica at neutral pH. The increase in concentration of ions in the interface would lead to the nucleation of HA. Later P. Li et al. (Li94) confirmed the role of the negative surface potential by showing that HA precipitation occurs on silica and titania substrates, both presenting negative surface charge, but it does not occur on

alumina, which presents a positive surface charge. All substrates were porous, produced by a sol-gel process.

The concept of enhanced ionic activity associated with the electrical double layer can be extended to support the hypotheses that pores are nucleation sites for hydroxyapatite. Inside a pore a superposition of the surface potential will increase the ionic activity as compared to a flat surface. Thus, the ionic concentrations inside the pores will be higher than at any other part of the surface and the degree of supersaturation required for heterogeneous nucleation is more likely to occur inside the pore.

In order for supersaturation to be reached inside the pores, diffusion of ions from solution must occur. Kunetz (personal communication) studied the diffusion of several cations into silica gels with different pore sizes. The diffusion coefficient was dependent on the ions present in solution, the solution pH and on the pore size of the gel. A very large decrease in the diffusion coefficient was observed as the pore size decreased. Thus, restricted diffusion into small pore size gels must be a factor that affects the nucleation of HA inside the pores. It should be noted that the studied gel-glasses having a very low average pore radius, also have a larger fraction of small pores including pores with a radii below 1.0 nm (see Fig. 4.1b). Diffusion into these very small pores may not be possible and will depend on the size of the ion and its hydration sphere.



In considering the diffusion of ions into the pores of gel-silica it is reasonable to consider that parameters such as ionic radius might have a large effect. In particular, the diffusion of  $\text{HPO}_4^{2-}$  ion, which has with its hydration layer a diameter of approximately 4-6 Å, should limit the rate of HA nucleation. It should also be remembered that in the experiments considered here, the SBF solution used contains besides  $\text{Ca}^{2+}$  and  $\text{HPO}_4^{2-}$  several other cations. A competition for diffusion into the pores to form the electric double layer should therefore be expected. This could explain the observation that  $\text{Mg}^{2+}$  (ionic radius=0.66Å) which has an ionic radius smaller than  $\text{Ca}^{2+}$  (ionic radius=0.99Å) slows down the nucleation of HA (Fil93, Li93a). As the magnesium concentration in solution increases, the electrical double layer becomes enriched with this ion and the induction time for HA nucleation increases.

The above discussion shows that the textural effects (pore size and pore volume) on the formation of HA can be understood if we assume pores to serve as nucleation sites. As pore volume decreases the number of nucleation sites decrease and consequently the nucleation rate decreases. Increasing the treatment temperature of the gels decreases the pore volume and an increase in the induction time for HA nucleation is observed. As the pore size decreases, restricted diffusion of ions into the pores becomes a limiting factor and nucleation rate decreases. This analysis does not exclude the role of the hydroxyl coverage on the HA



nucleation, since the rehydration and establishment of the electrical double layer will depend on this parameter.

#### 4.5 Conclusions

The rate of HA formation depends on the composition of sol-gel derived glasses in the system  $\text{CaO-P}_2\text{O}_5\text{-SiO}_2$ . HA precipitation occurs on the three component gel-glasses as well as in pure silica gel-glasses. The general requirement for precipitation appears to be a porous, negatively charged substrate. The nucleation rate increases with ion concentration and pH of the solution. Besides solution parameters, the texture of the substrate, which depends on method of preparation and thermal history, greatly affects the nucleation rate. The induction time for HA nucleation increases as pore volume and pore size decrease. The nucleation of HA likely occurs inside the pores through the establishment of an electrical double layer with higher ionic concentration. The number of nucleation sites, defined by the textural characteristics of the gel, and the diffusion of ions into the pores are parameters that control the nucleation rate, not the surface hydroxyl concentration.

CHAPTER 5  
MECHANISMS OF HYDROXYAPATITE  
FORMATION ON SILICA SUBSTRATES: A REVIEW

5.1 Introduction

The past 20 years of research on bioactive glasses and glass-ceramics has revealed much about the various aspects of the unique characteristic of these materials, the bone-bonding ability. Information on both the material response and the host tissue response has helped to understand the biological performance of these bioactive materials. The results of in vivo and in vitro studies, through the use of many analytical tools, has led to the conclusion that in all cases in which bone bonding occurs, it does so through the formation of a biologically active hydroxy carbonate apatite (HCA) layer. This appears to be the only common characteristic of all the known bioactive implants.

The knowledge that the interfacial bonding involves the formation of an HCA layer stimulated research groups around the world to investigate the parameters that control its formation and to propose mechanisms of apatite nucleation. In the case of bioactive glasses and some glass-ceramics it is generally a consensus that a silica gel layer plays an essential role in the nucleation and crystallization of

apatite. However, many questions concerning the mechanism of hydroxyapatite (HA) induction remain to be answered and some hypothesis lack experimental evidence. To mention some of those questions:

- Is soluble silicon involved in the nucleation of hydroxyapatite?
- Is the formation of a silica gel layer a necessary step in establishing bioactivity?
- How do the textural features of the silica gel layer affect the nucleation of HA?
- What is the effect of surface charge on HA induction?
- Many publications suggest that silanol groups present on the surface of the silica gel act as nucleation sites for apatite formation. Is there evidence to support this hypothesis? Will silanol concentration be a rate determining factor?
- Are trisiloxane ring concentration and its effect of the rehydration of the silica surface rate determining for HA induction?
- Does the rate of HA induction control the level of bioactivity? If so, why?

In this chapter we discuss possible answers to these questions by presenting a review of the literature up to date on the subject of HA formation on silica substrates. The parameters known to affect HA nucleation are reviewed. The proposed mechanisms and the experimental evidence to support them are discussed.

## 5.2 Effect of Solution Parameters on Apatite Formation

The solution parameters pH, temperature, and ionic concentration have a large effect on the type of calcium phosphate (CP) precipitated from solutions containing  $\text{Ca}^{2+}$  and  $\text{HPO}_4^{2-}$  ions and their rate of formation. This is well established for spontaneous precipitation as well as for heterogeneous precipitation of calcium phosphates (LeG91). This discussion is concerned only with the heterogeneous precipitation of hydroxyapatite (HA) on silica substrates. For this particular case it was determined that as pH (in the range 7.0 to 7.4) and concentration of the ions  $\text{Ca}^{2+}$  and  $\text{HPO}_4^{2-}$  increase the rate of HA formation increases (Li93f, Per94).

When studying the heterogeneous precipitation of HA on silica substrates it is important to establish the conditions for which homogeneous precipitation may also occur. We evaluated the stability of calcium and phosphate containing solutions with respect to homogeneous precipitation of CP. Three solutions were evaluated (Table 5.1): a Simulated Body Fluid solution (SBF), and two other solutions obtained by adding extra  $\text{Ca}^{2+}$  ions to the SBF, as calcium chloride. All solutions were prepared with a pH = 7.25.

Ca and P concentrations were measured by Inductively Coupled Plasma (ICP) atomic emission spectroscopy analysis of the solutions as prepared and after maintaining at 37°C



Table 5.1  
Nominal Ca Concentration in the SBF Solutions.

Solution	Extra Ca <sup>2+</sup> Added (mM)	Total Ca <sup>2+</sup> (mM)	Total Ca <sup>2+</sup> (ppm)
SBF	-	2.5	100
SBF/Ca200	2.5	5.0	200
SBF/Ca300	5.0	7.5	300

Table 5.2  
Measured Ca and P Concentrations in SBF Solutions  
Before and After Maintaining at 37°C for the Period  
Indicated.

	Ca (ppm)			P (ppm)		
	0	20 days	60 days	0	20 days	60 days
SBF	91	91	91	30	30	30
SBF/Ca200	164	117	-	30	2.8	-

\* error =  $\pm 5\%$

for several time periods in a polyethylene container. The results are presented in Table 5.2. No decrease in the Ca and P concentrations was observed for the SBF solution maintained at 37°C for up to 60 days. A decrease in concentration of both elements was observed in the SBF/Ca200 solution maintained at 37°C for 20 days, although no apparent precipitation had occurred. No measurements were performed on the SBF/Ca300 since precipitation could be visually observed after only two days. These results confirm that SBF, although supersaturated with respect to HA (Neu58), is a metastable solution. The precipitation of HA from SBF on a pure silica substrate can therefore be considered as occurring exclusively through a heterogeneous nucleation process. However when other bioactive glasses or glass-ceramics are immersed in SBF, the release of  $\text{Ca}^{2+}$  ions into solution due to the glass dissolution may increase the concentration to about 200 ppm or above. For this supersaturation level homogeneous precipitation may occur concurrently with heterogeneous precipitation. This fact should be taken into account when reaction rates are measured and mechanisms of HA nucleation are proposed for bioactive materials.

### 5.3 The Silica-Rich Gel Layer Requirement

The development of the hydroxyapatite layer on top of a silica-rich layer was detected on Bioglass® (Pan74, Cla76,

Hen82, Kim89), other bioactive glasses derived from Bioglass® (And90a), and on the glass-ceramic Bioverit® (Hol85). Discussions of the mechanism of HA formation on those materials have included the role of the silica gel layer. On the glass-ceramics Ceravital® and A-W, a silica-rich layer was not detected (Kit87, Oht91, Neo92). In this case, other mechanisms have been proposed that do not include a silica gel layer as a necessary step.

Kokubo (Kok90a) suggests that the silicate ions dissolved from the glassy matrix might play a role in providing favorable sites for the nucleation of the apatite on the glass-ceramic A-W. The validity of this hypothesis is discussed in the next topic. However, if the changes occurring in the phases present in the glass-ceramics when immersed in aqueous medium are considered, the involvement of a silica gel is still a possibility. The glass-ceramic A-W consists of two crystalline phases, apatite and wollastonite ( $\text{CaO-SiO}_2$ ), and a glassy phase. The glassy phase is about 28 wt % of the glass-ceramic and consists of 16.6 MgO, 24.2 CaO, 59.2  $\text{SiO}_2$  (Kok90a). The calcium and silicate ions released in solution originate from the dissolution of wollastonite and the glassy matrix. Therefore, after exposure to SBF the material consists of a basically unchanged apatite phase, mixed with a calcium depleted glassy phase and wollastonite. Although a silica layer is not detected, a silica-rich gel matrix should be present, especially at grain boundaries.

Another possibility in the case of A-W glass-ceramic is the occurrence of homogeneous precipitation. The changes in concentration of the elements in SBF upon immersion of A-W glass-ceramic shows that after 1 day immersion the calcium concentration reaches approximately 180 ppm and increases to above 300 ppm in 5 days (Kok90a). The concentrations near the glass interface may actually be higher as the glass starts to dissolve. Therefore homogeneous nucleation is a real possibility. The HA formed may then deposit on the rough surface formed by the preferential dissolution of the wollastonite phase and the glassy matrix.

In conclusion, a silica-rich gel is always involved in the nucleation of apatite on bioactive glasses. In the case of glass-ceramics it may be involved but other mechanisms, such as homogeneous nucleation, are possible as well.

#### 5.4 Soluble Silicate Species on Apatite Nucleation

The hypothesis that soluble silicate ions are involved in the nucleation of apatite was investigated by Kokubo (Kok90a). He showed that when alumina (6.3 wt%) was included in an apatite-wollastonite glass-ceramic A-W(Al) no apatite formed on the surface even after 60 days immersion in SBF. This effect was attributed to the fact that the aluminum ions concentrated in the glassy matrix suppressed the dissolution of calcium and silicate ions. He then added these two ions to the SBF solution individually and together



and examined the formation of an apatite layer. The apatite layer was not formed on the surface of A-W(Al) immersed in SBF when  $\text{Ca}^{2+}$  or  $\text{HSiO}_3^-$  ions were added individually, whereas it formed when  $\text{Ca}^{2+}$  was added in combination with  $\text{HSiO}_3^-$  ions. These results suggested that the silicate ion might provide favorable sites for nucleation of apatite.

However, no direct information was presented on whether the soluble silicate added remained as a soluble species in solution. The concentration of  $\text{HSiO}_3^-$  added (1.8 mM) in addition to silicate ions that dissolve from the glass-ceramic (1.2 mM) reach a value higher than 2 mM, a concentration above which polymerization occurs, initially forming polysilicic acids of low molecular weight (Ile79).

The effect of soluble silicate species on the precipitation of HA was also investigated by Damen and Ten Cate (Dam89, Dam92). They analyzed the rate of precipitation of calcium phosphate by the change in the concentration of free calcium from solutions containing silicic acid. Two stock solutions, containing 2 and 20 mM silicic acid, were used to introduce silicon ions. In the 2 mM solution > 98% of the silicic acid was present as monomers. In the 20 mM solution, from 92 to 95% of the silicic acid was polymerized. They observed that stimulation of calcium phosphate precipitation could only be achieved by use of the stock solution that contained silicic acid largely in polymeric form. The stimulation effect was observed for rather low concentrations of silicic acid present (about

0.12 mM). The calcium phosphate precipitate was identified by x-ray diffraction as hydroxyapatite.

Damen and Ten Cate (Dam89) also tested the ability to stimulate HA precipitation using two types of silica powders. Both types of silica were effective, but at concentrations approximately 15 times higher than those necessary to achieve results equivalent with the polymerized silicic acid solution. The authors point out that this probably reflects a substantial difference in size and surface area between the particles in the silica powders and the silicic acid solutions. Hydroxyapatite precipitation was also observed on colloidal silica particles (Ada93) and on monolithic silica gels (Li92a, Per94).

Therefore, the experimental evidence indicates that hydroxyapatite precipitation involves the surface of silica particles, either colloidal, micron size or condensed into a gel, or oligomers of hydrated silica, rather than soluble monomeric silicate species, i.e., silicic acid.

### 5.5 Porous vs. Dense Substrates

The evidence discussed so far indicates that the hydrated silica surface stimulates the precipitation of hydroxyapatite. The next logical step is to question how the physical and chemical characteristics of the surface affect the nucleation of the precipitate. The following topics

discuss particular aspects of the silica surface and their relation with calcium phosphate precipitation.

A physical aspect of the silica surface that has been considered critical in HA precipitation is the porosity. It was first investigated by Walker (Wal77) on bioactive glasses of several compositions. He correlated the bonding ability of the glasses with the ability of that glass to react in aqueous solution to form a highly porous surface film. He established that the specific surface area of reaction films formed on bioactive glass surfaces depended on composition and that bone bonding occurred if the porosity resulted in surface areas greater than  $80 \text{ m}^2/\text{g}$ . He also observed bone bonding for Vycor®, which is a porous silica rich substrate. The importance of substrate porosity was further evaluated by P. Li and colleagues (Li92a). They showed that hydroxyapatite formed on silica gel immersed in SBF but not on dense silica glass or quartz. Unfortunately, they did not characterize the texture of the silica gels and the pore size distribution and volume fraction of porosity is unknown. Our results presented in the previous chapter also show that apatite forms on silica gels and porous Vycor® but not on dense borosilicate glass or quartz, confirming the findings of P. Li.

Calcium phosphate formation was also reported on colloidal (Ada93, Dam89) and micron size (Dam89) silica particles. However no information was available on the density or porosity of these particles.



Therefore, the available experimental evidence indicates that hydroxyapatite precipitates on porous silica substrates. Further evidence is needed to confirm if it can also form on dense silica particles or if there is a relationship between the particle size and the rate of hydroxyapatite nucleation.

### 5.6 Effect of Surface Charge

It is well known that silica presents a negative surface charge at neutral pH values which leads to the establishment of an electrical double layer with an increased concentration of cations at the interface. P. Li and Zang (Li90) applied the concept of the electrical double layer to the analysis of HA precipitation on bioactive glasses. They showed that the reactions occurring on the glass surface lead to the development of a negative surface charge and establishment of an electrical double layer. The consequent increase in concentrations of cations in the interface then lead to the nucleation of HA. P. Li et al. (Li93b, Li94) later extended this work by studying the precipitation of HA on three different oxides, silica, titania and alumina, immersed in SBF solution. All three substrates were porous, produced by a sol-gel process. They showed that HA precipitation occurred on silica and titania substrates, both presenting negative surface charges at physiological solution pH (Par65), but HA precipitation did



not occur on alumina, which presents a positive surface charge.

Zhong studied the precipitation of HA on silica gels immersed in SBF with and without the addition of  $\text{Al}^{3+}$  ions. He observed that the presence of  $\text{Al}^{3+}$  ions inhibited the formation of HA (personal communication). He suggests that these ions adsorb on the negative silica surface converting the surface potential to a positive charge.

Besides silica, HA precipitation was also observed on other negatively charged materials such as sephadex beads (Kru90) and collagen (Ban77).

These results indicate that heterogeneous HA precipitation is generally associated with negatively charged surfaces. However, quartz and dense silica glass, which also present negative surface potential at neutral pH, do not induce HA nucleation, as discussed before. Besides having a negative charge the oxide materials that were able to induce HA precipitation were porous substrates.

In summary, a negative surface potential is necessary but not a sufficient condition for the induction of heterogeneous precipitation of hydroxyapatite.

### 5.7 Effect of the Texture of Silica

Porous silica substrates induce the precipitation of hydroxyapatite. The rate of HA formation depends on the texture of the substrate as shown in the previous chapter.

For silica gels treated at the same temperature, the induction time for nucleation of hydroxyapatite increased as pore size and pore volume decreased.

For those gel-glasses the chemical characteristics of the surface, i.e., the concentration of hydroxyl groups, is the same. As shown by Zhuravlev (Zhu87), for a given treatment temperature the hydroxyl coverage is independent of the textural characteristics and method of preparation of the gel. Therefore, the change in nucleation time can be attributed solely to the textural variation between the gel-glasses.

To explain the textural effects observed we propose that the pores present in the gel structure act as nucleation sites. The superposition of the surface potentials inside the pores increases the ionic concentration and the degree of supersaturation required for heterogeneous nucleation. Thus, precipitation of HA is more likely to occur inside the pores. The rate of nucleation is then controlled by the number of sites available and by the diffusion of ions into the pores, both parameters related to the texture of the gel. As pore volume decreases the number of nucleation sites decrease and consequently the nucleation rate decreases. As the pore size decreases restricted diffusion of ions into the pores becomes a limiting factor and the nucleation rate decreases.

### 5.8 Hydroxyl Groups as Nucleation Sites for Hydroxyapatite

The discussion presented in the previous topics has shown that the induction of hydroxyapatite on the surface of silica substrates is affected by the physical aspects of the surface. The present topic focuses on the surface chemistry and its relation to the apatite nucleation process.

It has been suggested that the ability of a silica gel to induce the formation of hydroxyapatite is related to its state of hydration, i.e., the large amount of hydroxyl groups present on its surface (Hen91a, Li91a, Li92a). This hypothesis assumes that the silanol groups act as nucleation sites for HA. Attempts have been made to provide evidence for this theory, both experimentally (Li92a, Li93a, Li93c-f) and through the use of molecular orbital modeling (Wes92).

A large amount of work was done by P. Li and colleagues trying to provide experimental evidence for the involvement of silanol groups in the nucleation process. Initially, it was shown that apatite can form on the surface of silica gels immersed in a SBF solution but not on dense silica glass or quartz (Li92a). We confirmed those results as shown in the previous chapter. The assumption was made that the reason for this observation was the higher density of silanol groups on the surface of gels as compared to dense silica substrates. This is not enough evidence to support the involvement of silanols in the nucleation process. It can be argued that other differences exist between the gel-



glass and the dense glass such as: the presence of porosity in the gel-glass and the consequently different surface energy associated with the pore walls; the possibility of superposition of surface potentials inside the pores affecting the ionic distribution near the interface as discussed in Chapter IV; the different distribution of sizes of the silica rings constituting the gel-glass and the dense glass, especially the presence of metastable trisiloxane rings in the gel-glass.

A second set of experimental evidence P. Li and colleagues used to support the hypotheses of silanol involvement was the decrease of the rate of hydroxyapatite formation on silica gel as the heat treatment temperature of gels increased from 900 to 1200°C (Li93c). They point out that the concentration of hydroxyl groups and the consequent rate of rehydration of the silica surface decrease with temperature. This is a correct statement that has been confirmed by several investigators (You58, Bun89, Wal93). They then attribute the decrease in the rate of apatite nucleation to the decrease in the rate of rehydration. This correlation however is not necessarily true. First, it is well known that heat treatment affects not only the surface chemistry, i.e., concentration of silanols, but also the texture of the gels (Hen88b, Bri90). As shown in Chapter IV the rate of apatite formation is affected by the texture of the silica substrate. In his work, P. Li does not present any data on the texture of the gels or the change in texture



with temperature, and no reference is made to textural effects on HA formation. Second, a comparison of results presented in two different publications by the same authors (Li92a, Li93c) shows that gels treated at 400°C have an induction time for apatite nucleation approximately the same as gels treated at 900°C, although the gels have a large difference in hydroxyl concentration. Therefore, this prior work does not present evidence that the rate of hydroxyapatite formation is dependent on the hydroxyl concentration nor that the nucleation process involves hydroxyl groups.

Another experimental attempt to show the importance of Si-OH groups in nucleating hydroxyapatite was the addition of fluorine ions to the SBF solution in which silica gels were immersed (Li93a). No apatite formation was observed on silica gel when the F<sup>-</sup> concentrations was in the range 2.4 to 3.6 mM. This result was interpreted by the author as an indication that F<sup>-</sup> ions poison the silica surface with respect to its ability to induce apatite formation, by replacing OH groups to form Si-halogen bonds. They suggest that this chemical dehydroxylation reduces the concentration of hydroxyl groups on the surface so that apatite nucleation can not occur.

The equilibrium reaction between silica and fluorine ions has been described in the literature (Ile79):



Although the formation of  $\text{SiF}_6^{2-}$  is possible at physiological pH, the reactions above indicate that it is favored by acidic conditions. There is no direct evidence that the Si-halogen bonds were actually formed at the conditions of the experiment. Therefore, these results are not conclusive evidence of the involvement of silanols in the HA nucleation process.

A different approach to the possibility of the nucleation of HA through silanol groups was presented by West and Hench (Wes92). They use a semi-empirical molecular orbital modeling theory to analyze the possible mechanisms of HA nucleation on a hydrated silica cluster. In their model they compare the enthalpy of formation for Ca-P chain structure bonded to a tetrasiloxane ring with a Ca-P ring structure bonded to a tetrasiloxane ring. This approach differentiates the nucleation on silanol groups present in particular silica-ring structures. Therefore, it has the potential for being much more selective in terms of determining possible low energy pathways for apatite nucleation. It might show that nucleation occurs indeed through surface silanol groups, but only those bonded to a specific silica unit. However the work mentioned above is only the beginning step in the calculation process. It simply shows that Ca-P chains bonded to tetrasiloxane rings are more stable than Ca-P rings bonded to the same structure.

Another theory that calls for the involvement of specific silanol groups on the nucleation process was proposed by Karlsson et al. (Kar89). They suggest that  $\text{Si-O}^-$  pairs form chelates with phosphate ions, and that this is an essential step in the apatite formation. The specificity in this theory is related to the spatial distances involved. According to the authors, the silica gel is "flexible" enough to provide the same oxide-oxide spatial requirements to match the apatite lattice, thereby providing epitaxial sites for the apatite growth. However, there is little experimental evidence to support the epitaxy mechanism. Molecular orbital modeling may be used to evaluate the energy of formation of such phosphate complexes but has not been done.

A considerable amount of additional work has to be done to define a HA nucleation mechanism using the MO modeling approach. The following steps must include the comparison of different silica-ring sizes, bonding of the Ca-P structure to both closed and opened rings, etc. Naturally, this approach has the inherent limitations of molecular orbital modeling, such as a limitation on the sizes of the clusters for which calculation is feasible considering the computational times involved. As pointed out by West and Hench, another limitation in this particular case is the restriction to the use of XHMO model (Extended Huckel Molecular Orbital) , since modeling of structures containing Ca is not presently possible with other models that have



higher physical accuracy. New MO codes are coming available which will circumvent both of these limitations and use of them together with laser spectroscopy experiments will probably be needed to determine the molecular mechanism for HA nucleation.

#### 5.9 Hydroxyl Concentration as a Rate Determining Factor in Hydroxyapatite Formation

The discussion in the last section shows that the involvement of silanol groups in the HA nucleation process is possible, but there is still no conclusive evidence of the importance of silanols. If silanols are demonstrated to be involved, a second question follows: is the rate of HA formation controlled by the hydroxyl concentration on the silica surface?

To determine the effect of hydroxyl concentration and rehydration rate on the rate of hydroxyapatite nucleation the following experiment was performed. Silica gel samples with an average pore radius of 3.0 nm were heated to 600, 950 and 1050°C and maintained at temperature for 3 hours. The textural characteristics of the gel-glasses, measured by N<sub>2</sub> adsorption isotherms, are presented in Table 5.3. The hydroxyl concentrations, as indicated by Zhuravlev (Zhu87), are included in this table. Samples treated at 950 and 1050°C were rehydrated, by soaking in deionized water and maintaining at 100°C for 48 hours, and then dried with a schedule ending at 180°C. Rehydration of the surface should



Table 5.3  
Texture of Gel-Silica Glass 1S3.1 Treated at the  
Indicated Temperature and Correspondent Hydroxyl Coverage.

Temperature (°C)	Surface Area (m <sup>2</sup> /g)	Pore Volume (cm <sup>3</sup> /g)	Pore Size (nm)	OH/nm <sup>2</sup>
180	561	0.87	3.1	4.9
600	527	0.82	3.1	1.5
950	473	0.57	2.4	0.3
1050	253	0.26	2.1	0.15

Table 5.4  
Induction Time (days) for Nucleation of  
Hydroxyapatite on Gel-Silica Glass 1S3.1.

Condition	Temperature T		
	600°C	950°C	1050°C
Dehydroxylated at T	6 1	6 1	7 1
Dehydroxylated at T and Rehydrated	-	6 1	7 1

be complete after this treatment (Ile79) and the hydroxyl coverage is expected to be approximately the same as the original gel in the dried state. No significant changes in texture were observed after the rehydration procedure. Samples in both conditions, dehydroxylated and rehydrated, were soaked in SBF solution for several time periods, then removed and dried in air. The surfaces were analyzed by FTIRS.

The induction times for apatite nucleation based on the FTIRS results are presented in Table 5.4. A slight decrease in the induction time is observed for the samples treated at 1050 C. No significant difference is observed between the dehydroxylated and the rehydrated samples. These results show that the rate of apatite formation is not determined by the concentration of hydroxyl groups on the silica surface.

#### 5.10 Conclusions

It is clear that silica substrates induce the formation of hydroxyapatite. The experimental evidence indicates that the precipitation process involves the surface of silica particles or oligomers of hydrated silica, rather than soluble monomeric silicate species. Physical aspects of the silica surface, the negative surface charge and the presence of porosity, are directly responsible for HA precipitation. The rate of HA nucleation is affected by the texture of the silica substrate, increasing as pore size and pore volume

increase. Contrary to what was previously proposed by other investigators, the concentration of hydroxyl groups on the silica surface does not control the rate of HA formation. The involvement of silanol groups in the nucleation process, although possible, is not supported by the evidence presented so far.

CHAPTER 6  
IN VIVO EVALUATION OF BIOACTIVE  
SOL-GEL DERIVED GLASSES

6.1 Introduction

The biological performance of any biomaterial relies on both the material response and the host tissue response (Gro88). The material response depends on the physical and chemical properties of the material and on the environmental conditions in the implantation bed. The host response is by definition the particular response of the implantation bed elicited by the chemical and physical properties of the implant material (Gro88). An evaluation of the material response, represented mainly by its reactivity in the physiological environment, can be done by in vitro experimentation, as extensively used in the study of bioactive glasses and glass-ceramics. However, the assessment of the material response for a particular implant situation as well as the host tissue response are better accomplished by in vivo studies. Therefore a complete picture of the biological performance of a biomaterial is obtained by combining the results of in vitro and in vivo analysis.



The in vitro behavior of sol-gel derived bioactive glasses has been described earlier (Li91a-b). Chapters II and III of this work also present the in-vitro characterization of glasses produced by an alternative all alkoxide sol-gel process that yields a more homogeneous material. The studies show that these materials undergo very fast surface reactions resulting in a rapid rate of hydroxyapatite formation (Li91a, Per93b). Until now there has been no in vivo evaluation of bioactive glasses produced by the sol-gel process. This is the subject of the present chapter.

The application selected for the in vivo testing of the bioactive sol-gel derived materials was direct pulp cap therapy. Pulp capping is the treatment used for mechanical or traumatic dental pulp exposures and also asymptomatic teeth with deep caries. This procedure is commonly done with calcium hydroxide products (Cve78, Mar77). However, the use of this treatment has been questioned, because some investigators have demonstrated degenerative changes, such as persistent inflammation and ectopic calcifications, in the remaining pulp tissue (Mas65, Pat67). Alternative materials have been tested but limited success has been reported. Recently, a bioactive glass (Bioglass 45S5) was tested for use as a pulp capping agent (Ogu93). The results indicate a similar bridging with reparative dentin formation as occurs with calcium hydroxide, but with a lower inflammatory response. It is expected that the sol-gel

derived glasses present a better or at least similar performance as the conventional bioactive glass (45S5 Bioglass®).

The purpose of this study is to evaluate the safety and efficacy of bioactive powders produced by sol-gel processing as a pulp capping agent and to compare the biological performance of these materials with that of a conventionally produced bioactive glass, as well as a conventional pulp capping material, calcium hydroxide.

## 6.2 Experimental Procedures

Procedures were performed in accordance with ANS/ADA Document No. 41 regarding Recommended Standard Practices for Biological Evaluation of Dental Materials. This document calls for the use of subhuman primates or dogs for pulp cap testing. Adult mongrel dogs were selected as they are easier to handle and less expensive to procure and maintain. Pulp-capping procedures were carried out in 28 teeth in each animal in order to yield a minimum of 7 teeth to be evaluated for each experimental product to be tested at each of three time periods (7 days, 60 days, and 1 year). The pulp exposures were treated with experimental and control materials, then restored conventionally.

### 6.2.1 Experimental and Control Materials

Two compositions of sol-gel derived bioactive glass powders having a higher and a lower silica content were used. For comparison two glasses produced by conventional glass technology were also used. Table 6.1 presents the nominal glass compositions.

The sol-gel derived glasses were prepared according to a procedure developed by R. Li (Li91a) in which calcium nitrate is used as the CaO precursor. Although the powders produced by this procedure are not homogeneous in terms of calcium distribution in the glass network, as discussed in Chapter II, they were used in this study for two reasons: 1) at the time these experiments started the more homogeneous calcium alkoxide derived glasses (Chapter II) were still not developed, 2) despite its heterogeneity, the calcium nitrate derived glasses showed high bioactivity according to in vitro tests (RLi91b). The samples were prepared from tetraethyl orthosilicate (TEOS), triethyl phosphate [OP(OEt)<sub>3</sub>] and calcium nitrate (CaNO<sub>3</sub>·4H<sub>2</sub>O). Nitric acid was added to accelerate the hydrolysis reaction of TEOS. After mixing the components, the sol was cast into polyethylene containers and placed inside an oven at 60°C where the sol gelled and aged. The samples were then dried with a heating schedule ending at 180°C. The dried gels were heated in a silica crucible at a temperature of 600°C for 3 hours and

Table 6.1  
Composition of Experimental Materials in Mole %.

Material	Processing	SiO <sub>2</sub>	Na <sub>2</sub> O	CaO	P <sub>2</sub> O <sub>5</sub>
45S5	Conventional	46.1	24.2	26.9	2.6
60S	Conventional	60.1	17.7	19.6	2.6
54S	Sol-Gel	55.0	-	41.0	4.0
77S	Sol-Gel	80.0	-	16.0	4.0



subsequently at 700°C for 30 minutes. The material was then ground into powders with a particle size range of 106-250 $\mu$ m.

The conventional glasses were prepared by melting the raw materials in a crucible for 24 hours at 1350°C. The molten material was poured into distilled water, producing a glass frit, which was ball-milled and sieved to produce the powders in the same particle size range.

The in vitro bioactivity of the powders was analyzed according to the procedure described for powders in Chapter III. FTIR spectra of the powders immersed in a tris-buffer solution for 20 hours are presented in Figure 6.1. All materials show the formation of a hydroxyapatite layer indicating their bioactivity, except for the melt derived 60S glass. This glass is in the compositional boundary of bioactivity for melt derived glasses and is used here as a negative control of bioactivity.

A calcium hydroxide ( $\text{Ca}(\text{OH})_2$ ) product was used as a positive control. This material has proven efficacy as a pulp capping agent (Cve78, Cve87).

Before use, all the powders were sterilized in ethylene oxide.

#### 6.2.2 Pulp-Capping Procedure

The assignment of materials in each tooth was done by random selection before the surgical procedure. Table 6.2 summarizes the experimental design.

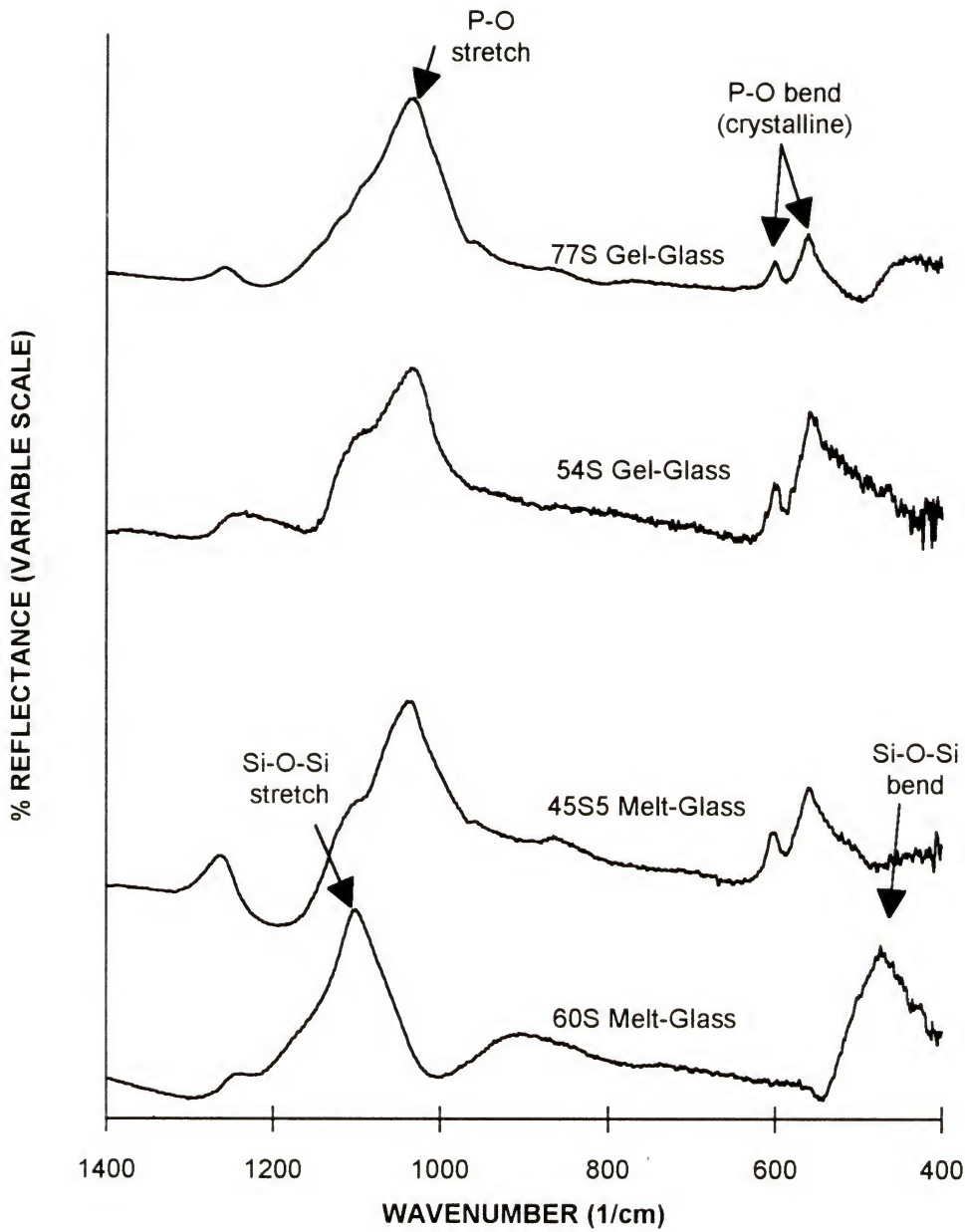


Figure 6.1 FTIR spectra of experimental bioactive glass powders after reaction in Tris buffer for 20 hours.

Table 6.2  
Experimental Design  
for Pulp Capping Treatment.

Material	Total No. of Teeth Treated		
	7 Days	60 Days	1 Year
Melt-Glass			
45S5	9	11	5
60S	8	11	4
Gel-Glass			
54S	12	13	5
77S	12	13	6
Ca(OH) <sub>2</sub>	16	14	8

The animals were anesthetized by induction with Ketamine 10mg/Kg and Xylazine 0.02 mg/Kg and maintained on Halothane. The selected teeth were cleaned, dried and disinfected with betadine. Approximately 4 mm diameter class five cavity preparations were made using sterile burs and high speed hand pieces under adequate water spray. Pulpal exposures 1-2 mm in diameter were made in the center of the cavity under sterile normal saline spray. Pulpal hemorrhage was controlled by continued irrigation of the exposure site with sterile saline and by placing a cotton pellet against the exposure site until hemostasis was obtained. The selected pulp capping agent was gently applied directly over the exposure, a Teflon disc was laid over the capping material and the cavity was restored with a zinc-oxide-eugenol cement.

The animals were sacrificed after 7 days, 60 days and 1 year. Block sections containing the teeth and the coronal 3 mm of the roots were removed immediately and fixed in 10% buffered formalin. All the fixed specimens corresponding to the 7 days and 1 year period were demineralized and 6  $\mu$ m serial sections prepared. The specimens for the 60 days period were divided in two groups: 1) one group was used for preparation of light microscopy serial sections, similarly to samples of the other time periods; 2) in the other group, the specimens were dehydrated, embedded in PMMA and thick sections (30  $\mu$ m thickness) were cut through the exposure site on a saw microtome (Leitz 1600).



### 6.2.3 Microscopic Examination

The 6  $\mu\text{m}$  serial sections made through the exposure site in each demineralized specimen were stained with hematoxylin and eosin. The sections were examined by an independent oral pathologist and the pathological changes in the dental pulp were recorded. The reparative dentin formation was recorded as none, partial or complete, based on its extent over the exposure site.

### 6.2.4 Scanning Electron Microscopy Examination

The thick sections obtained from the 60 days specimens were mounted in carbon discs, carbon coated and analyzed by scanning electron microscopy (SEM) with energy dispersive X-ray analysis (EDXA). This analysis allows the evaluation of the extent of surface reactions on each of the experimental materials.

## 6.3 Results

### 6.3.1 Microscopic Observations

The examination of the serial sections of the 7 and 60 days specimens showed that in general the capping materials were pushed (impacted) into the dental pulp, in some instances even up against the lingual wall. In a correct

surgical procedure the material should be localized outside the dental pulp, just laying on top of the exposure site. An evaluation of the problem led to the conclusion that it was caused because the Teflon discs used were too large for the cavity preparations, causing the capping material to be forced into the dental pulp. The results of the pathological examination of these specimens is therefore not reported here.

The pulp capping procedure was then repeated for the 60 days period. Two beagle dogs were used. The exposures were made and filled to yield 8 teeth capped with each experimental and control material. The surgical procedure was the same described before, except that the Teflon discs used were smaller. Two different sizes were used according to the size of the teeth and cavity preparation. The histological sections were examined and the results are reported below.

In general, the sections demonstrated generalized leukocyte infiltration, pus and hemorrhage. In some teeth complete necrosis of the pulp tissue occurred under the pulp capping agent. The inflammatory responses were not dependent on the pulp capping material used suggesting that the changes seen are related to causes other than material toxicity.

Very few specimens showed any dentin bridge formation. Specimens capped with gel-glasses 54S and 77S showed beginning of matrix (reparative dentin) formation and with

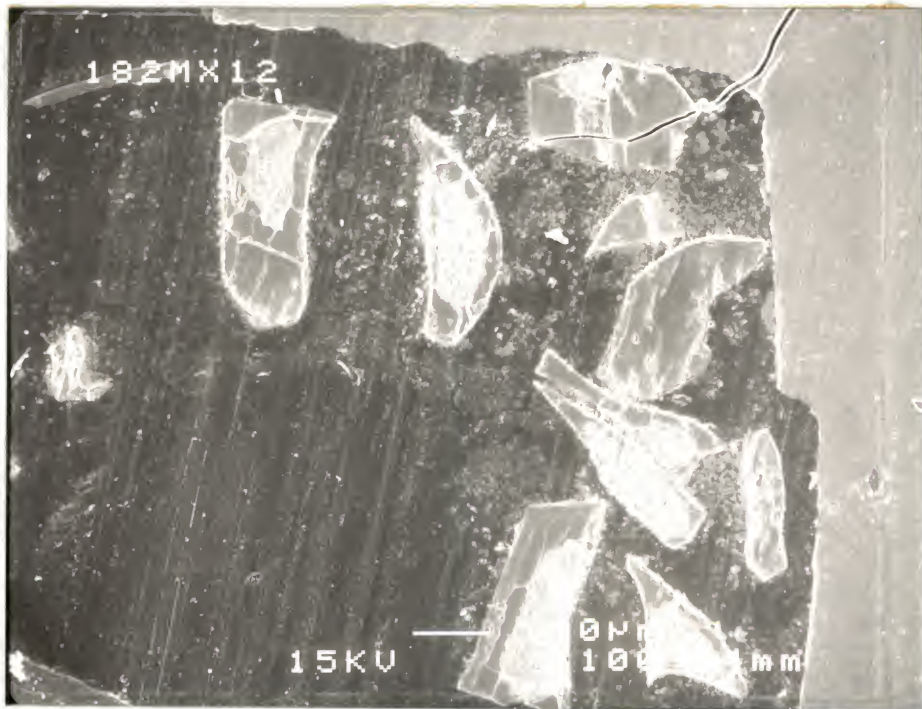
some pulps remaining vital despite severe degrees of inflammation. The matrix formation however was seen in only 1 out of 4 teeth examined. No dentin bridge formation was observed on teeth capped with  $\text{Ca(OH)}_2$ . Usually, good bridging occurs in 70 to 80% of specimens capped with this material.

### 6.3.2 SEM Observations

Figure 6.2 presents SEM micrographs of cross sections through the exposure site on 60 days specimens capped with melt derived glasses 45S5 and 60S. Three distinct regions can be observed on the particles of 45S5 Bioglass : a center region of rough appearance containing Si, Ca, Na, and P, similar to the original glass composition; an intermediate smooth layer consisting basically of Si; and an external layer, close to the edge of the particle, rich in Ca and P. These layers have been previously observed on bulk 45S5 Bioglass in several different implantation sites. These layers have been commonly described as the silica-rich layer and a calcium phosphate-rich or hydroxyapatite layer. Only two regions can be observed on the higher silica containing melt derived glass 60S: the center region with composition similar to the original glass composition and a thin layer depleted in Ca and Na, i.e., a silica rich layer. As observed before, this glass is at the boundary of



a)



b)

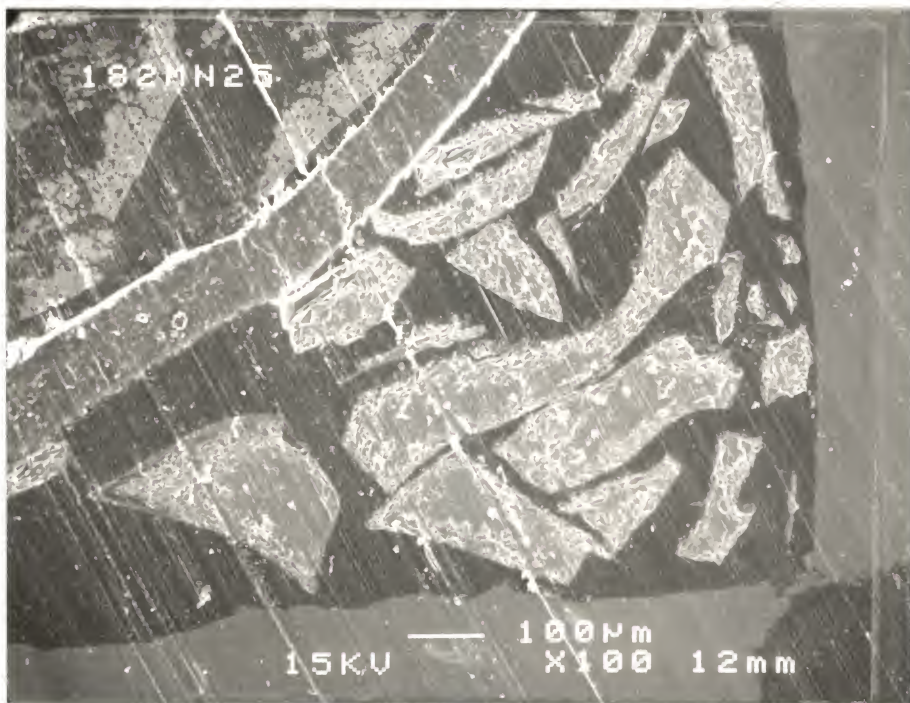


Figure 6.2 SEM micrographs of specimens capped with melt derived glass 45S5 Bioglass (a) and melt derived glass 60S (b); time period: 60 days.



bioactivity of melt derived glasses, and is not able to develop an external hydroxyapatite layer.

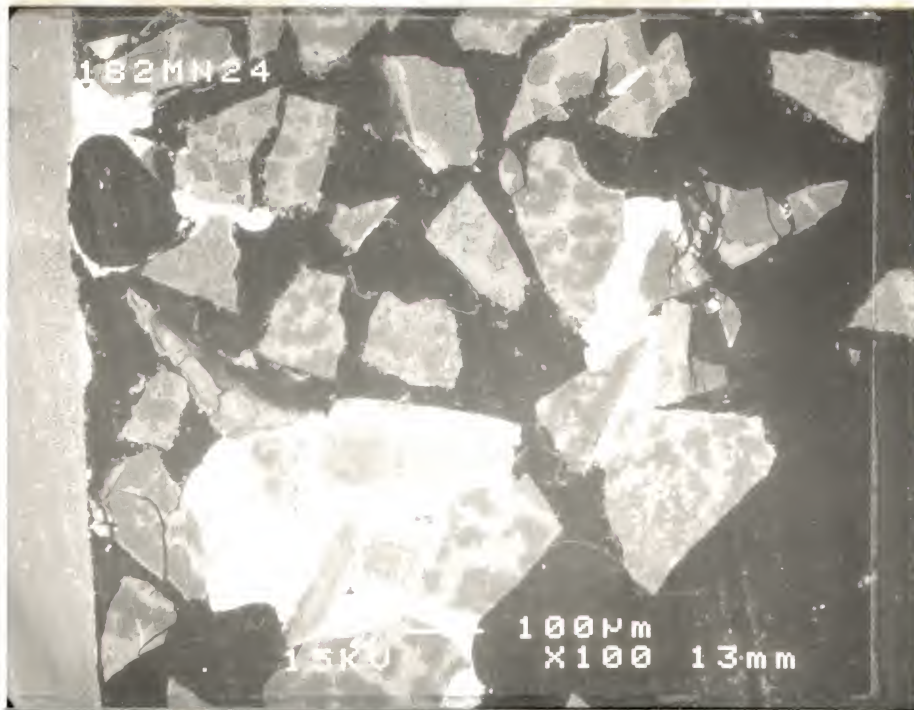
SEM micrographs of specimens capped with sol-gel derived glasses 54S and 77S are presented in Figure 6.3. Two regions are observed on the particles of the gel-glass 54S. The EDXA spectra show that the darker gray region has variable composition, going from points having Ca, P, and Si as in the original glass composition to points consisting basically of Si or Ca and P rich. The lighter gray pattern on the particles also varies in composition, being in general enriched with Ca and P. The white regions between the particles consist of calcium deposits. No distinct layers can be observed on the particles of gel-glass 77S. EDXA analysis show that the particles contain Ca, P and Si as in the original glass. However some particles analyzed showed a Ca and P enriched layer close to the edge.

#### 6.4 Discussion

The histological examination showed severe pulpal inflammation and poor or no reparative dentin formation for the experimental materials as well as for the control material. These results are very different from previous similar studies that used Bioglass and  $\text{Ca(OH)}_2$  as pulp capping agents (Ogu93, Cve78).

The pulpal inflammation was predominantly leukocyte in nature. This type of acute inflammation and pus formation is

a)



b)

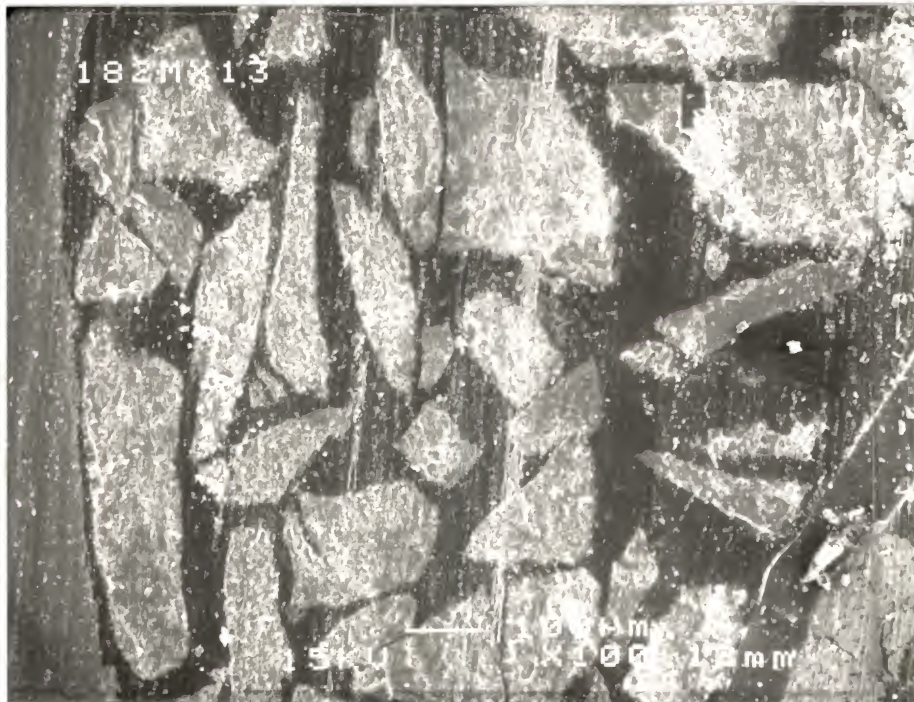


Figure 6.3. SEM micrographs of specimens capped with gel-glasses 54S (a) and 77S (b); time period: 60 days.



characteristic of a secondary bacterial infection. If material toxicity was the principal cause of the inflammatory response, the cellular infiltrate should contain chronic inflammatory cells such as lymphocytes, macrophages and plasma cells. Moreover, the inflammatory response was not a function of the pulp capping agent used, again suggesting that the changes seen are related to causes other than material toxicity.

In the present study dogs were used as the experimental model because this animal model is listed in the ANS/ADA Document No. 41 regarding Recommended Standard Practices for Biological Evaluation of Dental Materials. However, after reviewing pulp capping studies in the literature it appears that possible causes of the poor results encountered in this study are related to the particular experimental model used. The basis for this conclusion is described below.

Many pulp capping studies have been performed with the teeth of rats and primates and satisfactory results have been reported for  $\text{Ca(OH)}_2$  pulp capping (Tro74, Ave75, Pat76, Mar77, Cox82). Pigs were used in a previous study in which Bioglass 45S5 and  $\text{Ca(OH)}_2$  were compared (Ogu93) and good results were also reported. In contrast, pulp capping experiments performed in dogs (Bro79, Bim81, Wat81, For85) show that the results have been equivocal and not as predictable as with humans or non-human primates. In studies where partial success was reported, some special precautions were taken to reduce the oral bacterial flora.

The animals for which results are reported in this experiment were beagle dogs. It appears that the oral microflora of this dog contains a large percentage of anaerobic bacteria (Wun76). It is recommended that pulp capping experiments be performed via exposures in buccal class V cavities with the teeth of these animals. The location of these cavity preparations in the gingival makes it difficult to isolate with a rubber dam and therefore impossible to maintain complete asepsis. To counter this problem, previous investigators used antibacterial agents such as chlorexidine to prepare the teeth and remaining tissues prior to pulp exposures. This study used betadine for oral disinfection, but this was probably not adequate to render the area free of the anaerobic bacteria.

To confirm that the inflammatory response observed was caused by anaerobic bacteria, sections stained according to Brown and Brenn are currently being prepared for examination. Also, specimens from the 1 year animal are currently being analyzed. A preliminary evaluation has shown a higher degree of bridging with reparative dentin formation. It is possible that this particular species requires a longer post-operative time interval for complete healing. A definition of the direction to be taken will depend on the final evaluation of the results.

The SEM analysis showed that the extent of surface reaction on the glass particles depends on the composition of the glass, as previously observed for bulk implants. The



melt derived glass 45S5 and the gel-glass 77S present the formation of an external layer of calcium phosphate in accordance with the in-vitro results. Gel-glass 54S also showed the formation of a calcium phosphate layer on the particles. However, instead of a defined surface layer it appears as patches in the glass particles. Regions consisting only of calcium, probably  $\text{CaO}$ , are also present near the glass particles. These results show a very irregular reaction pattern which is probably due to the heterogeneous nature of the gel-glass. It may also be due to the inflammatory process in the sites which would produce a variable pH locally. The gel-glasses used in this study were produced by the calcium nitrate process. As discussed in Chapter II, the gel-glasses are heterogeneous in terms of the calcium distribution, specially when the calcium content is high as in the gel-glass 54S.

### 6.5 Conclusions

The histological examination showed that in general the sections presented a severe inflammatory response irrespective of the pulp capping agent used. Very few sections showed any reparative dentin formation. The uniform tissue response to all materials, including the controls, indicates that the response is not due to material toxicity. It is suggested that the reasons for these results are related to the surgical protocol and/or the experimental

model used. Nevertheless, the bioactive glasses exhibiting some matrix formation should be examined further.

The SEM observation showed that the extent of surface reaction depends on the composition of the glass particles. It also confirmed the heterogeneity of sol-gel derived glasses produced by the calcium nitrate process.

## CHAPTER 7

### CONCLUSIONS AND SUGGESTIONS FOR FUTURE WORK

The use of sol-gel processing offers a new approach for the preparation of bioactive glasses and extends the compositional range of bioactivity from a three component system-- $\text{CaO-P}_2\text{O}_5\text{-SiO}_2$ --to one component system--porous  $\text{SiO}_2$  gel-glass. Based on this fact, the present work was developed with the intent to provide information in two distinct areas: 1) the production and use of bioactive glasses prepared by sol-gel processing; 2) the study of parameters that control the induction of calcium phosphate formation on silica gels.

In the area of sol-gel processing of bioactive glasses a specific objective was to develop alternative procedures for producing glasses in the multicomponent  $\text{CaO-P}_2\text{O}_5\text{-SiO}_2$  system with better homogeneity than the gel-glasses previously produced. To accomplish this objective, modifications in the mixing and drying steps of the calcium nitrate process were tried. No significant improvement in homogeneity was obtained. A process in which all the precursors are alkoxides was then developed. Gel-glasses were prepared using tetraethyl orthosilicate, triethyl phosphate and calcium metoxiethoxide as precursors. The components were mixed, cast and slowly hydrolyzed with

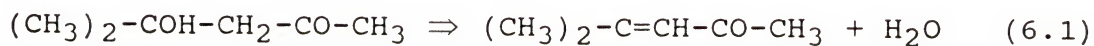
moisture from the atmosphere. By use of all alkoxide precursors monolithic, transparent gel-glasses were obtained with a low heterogeneity level of about 1%. Details about the preparation procedure and the homogeneity evaluation are presented in Chapter II.

The characteristic features of the all-alkoxide gel derived glasses measured using FTIR reflection spectroscopy, X-ray diffraction analysis, thermal analysis, and nitrogen adsorption are presented in Chapter III. The results show that all the compositions studied exhibit amorphous X-ray diffraction spectra. The absence of crystalline phases is confirmed by the DTA analysis, which shows only an endothermic band corresponding to the oxidation of residual organic compounds. The FTIR spectra are similar to those of melt derived glasses showing peaks corresponding to the bending and stretching vibrations of Si-O. The good reproducibility in the FTIR spectra also shows the homogeneity of these glasses. The compositions tested (S60 to S80) present high surface areas ranging from 250 to 450 m<sup>2</sup>/g. The textural characteristics depend on the rate of hydrolysis and the gelation time which may be controlled by the ambient conditions. A more detailed evaluation of the effect of relative humidity on the texture and structure of the gel-glasses is necessary.

Although the all-alkoxide procedure developed results in homogeneous gel-glasses, the process is lengthy due to the slow hydrolysis and aging required (7 days). The



monolithic forms that can be obtained are limited to those for which the level of solution in the casting container is below about 12 mm. Other hydrolysis procedures need to be tried. One possibility is to add components to the sol that slowly liberate water through a side chemical reaction. A preliminary study was done in which acetone alcohol was added to the alkoxides mixture. This organic compound dehydrates at about 60-80°C under acidic conditions, liberating one water molecule:



A dark-brown gel was obtained with this procedure, but it turned black after drying and white opaque after treatment at 700°C. The glass yield is low with this process because of the large amount of organic compounds used. No further studies were conducted with this approach.

Besides production of monoliths and powders, the sol produced with the all-alkoxides method can be used for coating of metal and organic substrates. It is promising for this application since the drying of the gels could be accomplished without cracking.

The bioactivity of the gel-glasses produced by the calcium alkoxide process was investigated and the results are presented in Chapter III. The gel-glasses are able to induce the formation of hydroxyapatite both in Tris buffer and simulated body fluid (SBF) solutions, indicating that they are bioactive. Similar to what was observed for the

calcium nitrate derived glasses, the bioactivity extends to gel-glasses with higher silica contents than melt derived glasses. A comparison between the rate of apatite formation in Tris buffer and SBF shows that the thickness of the hydroxyapatite layer grows rapidly in SBF whereas it remains constant in Tris buffer up to 15 days immersion time. It is proposed that the low concentration of phosphorus released into solution is the limiting factor for the growth of the HCA layer in a Tris buffer solution. An additional experiment that could be tried is to produce glasses with higher phosphorus content and test if they present higher bioactivity.

Although the results of in vitro bioactivity tests show that sol-gel derived glasses are highly bioactive, it is important to correlate the observed in vitro responses with in vivo results. A comparative study of the in vivo behavior of melt derived and sol-gel derived bioactive glasses was presented in Chapter VI. The application chosen for the study was pulp capping. Unfortunately, the results of this study showed that a severe inflammatory response occurred for the experimental materials as well as for the control material. Very few sections showed any reparative dentin formation. It is suggested that the reasons for these poor results are related to the experimental animal model used. Experiments using another animal model should be performed to confirm the above conclusion and to allow the evaluation

of the performance of the experimental materials, proposed but not accomplished in this study.

An important result came from this study, nevertheless. The SEM analysis showed that the gel-glass 54S produced by the calcium nitrate process presents a very irregular reaction pattern, having an uneven accumulation of calcium in localized regions. This observation is in accord with the in vitro homogeneity analysis presented in this work, which shows that the calcium nitrate derived gel-glasses are heterogeneous and that the heterogeneity level increases as the calcium content in the glass increases. It therefore confirms the importance of obtaining homogeneous materials to ensure high performance in a biomedical application.

The second area focused on in this work was the analysis of the mechanism of hydroxyapatite formation on silica substrates. A study was conducted on pure silica substrates to evaluate the effects of surface chemistry and the physical aspects of the surface on the nucleation process. In Chapter IV it was shown that the texture of the silica substrate has a direct effect on the nucleation rate. The induction time for nucleation of HA increases as pore size and pore volume decreases. It is proposed that the HA nucleation occurs inside the pores and that the number of pores and the diffusion of ions into the pores are the parameters that control the nucleation rate. It was also shown that the concentration of ions and the solution pH have a large effect on the HA nucleation rate.



The effect of surface chemistry on the formation of HA was extensively discussed in Chapters IV and V. Contrary to what several investigators in the field have hypothesized, it was shown that the concentration of silanol groups on the silica surface does not control the rate of HA nucleation and that there is not enough evidence to support the involvement of silanol groups on the nucleation process. However, silanol involvement is still a viable hypothesis. It is possible that the nucleation occurs through a very specific site, i.e., a silanol group bonded to a specific silica unit. The definition of a molecular mechanism of apatite formation involving those silica units may be possible through the use of Molecular Orbital modeling.

The discussion in Chapter V, reviewing the important parameters in the heterogeneous nucleation of hydroxyapatite on a silica substrate, shows that obtaining experimental evidence for a molecular level mechanism is not an easy task. In some cases the apparent evidence has been proven invalid by additional experiments or by careful interpretation. A complete understanding of the nucleation mechanism of HA will require more experimental information combined with a theoretical analysis, such as MO modeling, to eliminate the present uncertainties.

It is hoped that the results and discussion presented in this work have added a step in this direction.



## REFERENCES

- Ada93 J. Adair, T. Nagira, C. M. Brown, S. R. Khan, and W. C. Thomas Jr., "Heterogeneous Deposition of Calcium Phosphates at the Silicon (Hydrous) Oxide-Water Interface," in *Urolithiasis 2*, R. Ryall, eds., Plenum Press, 1993.
- Ael50 A. Aelion, A. Loebel, and F. Eirich, "Hydrolysis of Ethyl Silicate," *J. Am. Chem. Soc.*, **72** (1950), 5702.
- Agr90 D. K. Agrawal, A. R. Maslowski, and J. H. Adair, "Evolution of the Formation of Inorganic Polymers in the CaO-SiO<sub>2</sub>-P<sub>2</sub>O<sub>5</sub> System Using Metal Alkoxides," *J. Am. Ceram. Soc.*, **73** (1990) 430-434.
- And90a O. H. Andersson, "The Bioactivity of Silicate Glasses," Ph.D. Dissertation, Åbo Akademi University, Turku, Finland, 1990.
- And91 O. H. Andersson, and K. Kangasniemi, "Calcium Phosphate Formation at the Surface of Bioactive Glass In Vitro," *J. Biomed. Mater. Res.*, **25** (1991), 1019-1030.
- And90b O. H. Andersson, K. H. Karlsson, and K. Kangasniemi, "Calcium Phosphate Formation at the Surface of Bioactive Glass In Vivo," *J. Non-Cryst. Solids*, **119** (1990), 290-296.
- And92 O. H. Andersson, G. Latorre, and L. L. Hench, "The Kinetics of Bioactive Ceramics, Part II: Surface Reactions of Three Bioactive Glasses," in *Bioceramics*, Vol. 3, J. E. Hulbert and Samuel Hulbert, eds., Rose-Hulman Institute of Technology, Terre Haute, Indiana, 1992, pp. 46-53.
- Ave75 J. K. Avery, "Response of the Pulp and Dentine to Contact with Filling Materials," *J. Dent. Res.*, **54** (1975), B188-197.
- Bae86 C. F. Baes, and R. E. Mesmer, *The Hydrolysis of Cations*, Robert E. Krieger, Malabar, 1986.

- Ban77 E. Banks, S. Nakajima, L. C. Shapiro, O. Tilevitz, J. R. Alonzo, and C. Chianelli, "Fibrous Apatite Grown on Modified Collagen," *Science*, **198** (1977), 1164-1166.
- Bel70 R. J. Bell, and P. Dean, "Atomic Vibrations in Vitreous Silica," in *Discuss. Faraday Soc.*, **50** (1970), 55-61.
- Bim81 E. Bimstein and S. Shoshan, "Enhanced Healing of Tooth-Pulp Wounds in the Dog by Enriched Collagen Solution as a Capping Agent," *Archs. Oral Biol.*, **26** (1981), 97-101.
- Bri81 C.J. Brinker, S. P. Mukherjee, "Conversion of Monolithic Gels to Glasses in a Multicomponent Silicate Glass System," *J. Mat. Sci.*, **16** (1981), 1980-1988 .
- Bri90 C. J. Brinker, and G. W. Scherer, *Sol-Gel Science*, Academic Press, New York, 1990.
- Bro77 H. Brömer, K. Deutscher, B. Blencke, E. Pfeil, and V. Strunz, "Properties of the Bioactive Implant Material Ceravital," *Science of Ceramics*, **9** (1977), 219-225.
- Bro73 H. Brömer, E. Pfeil, and H. H. Käs, German patent No. 2,326,100 (1973).
- Bro79 M. Bromström and T. Strömberg, "Experiment with Pulp Capping," *Oral Surg.*, **48** (1979), 347-352.
- Bro81 W. E. Brown, and L. C. Chow, "Thermodynamics of Apatite Crystal Growth and Dissolution," *J. Crystal Growth*, **53** (1981), 31-41.
- Bun89 C. Bunker, D .M. Haaland, T. A. Michalske, and W. L. Smith, "Kinetics of Dissociative Chemisorption on Strained Edge-Shared Surface Defects on Dehydroxylated Silica," *Surface Sci.*, **222** (1989), 95-118.
- Cla76 A. E. Clark, C. G. Pantano, L. L. Hench, "Auger Spectroscopic Analysis of Bioglass Corrosion Films," *J. Amer. Ceram. Soc.*, **59** (1976), 37-39.
- Cox82 C. F. Cox, G. Bergenholtz, M. Fitzgerald, D. R. Heys, R. J. Heys, J. K. Avery, and J. Baker, "Capping of the Dental Pulp Mechanically Exposed to the Oral Microflora--a 5 Week Observation of Wound

- Healing in the Monkey," *Oral Pathology*, **11** (1982), 327-339.
- Cve78 M. Cvek, "A Clinical Report on Partial Pulpotomy and Capping with Calcium Hydroxyde in Permanent Incisors with Complicated Crown Fractures," *J Endodont.*, **4** (1978), 232-237.
- Cve87 M. Cvek, L. Granath, P. Cleaton-Jones, and J. Austin, "Hard Tissue Barrier Formation in Pulpotomized Monkey Teeth Capped with Cyanoacrylate or Calcium Hydroxide for 10 and 60 Minutes," *J. Dent. Res.*, **66** (1987), 1166-1174.
- Dam89 J. J. M. Damen, and J. M. Cate, "The Effect of Silicic Acid on Calcium Phosphate Precipitation," *J. Dent. Res.*, **68** (1989), 1355-1359.
- Dam92 J. J. M. Damen, and J. M. Cate, "Silica Induced Precipitation of Calcium Phosphate in the Presence of Inhibitors of Hydroxyapatite Formation," *J. Dent. Res.*, **71** (1992), 453-457.
- Deb58 J. H. deBoer, *The Structure and Properties of Porous Materials*, Butterworths, London, 1958.
- Dis83 Dislich, H. , "Glassy and Crystalline Systems from Gels: Chemical Basis and Technical Application," *J. Non-Cryst. Solids*, **57** (1983) 371-388.
- Duc87 P. Ducheyne, "Bioceramics: Material Characteristics versus *In Vivo* Behavior," *J. Biomed. Mater. Res.*, **21** (1987), 219-236.
- Dug64 D. L. Dugger, "The Exchange of Twenty Metal Ions With the Weakly Acidic Silanol Group of Silica Gel," *J. Phys. Chem.*, **68** (1964), 757-760.
- Fil93 M. R. Filgueiras, G. La Torre, and L. L. Hench, "Solution Effects on the Surface Reactions of a Bioactive Glass," *J. Biomed. Mater. Res.*, **27** (1993), 445-453.
- For85 T. R. Ford, "Pulpal Response to a Calcium Hydroxide Material for Capping Exposures," *Oral Surg.*, **59** (1985), 194-197.
- Fow74 B. O. Fowler, "Infrared Studies of Apatites, I. Vibrational Assignments for Calcium, Strontium, and Barium Hydroxyapatites Utilizing Isotopic Substitution," *Inorg. Chem.*, **13** (1974), 194-207.



- Gas70 P. H. Gaskell, "Vibrational Spectra of Simple Silicate Glasses," *Discuss. Faraday Soc.*, **50** (1970), 82-93.
- Gro88 U. Gross, R. Kinne, H. J. Schmitz, and V. Strunz, "The Response of Bone to Surface Active Glass/Glass-Ceramics," *CRC Critical Reviews in Biocompatibility*, **4** (1988), 2-15.
- Gro85 U. Gross, and V. Strunz, "The Interface of Various Glasses and Glass-Ceramics with a Bony Implantation Bed," *J. Biomed. Mater. Res.*, **19** (1985), 251-271.
- Gug88 M. Guglielmi, and G. Carturan, "Precursors for Sol-Gel Preparations," *J. Non-Cryst. Solids*, **100** (1988), 16-30.
- Hay80 T. Hayashi, and H. Saito, "Preparation of CaO-SiO<sub>2</sub> Glasses by the Gel Method," *J. Mater. Sci.*, **15** (1980), 1971-1977
- Hen80 L. L. Hench, "Biomaterials," *Science*, **208** (1980), 826-831.
- Hen88a L. L. Hench, "Bioactive Ceramics," *Annals N.Y. Acad. Sci.*, **523** (1988), pp. 54-71.
- Hen90a L. L. Hench, "Bioactive Glasses and Glass-Ceramics: a Perspective," in *Handbook of Bioactive Ceramics, Vol. I*, T. Yamamuro, L. L. Hench and J. Wilson, eds, CRC Press, Boca Raton, Florida, 1990, pp. 7-23.
- Hen91a L.L. Hench, "Bioceramics: from Concept to Clinic," *J. Am. Ceram. Soc.*, **74** (1991), 1487-1510.
- Hen92a L. L. Hench, "The Kinetics of Bioactive Ceramics, Part I: Reaction Rates," in *Bioceramics, Vol. 3*, J. E. Hulbert and Samuel Hulbert, eds., Rose-Hulman Institute of Technology, Terre Haute, Indiana, 1992, pp. 43-45.
- Hen91b L. L. Hench, O. A. Andersson, and G. P. LaTorre, "The Kinetics of Bioactive Ceramics Part III: Surface Reactions for Bioactive Glasses Compared with an Inactive Glass," in *Bioceramics Vol. 4*, W. Bonfield, G. W. Hastings, and K. E. Tanner, eds., Butterworth-Heinemann Ltd., Guildford, London, 1991, pp. 155-162.
- Hen93a L. L. Hench, F. G. Araujo, J. K. West, and G. P. LaTorre, "Gel-Silica Optics: Theory and Application," *J. Non-Cryst. Solids*, accepted.



- Hen82 L. L. Hench and E. C. Ethridge, *Biomaterials: An Interfacial Approach*, Academic Press, New York, 1982.
- Hen92b L. L. Hench, G. P. LaTorre, S. Donovan, J. Marotta, and E. Valliere, "Properties of Gel-Silica Optical Matrices with 4.5 and 9.0 nm Pores," in *Sol-Gel Optics II*, J. D. Mackenzie, ed., SPIE, Bellingham, WA, 1992, pp. 94-104.
- Hen74 L. L. Hench, and H. A. Paschall, "Histochemical Responses at a Biomaterial's Interface," *J. Biomed. Mater. Res.*, **5** (1974), 49-64.
- Hen71 L. L. Hench, R. J. Splinter, W. C. Allen, and T. K. Greenlee, Jr., "Bonding Mechanisms at the Interface of Ceramic Prosthetic Materials," *J. Biomed. Mater. Res.*, **2** (1971), 117-141.
- Hen77 L. L. Hench and M. Walker, US Patent 4171544 (1977).
- Hen88b L. L. Hench, S. H. Wang, and J. L. Nogues, "Gel-Silica Optics," *Multifunctional Materials 878*, R. L. Gunshor, ed., SPIE, Bellingham, Washington, 1988, pp. 76-85.
- Hen90b L. L. Hench, and J. K. West, "Sol-Gel Process," *Chem. Reviews*, **90** (1990), 7-23.
- Hen84 L. L. Hench, and J. Wilson, "Surface Active Biomaterials," *Science*, **226** (1984), 630-636.
- Hen93b *An Introduction to Bioceramics*, L. L. Hench and J. Wilson, eds., World Scientific, Singapore, 1993.
- Hol93 W. Höland and W. Vogel, "Machinable and Phosphate Glass-Ceramics," in *An Introduction to Bioceramics*, L. L. Hench and J. Wilson, eds., World Scientific, Singapore, 1993, pp. 125-137.
- Hol85 W. Höland, W. Vogel, K. Naumann, and J. Gummel, "Interface Reactions between Machinable Bioactive Glass-Ceramics and Bone," *J. Biomed. Mater. Res.*, **19** (1985), 303-312.
- Ile79 R. K. Iler, *The Chemistry of Silica*, John Wiley & Sons, New York, 1979.
- Jar76 M. Jarcho, J. F. Key, K. I. Gumer, R. H. Doremus, and H. P. Drobeck, "Tissue, Cellular and Subcellular

Events at Bone-Ceramic Hydroxyapatite Interface," *J. Bioengineering*, **1** (1976), 79-92.

- Joh85 D. W. Johnson, "Sol-Gel Processing of Ceramics and Glass," *Am. Ceram. Soc. Bull.*, **64**, 1597-1602 (1985).
- Kan90 K. Kangasniemi, and A. Yli-Urpo, "Biological Response to Glasses in the  $\text{SiO}_2\text{-Na}_2\text{O-CaO-P}_2\text{O}_5\text{-B}_2\text{O}_3\text{-AlO}_3$  System," in *CRC Handbook of Bioactive Ceramics Vol. I*, T. Yamamuro, L. L. Hench, and J. Wilson, eds., CRC Press, Boca Raton, Florida, 1990, pp. 97-108.
- Kar89 K. H. Karlsson, K. Froberg, and T. Ringbom, "A Structural Approach to Bone Adhering of Bioactive Glasses," *J. Non-Cryst. Solids*, **112** (1989), 69-72.
- Kim89 C. Y. Kim, A. E. Clark, and L. L. Hench, "Early Stages of Calcium Phosphate Layer Formation in Bioglasses," *J. Non. Cryst. Solids*, **113** (1989), 195-202.
- Kim92 C. Y. Kim, A. E. Clark, and L. L. Hench, "Compositional Dependence of Calcium Phosphate Layer Formation on Fluoride Bioglasses," *J. Mater. Sci.*, **26** (1992), 1147-1161.
- Kit87 T. Kitsugi, T. Nakamuro, T. Yamamuro, T. Kokubo, T. Shibuya and M. Takagi, "SEM-EPMA Observation of Three Types of Apatite-Containing Glass-Ceramics Implanted in Bone: the Variance of a Ca-P-rich Layer," *J. Biomed. Mater. Res.*, **21** (1987), 1255-1271.
- Kok90a T. Kokubo, "Surface Chemistry of Bioactive Glass-Ceramics," *J. Non-Cryst. Solids*, **120** (1990), 138-151.
- Kok87 T. Kokubo, T. Hayashi, S. Sakka, T. Kitsugi, T. Yamamuro, M. Takagi, and T. Shibuya, in *Ceramics in Clinical Applications*, P. Vicenzini, eds., Elsevier, Amsterdam, 1987, pp. 175-184.
- Kok90b T. Kokubo, S. Ito, Z. T. Huang, T. Hayashi, S. Sakka, T. Kitsugi, T. Yamamuro, "Ca-P-rich Layer Formed on High-Strength Bioactive Glass-Ceramic A-W," *J. Biomed. Mater. Res.*, **24** (1990), 331-343.
- Kok86 T. Kokubo, S. Ito, S. Sakka, and T. Yamamuro, "Formation of a High-Strength Bioactive Glass-Ceramic in the System  $\text{MgO-CaO-SiO}_2\text{-P}_2\text{O}_5$ ," *J. Mater. Sci.*, **21** (1986), 536-540.

- Kok85 T. Kokubo, S. Ito, M. Shigematsu, S. Sakka, and T. Yamamuro, "Mechanical Properties of a New Type of Apatite-Containing Glass-Ceramic for Prosthetic Application," *J. Mater. Sci.*, **20** (1985), 2001-2004.
- Kok92 T. Kokubo, H. Kushitani, C. Ohtsuki, S. Sakka, and T. Yamamuro, "Chemical Reaction of Bioactive Glass and Glass-Ceramics with a Simulated Body Fluid," *Materials in Medicine*, **3** (1992), 79-83.
- Kok90c T. Kokubo, H. Kushitani, S. Sakka, T. Kitsugi and T. Yamamuro, "Solutions Able to Reproduce In Vivo Surface-Structure Changes in Bioactive Glass-Ceramic A-W," *J. Biomed. Mater. Res.*, **24** (1990), 721-734.
- Kru90 M. Krukowski, R. A. Shively, P. Osbody, and B. L. Eppley, "Stimulation of Craniofacial and Intramedullary Bone Formation by Negative Charged Beads," *J. Oral Maxillofac. Surg.*, **48** (1990), 468-475.
- LeG91 R. Z. LeGeros, *Calcium Phosphates in Oral Biology and Medicine*, Karger, Basel, 1991.
- LeG78 R. F. Le Geros, G. Bone, and R. Le Geros, "Type of H<sub>2</sub>O in Human Enamel and in Precipitated Apatites," *Calcif. Tissue Res.*, **26** (1978), 111-118.
- LeG93 R. Z. LeGeros, and J. P. LeGeros, "Dense Hydroxyapatite," in *An Introduction to Bioceramics*, L. L. Hench and J. Wilson, eds., World Scientific, Singapore, 1993, pp. 139-180.
- Li93a P. Li, *In Vitro and In Vivo Calcium Phosphate Induction on Gel Oxides*, Ph.D. Dissertation, Leiden University, Leiden, 1993.
- Li93b P. Li, K. de Groot, "Calcium Phosphate Formation Within Sol-Gel Prepared Titania *In Vitro* and *In Vivo*," *J. Biomed. Mater. Res.*, **27** (1993), 1495-1500.
- Li93c P. Li, I. Kangasniemi, K. de Groot and T. Kokubo, "Apatite Crystallization from a Metastable Calcium Phosphate Solution on Sol-Gel Prepared Silica: Effect of Sintering Temperature of Silica Gel on Apatite Formation," *J. Non-Cryst. Solids*, (accepted).
- Li93d P. Li, K. Nakanish, and K. de Groot, "Induction and Morphology of Hydroxyapatite, Precipitated from



Metastable Simulated Body Fluids on Sol-Gel Prepared Silica," *Biomaterials*, **14** (1993), 963-968.

- Li94 P. Li, C. Ohtsuki, T. Kokubo, K. Nakanish, N. Soga, and K. de Groot, "A Role of Hydrated Silica, Titania and Alumina in Forming Biologically Active Bone-like Apatite on Implant," *J. Biomed. Mater. Res.*, **28** (1994), 7-15.
- Li92a P. Li, C. Ohtsuki, T. Kokubo, K. Nakanish, N. Soga, T. Nakamura, and T. Yamamuro, "Apatite Formation Induced by Silica Gel in a Simulated Body Fluid," *J. Amer. Ceram. Soc.*, **75** (1992), 2094-2097.
- Li93e P. Li, C. Ohtsuki, T. Kokubo, K. Nakanish, N. Soga, T. Nakamura, and T. Yamamuro, "Process of Formation of Bone-Like Apatite Layer on Silica Gel," *Materials in Medicine*, **4** (1993), 127-131.
- Li93f P. Li, C. Ohtsuki, T. Kokubo, K. Nakanish, N. Soga, T. Nakamura, and T. Yamamuro, "Effect of Ions in Aqueous Media on Apatite Formation on Silica Gel and its Relevance to Bioactivity of Bioactive Glasses and Glass-Ceramics," *J. Appl. Biomat.*, **4** (1993), 221-229.
- Li90 P. Li and F. Zhang, "The Electrochemistry of Glass Surface and its Application to Bioactive Glass in Solution," *J. Non-Cryst. Solids*, **119** (1990), 112-118.
- Li91a R. Li, *Sol-Gel Processing of Bioactive Glass Powders*, Ph.D. Dissertation, University of Florida, Gainesville, 1991.
- Li91b R. Li, A. E. Clark, and L. L. Hench, "An Investigation of Bioactive Glass Powders by Sol-Gel Processing," *J. Appl. Biomater.*, **2** (1991), 231-239.
- Li92b R. Li, A. E. Clark, and L. L. Hench, "Effects of Structure and Surface Area on Bioactive Powders by Sol-Gel Process," in *Chemical Processing of Advanced Materials*, L. L. Hench and J. West, eds., John Wiley & Sons, New York, 1992, pp. 627-633.
- Mac82 J. D. Mackenzie, *J. Non-Cryst. Solids*, **41** (1982), 1-10.
- Mar77 D. M. Martin and H. S. M. Crabb, "Calcium Hydroxide in Root Canal Therapy," *Brit. Dent. J.*, **142** (1977), 277-283.



- Mas65 J. B. Masterton, "Internal Resorption of Dentin: A Complication Arising from Unhealed Pulp Wounds," *Br. Dent. J.*, **118** (1965), 241-249.
- Muk84 S. P. Mukherjee, "Homogeneity of Gels and Gel-Derived Glasses," *J. Non-Cryst. Solids*, **63** (1984), 35-43.
- Nak85 T. Nakamura, T. Yamamuro, S. Higashi, T. Kokubo, and S. Ito, "A New Glass-Ceramic for Bone Replacement: Evaluation of its Bonding to Bone Tissue," *J. Biomed. Mater. Res.*, **19** (1985), 685-689.
- Neo92 M. Neo, S. Kotani, T. Nakamura, T. Yamamuro, C. Ohtsuki, T. Kokubo, and Y. Bando, "A Comparative Study of Ultrastructures of the Interfaces Between Four Kinds of Surface-Active Ceramics and Bone," *J. Biomed. Mater. Res.*, **26** (1992), 1419-1432.
- Neu58 W. Newman and M. Newman, *The Chemical Dynamics of Bone Mineral*, University of Chicago, Chicago, Illinois, 1958, p. 34.
- Ogi80 M. Ogino, F. Ohuchi, and L. L. Hench, "Compositional Dependence of the Formation of Calcium Phosphate Films on Bioglass<sup>®</sup>," *J. Biomed. Mater. Res.*, **14** (1980), 55-64.
- Ogu93 B. Oguntebi, A. Clark, and J. Wilson, "Pulp Capping with Bioglass and Autologous Dentin in Miniature Swine," *J. Dent. Res.*, **72** (1993), 484-489.
- Oht92a C. Ohtsuki, T. Kokubo, and T. Yamamuro, "Mechanism of Apatite Formation on CaO-SiO<sub>2</sub>-P<sub>2</sub>O<sub>5</sub> Glasses in a Simulated Body Fluid," *J. Non-Cryst. Solids*, **143** (1992), 84-92.
- Oht92b C. Ohtsuki, T. Kokubo, and T. Yamamuro, "Compositional Dependence of Bioactivity of Glasses in the System CaO-SiO<sub>2</sub>-Al<sub>2</sub>O<sub>3</sub>: Its *In Vitro* Evaluation," *Materials in Medicine*, **3** (1992), 119-125.
- Oht91 C. Ohtsuki, H. Kushitani, T. Kokubo, S. Kotani, and T. Yamamuro, "Apatite Formation on the Surface of Ceravital-Type Glass-Ceramic in the Body," *J. Biomed. Mater. Res.*, **25** (1991), 1363-1370.
- Ohu91 K. Ohura, T. Nakamura, T. Yamamuro, Y. Ebisawa, T. Kokubo, Y. Kotoura, and M. Oka, "Bone-Bonding

- Ability of  $P_2O_5$ -Free  $CaO.SiO_2$  Glasses," *J. Biomed. Mater. Res.*, **25** (1991), 357-365.
- Ohu92 K. Ohura, T. Nakamura, T. Yamamuro, Y. Ebisawa, T. Kokubo, Y. Kotoura, and M. Oka, "Bioactivity of  $CaO.SiO_2$  Glasses Added with Various Ions," *Materials in Medicine*, **3** (1992), 95-100.
- Pan84 F. Pancrazi, J. Phalippou, F. Sorrentino, and J. Zarzicki, "Preparation of Gels in the  $CaO-Al_2O_3-SiO_2$ ," *J. Non Cryst. Solids*, **63**, 811-93 (1984).
- Pan74 C. G. Pantano, A. E. Clark, and L. L. Hench, "Multilayer Corrosion Films on Bioglass Surfaces," *J. Amer. Ceram. Soc.*, **57** (1974), 412-413.
- Par65 G. A. Parks, "The Isoelectric Points of Solid Oxides, Solid Hydroxides, and Aqueous Hydroxy Complex Systems," *Chem. Rev.*, **65** (1965), 177-198.
- Pat76 R. C. Patterson, "Reaction of the Rat Molar Pulp to Various Materials," *Br. Dent. J.*, **140** (1976), 93-96.
- Pat67 S. S. Patterson, "Pulp Calcifications Due to Operative Procedures -- Pulpotomy," *Int. Dent. J.*, **17** (1967), 490-505.
- Per93a M. M. Pereira, A. E. Clark, and L. L. Hench, "Homogeneity of Bioactive Sol-Gel Derived Glasses in the System  $CaO-P_2O_5-SiO_2$ ," *Journal of Materials Synthesis and Processing*, accepted.
- Per93b M. M. Pereira, A. E. Clark, and L. L. Hench, "Calcium Phosphate Formation on Sol-Gel Derived Bioactive Glasses *In Vitro*," *J. Biomed. Mater. Res.*, accepted.
- Per94 M. M. Pereira, A. E. Clark, and L. L. Hench, "Effect of Texture on the Rate of Hydroxyapatite Formation on Silica Gel Surface," *J. Amer. Ceram. Soc.*, accepted.
- Pra84 M. Prassas, and L. L. Hench, "Physical Chemical Factors in Sol-Gel Processing," in *Ultrastructure Processing of Ceramics, Glasses and Composites*, L.L. Hench, and D. R. Ulrich, eds., J. Wiley and Sons, New York, 1984, pp. 100-125.
- Sho93 E. C. Shors, and R. E. Holmes, "Porous Hydroxyapatite," in *An Introduction to Bioceramics*, L. L. Hench and J. Wilson, eds., World Scientific, Singapore, 1993, pp. 181-198.

- Tho74 I. M. Thomas, U.S Patent 3,791,808, February, 1974.
- Tia88 F. Tian, "The NMR Studies of the  $P_2O_5$ - $SiO_2$  Sol and Gel Chemistry," *J. Non. Cryst. Solids*, **104** (1988), 129-134.
- Tra84 B. M. Tracy and R. H. Doremus, "Direct Electron Microscopy Studies of the Bone-Hydroxylapatite Interface," *J. Biomed. Mater. Res.*, **18** (1984), 719.
- Tre88 W. K. Tredway and S. H. Risbud, "Gel Synthesis of Glass Powders in the  $BaO$ - $Al_2O_3$ - $SiO_2$  System," *J. Non. Cryst. Solids*, **100** (1988), 278-283.
- Tro74 L. Tronstad, "Reaction of the Exposed Pulp to Dycal Treatment," *Oral Surg.*, **38** (1974), 945-953.
- Var87 A. K. Varshneya, and S. Nungil, "Sol-Gel Derived Soda-Lime-High-Silica Glass," *J. Am. Ceram. Soc.*, **70** (1987), C-21.
- Vil88 M. A. Villegas, and J. M. F. Navarro, "Hydrolytic Resistance of  $Na_2O$ - $B_2O_3$ - $SiO_2$  Gels Prepared By Sol-Gel Process," *J. Non-Cryst. Solids*, **100** (1988), 453-460.
- Vog86 W. Vogel, W. Holand, K. Naumann, and J. Gummel, "Development of Machinable Bioactive Glass-Ceramics for Medical Uses," *J. Non-Cryst. Solids*, **80** (1986), 34-51.
- Wal77 M. M. Walker, *An Investigation into the Bonding Mechanisms of Bioglass*, Ph.D. Dissertation, University of Florida, Gainesville, Florida, 1977.
- Wal93 S. Wallace, J. K. West, and L. L. Hench, "Interactions of Water with Trisiloxane Rings: Experimental Analysis," *J. Non-Cryst. Solids*, **152** (1993), 101-108.
- War89 L. D. Warren, A. E. Clark, and Hench L.L., "Quality Assurance of Bioglass Powders," *J. Biomed. Mater. Res.*, **23** (1989), 201-209.
- Wat81 A. Watts, L.D.S.R.C.S., and R. C. Patterson, "A Comparison of Pulp Responses to Two Different Materials in the Dog and the Rat," *Oral Surg.*, **52** (1981), 648-652.
- Wes92 J. K. West, and L. L. Hench, "Reaction Kinetics of Bioactive Ceramics Part V: Molecular Orbital



Modelling of Bioactive Glass Surface Reaction," in *Bioceramics 5*, T. Yamamuro, T. Kokubo, and T. Nakamura, eds., Kobunshi Kankokai, Japan, 1992, pp. 75-86.

- Wil90 J. Wilson, and D. Nolleti, "Bonding of Soft Tissues to Bioglass ," in *Handbook of Bioactive Ceramics, Vol. I*, T. Yamamuro, L. L. Hench and J. Wilson, eds, Boca Raton, Florida, 1990, pp. 283-302.
- Wil81 J. Wilson, G. H. Pigott, F. J. Schoen and L. L. Hench, "Toxicology and Biocompatibility of Bioglasses," *J. Biomed. Mater. Res.*, **15** (1981), 805-817.
- Wun76 J. A. Wunder, W. W. Briner, and G. P. Calkins, "Identification of Cultivable Bacteria in Dental Plaque from the Beagle Dog," *J. Dent. Res.*, **55** (1976), 1097-1102.
- Yol79 B. E. Yoldas, "Monolithic Glass Formation by Chemical Polymerization," *J. Mat. Sci.*, **14** (1979), 1843-1849.
- You58 C. J. Young, "Interaction of Water Vapor with Silica Surfaces," *J. Colloid Sci.*, **13** (1958), 67-85.
- You60 C. J. Young, and T. P. Bursh, "Immersion Calorimetry Studies of the Interaction of Water with Silica Surfaces," *J. Colloid Sci.*, **15** (1960), 361-370.
- Zhu87 L. T. Zhuravlev, "Concentration of Hydroxyl Groups on the Surface of Amorphous Silicas," *Langmuir*, **3** (1987), 316-318.



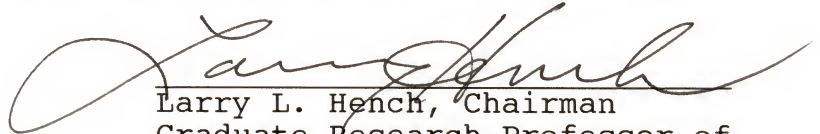
## BIOGRAPHICAL SKETCH

Marivalda de Magalhães Pereira was born June 9, 1960, in Guanhães, State of Minas Gerais, Brazil. She attended local schools and graduated from high school in 1978. In 1983 Ms. Pereira graduated from the *Universidade Federal de Minas Gerais* (Federal University of Minas Gerais), Belo Horizonte, Brazil, with the degree of Chemical Engineer. In 1984 she enrolled in the Graduate School of the *Universidade Federal de Minas Gerais*, from which she received the title of Specialist in Physical Metallurgy and the degree of Master of Science in metallurgical engineering in 1986.


In 1986 Ms. Pereira joined the faculty of the *Universidade Católica de Minas Gerais* (Catholic University of Minas Gerais) as a part-time assistant professor for the Mechanical Engineering Department. From 1987 to 1989 she worked for a research institution, *Fundação Centro Tecnológico de Minas Gerais*, in the area of physical metallurgy.

In the spring of 1990 she entered the Graduate School of the University of Florida, and since then she has pursued work toward the degree of Doctor of Philosophy in materials science and engineering.


I certify that I have read this study and that in my opinion it conforms to acceptable standards of scholarly presentation and is fully adequate, in scope and quality, as a dissertation for the degree of Doctor of Philosophy.

  
Larry L. Hench, Chairman  
Graduate Research Professor of  
Materials Science and  
Engineering

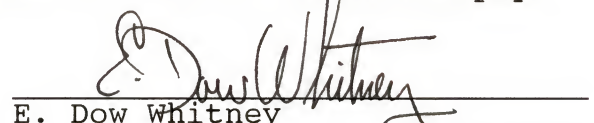
I certify that I have read this study and that in my opinion it conforms to acceptable standards of scholarly presentation and is fully adequate, in scope and quality, as a dissertation for the degree of Doctor of Philosophy.

  
Arthur E. Clark, Cochair  
Professor of Materials Science  
and Engineering

I certify that I have read this study and that in my opinion it conforms to acceptable standards of scholarly presentation and is fully adequate, in scope and quality, as a dissertation for the degree of Doctor of Philosophy.

  
David E. Clark  
Professor of Materials Science  
and Engineering

I certify that I have read this study and that in my opinion it conforms to acceptable standards of scholarly presentation and is fully adequate, in scope and quality, as a dissertation for the degree of Doctor of Philosophy.

  
E. Dow Whitney  
Professor of Materials Science  
and Engineering

I certify that I have read this study and that in my opinion it conforms to acceptable standards of scholarly presentation and is fully adequate, in scope and quality, as a dissertation for the degree of Doctor of Philosophy.



James H. Adair  
Associate Professor of  
Materials Science and  
Engineering

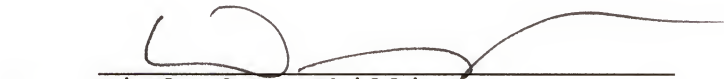
I certify that I have read this study and that in my opinion it conforms to acceptable standards of scholarly presentation and is fully adequate, in scope and quality, as a dissertation for the degree of Doctor of Philosophy.



Dinesh O. Shah  
Professor of Chemical  
Engineering

This dissertation was submitted to the Graduate Faculty of the College of Engineering and to the Graduate School and was accepted as partial fulfillment of the requirements for the degree of Doctor of Philosophy.

April 1994



Winfred M. Phillips  
Dean, College of Engineering

Karen A. Holbrook  
Dean, Graduate School